Speciation of Pu(III) in the Environmental System Humic Substances-Groundwater-Kaolinite

Thesis submitted for
attaining the degree of

"Doktor der Naturwissenschaften"
doctor rerum naturalium

at the
Department of Chemistry, Pharmacy,
and Geosciences
of the
Johannes Gutenberg-University Mainz

Buda Razvan Aurel
Born in Cluj-Napoca/Romania

Mainz, 2006

Index

Abstract

For the safety assessments of nuclear waste repositories, the possible migration of the radiotoxic waste into environment must be considered. Since plutonium is the major contribution at the radiotoxicity of spent nuclear waste, it requires special care with respect to its mobilization into the groundwater.

Plutonium has one of the most complicated chemistry of all elements. It can coexist in 4 oxidation states parallel in one solution. In this work is shown that in the presence of humic substances it is reduced to the Pu(III) and Pu(IV). This work has the focus on the interaction of Pu(III) with natural occurring compounds (humic substances and clay minerals bzw. Kaolinite), while Pu(IV) was studied in a parallel doctoral work by Banik (in preparation).

As plutonium is expected under extreme low concentrations in the environment, very sensitive methods are needed to monitor its presence and for its speciation. Resonance ionization mass spectrometry (RIMS), was used for determining the concentration of Pu in environmental samples, with a detection limit of 10^6- 10^7 atoms. For the speciation of plutonium CE-ICP-MS was routinely used to monitor the behaviour of Pu in the presence of humic substances. In order to reduce the detection limits of the speciation methods, the coupling of CE to RIMS was proposed. The first steps have shown that this can be a powerful tool for studies of pu under environmental conditions.

Further, the first steps in the coupling of two parallel working detectors (DAD and ICP_MS) to CE was performed, for the enabling a precise study of the complexation constants of plutonium with humic substances.

The redox stabilization of Pu(III) was studied and it was determined that NH_2OHHCl can maintain Pu(III) in the reduced form up to pH 5.5 – 6. The complexation constants of Pu(III) with Aldrich humic acid (AHA) were determined at pH 3 and 4. the logß = 6.2 – 6.8 found for these experiments was comparable with the literature.

The sorption of Pu(III) onto kaolinite was studied in batch experiments and it was determine dthat the pH edge was at pH ~ 5.5. The speciation of plutonium on the surface of kaolinite was studied by EXAFS/XANES. It was determined that the sorbed species was Pu(IV).

The influence of AHA on the sorption of Pu(III) onto kaolinite was also investigated. It was determined that at pH < 5 the adsorption is enhanced by the presence of AHA (25 mg/L), while at pH > 6 the adsorption is strongly impaired (depending also on the adding sequence of the components), leading to a mobilization of plutonium in solution.

Zusammenfassung

Um die Sicherheit nuklearer Endlager einschätzen zu können, muss eine mögliche Migration des radiotoxischen Abfalls in die Umwelt betrachtet werden. Da Plutonium den Hauptbestandteil der Radiotoxizität des Abfalls bis zu 10^6 Jahren ausmacht, benötigt die Untersuchung seiner Mobilisierung durch/in das Grundwasser besondere Aufmerksamkeit.

Plutonium besitzt ein sehr kompliziertes chemisches Verhalten. Es kann gleichzeitig in vier Oxidationsstufen in einer Lösung existieren. In dieser Arbeit wird gezeigt, dass in Anwesenheit von Huminstoffen höherwertiges Plutonium zu Pu(III) und Pu(IV) reduziert wird. Diese Arbeit ist auf die Wechselwirkungen von Pu(III) mit natürlich vorkommenden Bestandteilen (Huminstoffe und Tonminerale bzw. Kaolinit) fokussiert. Das Verhalten von Pu(IV) wird in einer parallelen Doktorarbeit von N. L. Banik, untersucht.

Da Plutonium in extrem geringer Konzentration in der Umwelt vorkommt, werden sehr empfindliche Methoden benötigt, um Pu nachzuweisen und seine Speziation zu ermitteln. Resonanzionisationsmassenspektrometrie (RIMS) wurde benutzt, um Pu in Umweltproben zu bestimmen. Die Nachweisgrenze liegt bei 10^6 bis 10^7 Atomen. Für die Speziation des Plutoniums in Anwesenheit von Huminstoffen wurde routinemässig die Kopplung Kapillarelektrophorese (CE) mit der ICP-MS (CE-ICP-MS) eingesetzt. Zur Verbesserung die Nachweisgrenze der Speziationsmethoden, wurde eine Kopplung von CE mit RIMS vorgeschlagen. Erste Ergebnisse haben ergeben, dass dies ein Verfahren zur Untersuchung von Pu unter Umweltbedingungen sein kann.

Weiterhin wurde die Kopplung von zwei parallel arbeitenden Detektoren, Dioden-Array-Detektor, DAD, und ICP-MS, nach der CE untersucht. Diese Technik sollte eine präzise Untersuchung der Komplexierungskonstanten von Pu mit Huminstoffen ermöglichen.

Die Redoxstabilität von Pu(III) wurde studiert. Dabei konnte gezeigt werden, dass NH_2OHHCl dreiwertiges Pu bis zu pH 5,5 – 6 stabilisiert. Die Komplexierungskonstanten von Pu(III) mit Aldrich-Huminsäure (AHA) wurden bei pH 3 und 4 bestimmt. Die ermittelten logß-Werte von 6,5±0,3 stimmen gut mit Literaturwerten für Am(III) überein.

Die Sorption von Pu(III) an Kaolinit wurde in Batch-Experimenten untersucht, und es wurde dabei eine pH-Kante bei pH ~ 5,5 bestimmt. Die Speziation des Pu auf der Oberfläche von Kaolinit wurde mittels Röntgenabsorptionspektroskopie (EXAFS/XANES) studiert. Als sorbierte Spezies wurde Pu(IV) ermittelt.

Der Einfluss von AHA auf die Sorption von Pu(III) an Kaolinit wurde ebenfalls bestimmt. Dabei wurde beobachtet, dass bei pH < 5 die Anwesenheit von AHA (25 mg / l) die Sorption erhöht, während es bei pH > 6 die Sorption reduziert, wobei dieser Effekt im Detail von der Reihenfolge der Zugabe der Reagenzien abhängt.

1. Introduction

Towards the end of the fourth decade of the last century, Otto Hahn and Fritz Straßmann were conducting a large series of experiments trying to identify radioactive products resulting from the neutron bombardment of uranium. In December 1938, they were confronted with a completely new and surprising discovery, namely the fission process.

The results were so unexpected, that Hahn and Straßmann were unable to offer a satisfactory explanation for what they observed. That explanation was provided by the physicists Lise Meitner and her nephew Otto Frisch. They presumed that after the absorption of a neutron, the uranium nucleus would become unstable and divide into two smaller drops. If this division takes place, the resulting drops (nuclear fragments) would be repelled by their respective positive charges. This process was termed fission by Meitner and Frisch (Meitner *et al*., 1939).

Furthermore, fission raised the possibility of a nuclear chain reaction**.** The scientists understood that if they would be able to control such a chain reaction, this could be a tremendous source of energy obtained from the fission of uranium atoms (Joliot *et al*., 1939).

The high energetic potential of the nuclear fission didn't remain unexploited, so in the 2nd of December 1942 Enrico Fermi and Leo Szilard brought the first atomic reactor to criticality. The era of nuclear power has begun.

In the World War II the race for more powerful weapons accelerated the research in the nuclear field, as scientists recognized the tremendous power potential of nuclear fission. On 16th of July 1945 in New Mexico, USA the first fission bomb exploded.

The use of radioactivity has become much more common in our days. Nuclear medicine, radioactive dating of archaeological, geological, and cosmical samples, radioactive analysis for different materials, radionuclide batteries for cardiac pacemakers or space mission vehicles (Stieve, 1976) are just some of the modern applications of radioactivity.

Besides all of the applications mentioned above, nuclear fission is used worldwide for the production of electrical power in nuclear power plants, providing around 17% of the consumed energy (IAEA, 2006). In Germany more than 30% of the electricity fed to the public grid is generated in nuclear power plants.

The nuclear power plants have a very low contribution to the greenhouse effect in contrary to fossil fuel reactors. The big disadvantage of nuclear power plants is that they produce long-lived radioactive waste.

Different strategies to reduce the amount of nuclear waste were developed and applied in the last decades, including the improvement of the so called "burn-up" of the fuel and reprocessing of the spent fuel. Uranium oxide or mixed oxides (MOX, which is $^{235}UO_2$+ $^{239}PuO_2$) are used to fuel the nuclear reactors. In the process of "burning" of the nuclear fuel, a big variety of nuclear reactions take place, producing a wide range of fission products and long-lived actinides as shown in Fig. 1. These products decay to non radioactive products in periods of time of up to 1.000.000 years or more.

The disposal of the spent nuclear fuel is still not a solved problem in most of the countries. The repositories would have to be able to withstand the most dramatic conditions over extremely long periods of time (up to 1.000.000 years) (Beckmerhagen *et al*. 2004).

A number of countries are developing geological disposal facilities for spent fuel and high-level radioactive waste. Preparations for the Yucca Mountain licence application continue in the United States, although a recent court decision is affecting the process. Finland continues to develop an underground research laboratory on the site designated for its geological disposal facility while Sweden continues with its site selection process. Switzerland is considering the possibility of disposing the high level and the long-lived intermediate-level waste and spent

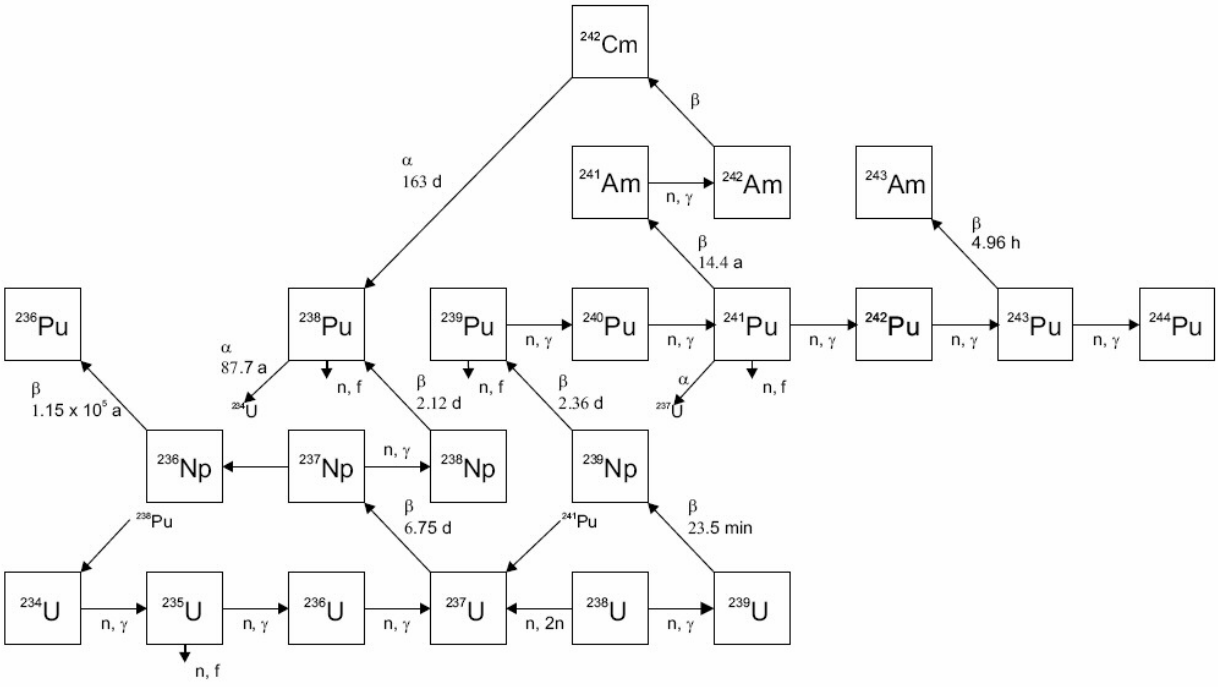

Figure 1: Production and decay chain of a few important long-lived isotopes in a nuclear reactor (IAEA, 1998)

nuclear fuel in a deep geological formation too. Work also continues in France on investigations at the Bure site. In view of its rapidly expanding nuclear power programme, China is considering accelerating its schedule for developing a geological disposal facility.

Many countries operate near surface disposal facilities for low and intermediate level radioactive waste. (Lidskog *et al*. 2001)

The German government has decided to stop the reprocessing of the spent nuclear fuel from 1st of July 2005 and to establish a deep geological repository for radioactive waste starting operation by ~ 2030 (Dobschütz *et al.* 2003). The storage will take place in casks in a dry way.

Figure 2: Disposal container design in Canada *(nuclearfaq.ca)*

Several options for disposal containers designs have been discussed. One example is shown in Fig. 2. The common point is that they all must be able to withstand the most extreme conditions for transport, as well as for long time deposition.

The containers were designed very robust so they were still intact after a collision with a locomotive in a crash test, as illustrated in the Fig. 3. Still, for an increased safety of the long term repositories, further barriers are being considered in order to protect humans and the environment from potential risks of contamination.

Figure 3: Nuclear waste casks crash tests performed at Sandia National Laboratories in the USA *(nuclearfaq.ca)*

As mentioned before, from the very beginning of industrial nuclear power use in the early sixties, it was the radioactive waste disposal policy in Germany that all types of radioactive waste were to be disposed of in deep geological formations (BfS, DBE, web site). As an example, a model of such a deep geological formation as planed in Finland is presented in Fig. 4.

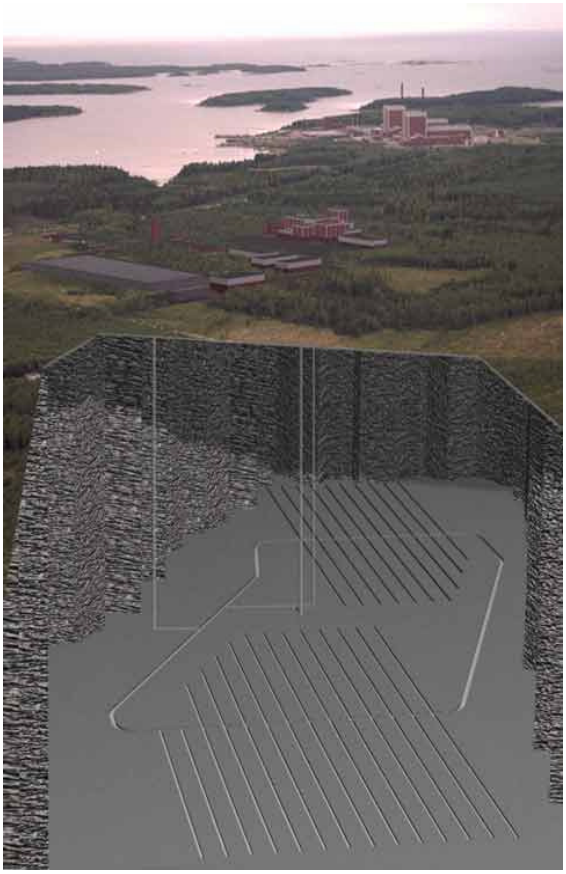

Figure 4: Illustration of the planned final disposal facility for spent nuclear fuel in Olkiluoto, Finland. (photo courtesy of World Nuclear Association).

Several criteria must be taken into account when analysing the safety of a repository to be constructed. The respective investigations and evaluations have to cover the following items:

- Criticality safety in the operational and post-closure phase
- Thermal influence upon the host rock by the decay heat of the radionuclides
- The possible exposure of the staff and of the public in the repository vicinity to radioactive substances released from the site via gaseous and liquid effluents
- Exposure to radiation in the repository surroundings due to radioactive substances released via the water path in the post-closure phase (radiological long-term effects).

This work has to be based on detailed site-specific geological and hydro-geological data, a sufficiently detailed concept of the repository including the planned mode of operation, and data concerning the types, quantities, and properties of the waste that is planned to be disposed off.

For the long term safety assessment of a deep geological nuclear waste repository, good knowledge on the chemical and physical properties of the waste materials, on the host rocks, hydrological conditions in the surroundings of the site, as well as the interactions between them is mandatory.

Germany still didn't come to a final decision concerning the position of a repository. Different types of rocks are used or investigated with respect to nuclear waste repositories. Table 1 presents some examples of final disposal concepts and underground laboratories.

Tabel 1. Comparison between different types of repositories and underground laboratories, and different types of host rocks (FZK, 2001).

Country	Location	Concept	Host Rock	Type of Waste
Germany	*Morsleben*	*1*	*Salt*	*MAW/LAW*
	Gorleben	*2*	*Salt*	*HAW*
	Schacht Konrad	*1*	*Clay*	*MAW/LAW*
Finland	*Olkiluoto*	*3*	*Granite*	*HAW*
	Olkiluoto	*4*		*MAW/LAW*
France	*Tournemire*	*3*	*Clay*	*HAW*
	Bure / Est	*3*	*Clay*	*HAW*
Sweden	*Äspö (Hard Rock Laboratory)*	*3*	*Granite*	*HAW*
Switzerland	*Felslabor Grimsel*	*3*	*Granite*	*HAW*
	Mount Terri	*3*	*Clay*	*MAW/LAW*
USA	*Carlsbad / New Mexico WIPP (Waste Isolation Pilot Plant)*	*1*	*Salt*	*HAW*
	Yucca Mountain	*1*	*Tuff*	*HAW*

Legend:

LAW – Low Active Waste
MAW – Middle Active Waste
HAW – High Active Waste

1 - Repository in deep geological formation
2 - Pilot mine in deep geological formation
3-– Experimental laboratory in deep geological formation
4 - Near surface underground repository

Two possible sites for the position of nuclear waste final repository have been considered in Germany. One is an old salt dome in Gorleben and the other one is the former iron ore mine Konrad.

From July 2003 several institutions across Germany *(Institut für Interdisziplinäre Isotopenforschung* in Leipzig *(IIF), Institut für Kernchemie* at *Johannes Gutenberg Universität Mainz, Institut für Nukleare Entsorgung (INE)* at *Forschungszentrum Karlsruhe*, *Institut für Radiochemie* at *Forschungszentrum Rossendorf,* as well as groups from *Technische Universität München, Universität Heidelberg, Universität Potsdam,* and *Universität des Saarlandes*) have combined their efforts in a project supported by the Bundesministerium für Wirtschatft und Technology (BMWi, Federal Ministry for Economy and Technology), entitled *"Migration von Actiniden im System Ton, Huminstoff, Aquifer"* (Migration of Actinides in the System Clay, Humic Substances, Aquifer). The main focus of this project was to acquire information on the interactions between actinides and the possible host rock clay, ground waters and their components, in the vicinity of nuclear waste repositories.

The "Institut für Kernchemie" at the Mainz University has focused its activity

on studying the interactions of plutonium and neptunium with humic substances and different clay minerals.

Plutonium represents the major contribution to the radiotoxicity of spent nuclear fuel over long time storage as shown in Fig. 5.

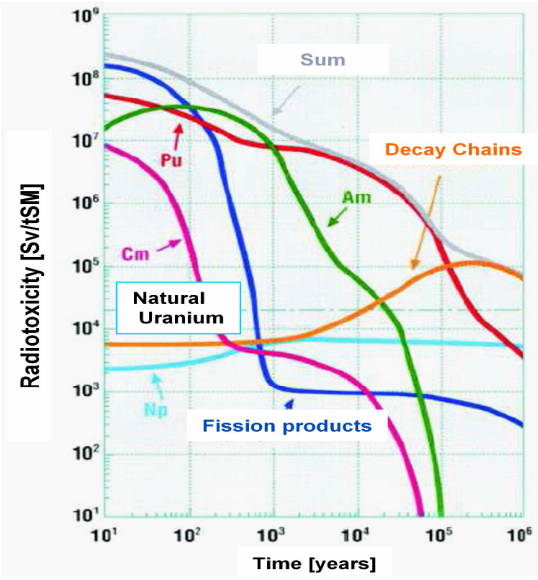

Figure 5: Chronological sequence of the radiotoxicity of spent nuclear fuel from a modern pressurized-water reactor (in Sievert Sv per ton heavy metal). (Primary enrichment in ^{235}U of the fuel elements 4%, burnout: 40GWd/t, radiotoxicity relating to ingestion) (Gomper, 2001)

Therefore, it is very important to predict in a very appropriate way the behaviour of this element in a so called "worst case scenario", when after an accidental release plutonium would come in contact with the geological elements.

It was considered in the past that plutonium introduced into the subsurface environment is relatively immobile owing to its low solubility in ground water (Nitsche *et al.* 1993) and strong sorption onto rocks (Triay *et al.* 1996). Nonetheless, colloid–facilitated transport of radionuclides over distances larger than one kilometre, were reported at the Nevada Test Site US, where hundreds of underground nuclear tests were conducted (Kersting *et al.* 1999). It has been argued that plutonium could have been sorbed onto colloids found in groundwater, or could have formed Eigen colloids, and thus its transport over longer distances has been enhanced.

The chemical and physical interactions between plutonium and clay minerals as well as organic substances like humic substances found ubiquitously in water, could lead to the mobilization or immobilization of the radiotoxic element. Many parameters have strong influences on the migration behaviour of this actinide. Of great importance are the pH, redox potential (E_h), temperature, ionic strength (I) of the aquatic solution as well as the oxidation state of plutonium (Allard *et al.* 1984), (Choppin, 1988). Plutonium can coexist under natural conditions in four oxidation states, III, IV, V, and VI.

Dissolved humic substances have a significant influence on the redox behaviour of a plutonium solution (Choppin, 1988), (Choppin, 2003), (Kim and Czerwinski, 1996). In the presence of humic substances, plutonium is reduced

from the higher oxidation states to the oxidation states III and IV (Kuczewski *et al.*, 2003) (Bürger, 2005), and this work.

The scientific research performed at the Institut für Kernchemie has been therefore concentrated on the study of the migration behaviour of Pu(III) and Pu(IV) under the conditions expected in the environment.

New speciation methods have been developed, in order to enable the investigation of plutonium under environmental conditions and its interaction with natural occurring substances.

2. History and chemistry of the actinides

The discovery of fission in 1938 by O. Hahn and F. Straßmann (Frisch, 1939) launched a intense campaign in the field of nuclear physics and chemistry. At Berkeley, Edwin Mattison McMillan first performed a simple experiment to measure the ranges of the energetic fission fragments, by exposing a thin layer of uranium oxide spread on a sheet of paper placed between several thin aluminium foils on either side, to the neutrons from 8 MeV deuterons striking a beryllium target in a 37-inch cyclotron. In another experiment he used cigarette papers instead of the aluminum foils, since the paper is a material that would not become itself radioactive.

In addition to the fission fragment activity which was strong in the cigarette paper, there was one component with a twenty-five-minute half-life and another of roughly two days that was concentrated in the uranium layer and was termed the "non recoiling activity". McMillan speculated that the twenty-five-minute activity was ^{239}U, identified earlier by Hahn and co-workers as a product of resonant neutron capture in uranium.

After he improved the separation of the irradiated uranium from the fission products, McMillan enlisted Emilio Segrè to study the chemical properties of the new physically separated product *i.e.* the non recoiling 2.3 d activity. They had expected that the new element (next to uranium) would behave similar to rhenium. But it was found that the new element behaved similar to rare earth elements.

In 1940 McMillan returned to the experiment, this time using a 60-inch cyclotron where 16 MeV deuterons were available. It was then clearly demonstrated that the 2.3 day activity could not be from a fission product and that the two activities, the twenty three minutes and the 2.3 day, were genetically linked. It was posted that the beta decay of ^{239}U was producing atoms of a new element $Z = 93$. It was named neptunium (Np) after Neptune, the planet immediately beyond Uranus.

Philip H. Abelson helped further McMillan in studying the chemical properties of the new element. They noticed that it resembled sometimes the properties of rare-earth elements. The key to that was the state of oxidation of the material. In the reduced state, the activity coprecipitated with rare-earth fluorides, whereas in an oxidized state, it did not. In the oxidised state, it behaved thus like uranium. (McMillan, 1964).

In the summer of 1940, Glen Seaborg, Arthur Wahl, and Joseph Kennedy, a group of chemists at Berkeley, began a

search for the next transuranium element, 94, which they thought to be a decay product (daughter) of Np-239. Continuing the search for element 94 in the winter of 1941, they bombarded uranium oxide with 16 MeV deuterons from the Berkeley cyclotron. They chemically identified another isotope of neptunium, Np-238, which decayed by beta emission to an isotope of element 94 (plutonium) that then emitted alpha particles. The reaction is summarized in Fig. 6.

$$^{238}_{92}U + ^{2}_{1}H \longrightarrow ^{238}_{93}Np + 2n \quad (1)$$

$$^{238}_{93}Np \xrightarrow[2.1d]{\beta-} ^{238}_{94}Pu \quad (2)$$

Figure 6: Formation of ^{238}Pu

The Pu alpha particle emitter was separated chemically from U, Np, and other reaction products and oxidized with potassium peroxydisulfate, ($K_2S_2O_8$), to a fluoride-soluble oxidation state. The other products of this neutron bombardment did not undergo oxidation with $K_2S_2O_8$ and thus remained insoluble. The Pu in solution was then reduced to a lower oxidation state with SO_2 and precipitated as a fluoride using Ce^{3+} and La^{3+} as carriers. This chemistry, based on oxidation, reduction, and precipitation reactions, would later prove the basis for the large-scale production of plutonium. The alpha particle energy and activity was unique and thus indicated a new element, identified later as ^{238}Pu. Simultaneously to the deuteron bombardment of ^{238}U (from deuterons on Be) leading to 86 a ^{238}Pu, there were performed neutron bombardments of ^{238}U producing $^{239}Np \xrightarrow{\beta-} ^{239}Pu$ (24.000 a). A. C. Wahl observed the growth of α activity from the Np precursor in both experiments and determined the range of the α particles in air, indicating that ^{238}Pu had a higher α energy than ^{239}Pu. The first weightable amounts of plutonium were from neutron bombardments of up to 90 kg of $UO_2(NO_3)\cdot 6H_2O$ which was dissolved in ether, (100 L) followed by oxidation – reduction cycles in which Pu was finally separated from Np and 37 μg of ^{239}Pu were isolated (Cunningham *et al.*, 1949).

Many different isotopes of elements with higher atomic numbers were produced in the following years. Americium (95) and curium (96) in 1944, berkelium (97) in 1949, californium (98) in 1950, einsteinium (99) and fermium (100) in 1952, mendelevium (101) in 1955, nobelium (102) in 1957 and lawrencium (103) in 1961. All this new discovered elements were radioactive as expected from their position at the end of the periodic table, and a good analogy between them and the rare earths elements

Table 2: The known oxidation states of the actinide elements; the most stable with bold characters, in brackets-unstable. (Bagnall 1972)

Ac	Th	Pa	U	Np	Pu	Am	Cm	Bk	Cf	Es	Fm	Md	No	Lr
						(2)						2	**2**	
3	(3)	(3)	3	3	3	**3**	**3**	**3**	**3**	**3**	**3**	**3**	3	**3**
	4	4	4	4	**4**	4	4	4	4					
		5	5	**5**	5	5								
			6	6	6	6								
				7	7									

have been recognized. They were called actinides.

A very important step in the processes of the identification and separation of new elements, was the use of a cation exchange resin with ammonium citrate solution as eluting agent. Later, α-hydroxi-isobutyrate was used as chelating agent. It was stated that the elution positions of the transcurium elements should be analogous to those of the transgadolinium elements in the ion-exchange column.

Table 3: Electronic configuration of the *4f* and *5f* elements (Bagnall 1972)

Xe core		**Rn core**	
La	$5d6s^2$	Ac	$6d7s^2$
Ce	$4f\,5d6s^2$	Th	$6d^27s2$
Pr	$4f^36s^2$	Pa	$5f^26d7s^2$ *or* $5f^26d7s^2$
Nd	$4f^46s^2$	U	$5f^36d7s^2$
Pm	$4f^56s^2$	Np	$5f^46d7s^2$ or $5f^57s^2$
Sm	$4f^66s^2$	Pu	$5f^67s^2$
Eu	$4f^76s^2$	Am	$5f^77s^2$
Gd	$4f^75d6s^2$	Cm	$5f^76d7s^2$
Tb	$4f^96s^2$	Bk	$5f^97s^2$ or $5f^86d7s^2$
Dy	$4f^{10}6s^2$	Cf	$5f^{10}7s^2$
Ho	$4f^{11}6s^2$	Es	$5f^{11}7s^2$
Er	$4f^{12}6s^2$	Fm	$5f^{12}7s^2$
Tm	$4f^{13}6s^2$	Md	$5f^{13}7s^2$
Yb	$4f^{14}6s^2$	No	$5f^{14}7s^2$
Lu	$4f^{14}5d6s^2$	Lr	$5f^{14}6d7s^2$

This was based on the relative changes in ionic radii which determine the relative separations in the ion-exchange adsorption method (Seaborg, 1964).

The (III) oxidation state is predominant in the actinide series, beginning with americium (Katz *et al.* 1986). The lighter actinides (Th to Pu) however, exhibit the property of oxidation to higher states with much greater ease than the heavier actinides and than their corresponding elements in the rare earths series (Tab. 2).

The most important reason for the formation of the large number of oxidation states among the first elements of the series, is the presence of the 6d and 5f electrons. As it can be seen in Tab. 3, in the actinides series from plutonium onwards, the elements generally have reciprocal electronic configurations as their lanthanide analogues, whereas the earlier members retain some d electrons in their ground state configuration.

The *5f* electrons are more delocalized as the *4f* electrons. An important aspect of this consideration is the fact that the *5f* and *6d* shells of these elements lie so close together, that the energy necessary for the shift from one shell to the other is in some cases within the energy of chemical binding energies (Seaborg, 1964) resulting in a much more complicated chemistry of the actinides. An unique effect is observed in the actinide series with the atomic volumes, due to the delocalization of the *f* electrons in the beginning of the series. Fig. 7 presents the changes of the atomic volume with the increasing number of *f* electrons in the actinide series. In actinides, one would expect the volume per atom to decrease linearly until curium. Instead, in the beginning of the actinides, there is a U shaped decrease until Pu which is typical for a d-transition element series. Then, between plutonium and americium the volume suddenly increases and then decreases slowly (Albers, 2001). The lighter actinides exhibit a typical *d* electronic level

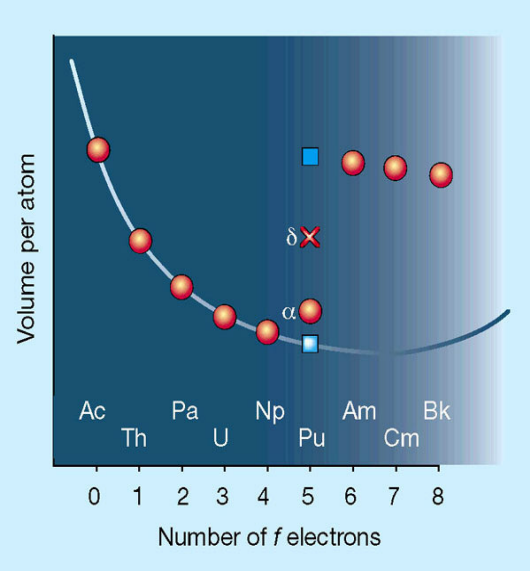

Figure 7: The changes in atomic volume of actinides with increasing atomic number (Albers, 2001)

behaviour, whereas the elements from americium upwards present similar properties as their analogues from the rare earths series. The same sequence of changes in the ionic radius is encountered on filling in the 5f electrons as occurs on

filling the 4f shell (lanthanide contraction) at the elements after americium.

Plutonium is one of the most complicated elements from the actinide group, due to the positioning of its outer f electrons at the border between localized and delocalized. Their position can be influenced by outer parameters like temperature and pressure (Albers, 2001). Further properties of this unique element are presented in the next chapter.

2.1. Plutonium, physical and chemical properties

2. 1. 1. Generalities

Plutonium, the element with the atomic number 94, was named after the planet Pluto (Seaborg *et al*., 1946). The metal exhibits six allotropic modifications having various crystalline structures. The densities of these vary from 16.00 to 19.86 g/cm^3 (Lide, 1998). It is a heavy metal, and in solid state has a silvery appearance when freshly cut, but it takes rapidly a yellow tarnish in air due to the oxidation (Bagnall, 1972), (IAEA, 1998).

Table 4: Half-life, mode of decay, and α energies of the most important plutonium isotopes (Pfenning, *et al*. 1998)

Isotope	$T_{1/2}$	Decay mode	Decay energy [MeV]	Rate
236	2.858 a	α	5.768	69.26
			5.721	30.56
238	87.74 a	α	5.499	70.91
			5.456	28.98
239	2.411 * 10^4 a	α	5.157	73.3
			5.144	15.1
			5.106	11.5
240	6563 a	α	5.168	72.8
			5.124	27.1
241	14.35 a	ß-		
242	3.733 * 10^5 a	α	4.901	77.5
			4.856	22.4
244	8.08 * 10^7 a	α	4.589	80.6
			4.546	19.4

It is pyrophoric at increased temperature, it starts burning at around 500 °C when in a massive metal form, and at 150-200 °C when it is in a powder form (IAEA, 1998). It has the melting point at around 640 °C, and boiling point at around 3220 °C (Holleman *et al.*, 1987).

All the known isotopes of plutonium are radioactive. The decay modes, the half-lives, and the typical decay energies of the most important isotopes are presented in Tab. 4.

The decay processes and the nuclear reactions of the most important isotopes, that occur in a nuclear reactor, are presented in Fig.1.

By far the most important isotope of plutonium is ^{239}Pu. It has a high cross section for fission with slow neutrons, and it serves thus as a nuclear fuel and as explosive charge in nuclear weapons (Katz, *et al.* 1986). The critical mass of a bare sphere of plutonium-239 metal is about 10 kilograms. It can be considerably lowered in various ways (IEER, 1992).

The electronic configuration of plutonium is presented in Tab. 3.

As mentioned before, plutonium is an interesting case to study, because its outer *f* electrons sit at the border between delocalized and localized, and can be driven one way or the other by changes in temperature and pressure. According to Savrasov (2001), in a plutonium atom, temperature changes can lead to an expansion of the atomic lattice, so that it undergoes a 25% increase in volume when the temperature changes from room temperature to about 600 K. Also, according to Savrasov, there are more than the two alternatives for the *f* electrons, localized or delocalized, as he explains that plutonium undergoes an intermediate transition that is only partly localized. This behaviour is unexpected and different from the one of the other actinides.

2. 1. 2. Plutonium in nature

The amount of natural plutonium is very small due to the fact that its half-life is much shorter than the age of the Earth. It can be stated that all the plutonium existing today is of anthropogenic origin. Only traces of natural plutonium can be found in nature.

The presence of plutonium in uranium of natural origin was established for the first time by G. T. Seaborg *et al.* (1948), (Garner, et al. 1948). They found alpha activity presumably from ^{239}Pu in uranium ores specifically the Canadian "Pitchblende" and the Colorado "Carnotite".

The actual global inventory for plutonium is very high, due to its artificial production in nuclear reactors for further use as nuclear fuel, or for nuclear weapons. It is therefore present in the environment mainly as a result of global fallout from the nuclear weapon tests, or by accidental release (Hardy *et al.*, 1973), (Hotzl *et al.*, 1983), (Jennings *et al.*, 1985), (Montero *et al.*, 2001). In 1998 the IAEA posted that around 4000 kg of plutonium (of which ≈ 3250 kg ^{239}Pu, ≈ 600 kg ^{240}Pu, and ≈ 100kg ^{242}Pu) were present in the atmosphere as a result of nuclear weapon tests, followed by ≈ 300 kg (mostly ^{239}Pu) originating from the civil reprocessing plants, and ≈ 15 kg ^{239}Pu/^{240}Pu from the Chernobyl accident. There were reported some other lower amounts of other isotopes like ^{238}Pu (0.9 kg) originating from the SNAP satellite accident in 1964. The most common isotopes of plutonium in environment are ^{239}Pu and ^{240}Pu.

Tab. 5 summarizes some of the typical concentrations of plutonium in soil samples (Watters et al., 1980), ocean (Baxter et al., 1995), and sweet water (Warneke et al., 2002). The fact that plutonium dissolves slowly in water explains its low concentration in the ocean, although most of the fall out dust fell in the oceans (Voelz *et al.*, 2000). Besides this, plutonium was introduced in the oceans by the nuclear powered submarines sunken after various accidents (Oughton *et al.*, 2004), (Baxter *et al.*, 1995).

Table 5: Typical concentrations of plutonium in the environment.

Source	Amount Pu [g/g]
Soil	* 15 ● 10^{-14}
Ocean	3 ● 10^{-18}
Sweet water	10^{-18} – 10^{-16}

* mean value

Although the concentrations of plutonium in environment are reduced, a high risk is associated with the incorporation of it, as it is considered as a toxic element (Cohen et al., 1989).

When plutonium enters the environment, the chemical interactions are complex because, in addition to natural waters, a vast amount of chemically active compounds and minerals exist in earth formations. Precipitation and dissolution of plutonium-bearing solids limit its concentration in solution.

It was long debated whether the low amounts of plutonium found under normal conditions in the environment are dangerous or not. It is known that plants absorb low levels of plutonium, but these levels are not high enough to cause bio magnification of plutonium up into the food chain, or accumulation in the bodies of animals (Delaney *et al.*, 1979). Further effects of plutonium on living beings will be discussed in the next paragraph.

2. 1. 3. Plutonium toxicity

As mentioned before, plutonium is considered as a very toxic element.

Besides the typical heavy metal toxicity, plutonium exhibits the radio-toxicity. To describe this, it can be posted that an α- particle emitted by a ^{239}Pu atom, travelling with a speed of about 1.5 x 10^7 m/s, can deposit its energy by ionizing the molecules or collide with molecules from the living tissues and break those molecules apart. The α- particles travel 3 to 5 centimetres in air and about 30 micrometers in living tissues as shown in Fig. 8.

The outer layer of intact skin would be able to block the passage of α- particles. It can be therefore posted that alpha emitters like plutonium are hazardous to human health only when they are inhaled, ingested or incorporated.

No human has ever died from acute toxicity due to plutonium uptake,(Voelz *et al.*, 2000) so the lethal doses could have been only estimated from the research on animals.

Assuming that animal (dogs) dose also apply to humans, the lethal dosis (LD) would be ≈ 0.32 mg Pu/kg body weight.

The most likely way for plutonium to enter the body is by inhalation of dust particles containing the element. According to the International Commission on Radiation Protection (ICRP, 1988), about 25% of the inhaled particles of the size 0.5 – 5 μm in diameter, deposit in the lungs and 5% gets into bones and an equal amount collects in the liver. This is the most dangerous way of incorporation as it is the easiest of all.

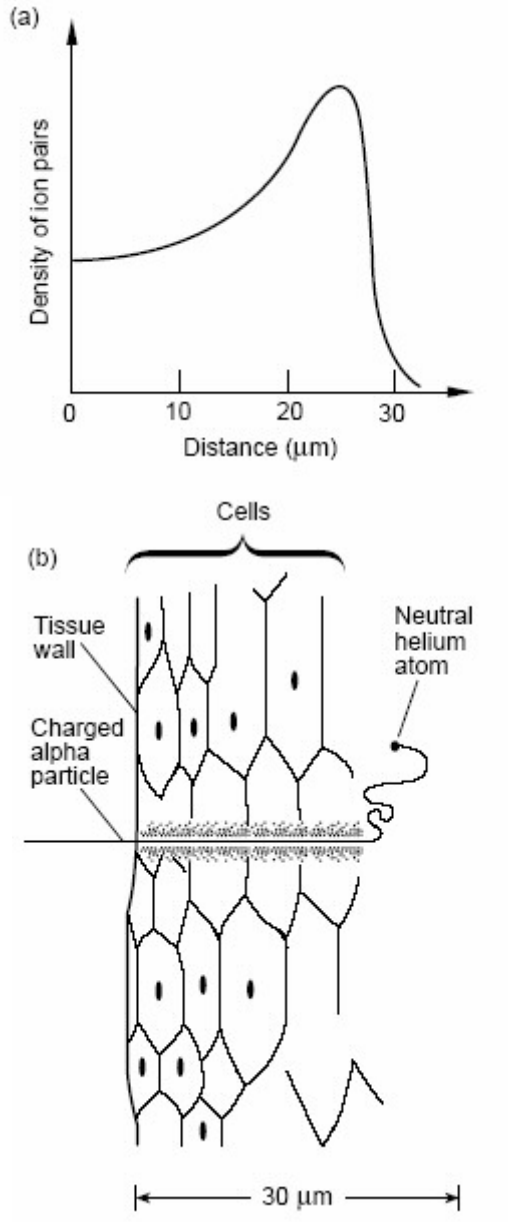

Figure 8: The ionizing path of alpha particles in a living tissue (Voelz et al. 2000).

The ingested plutonium is assimilated at an even lower rate, about 0.05 % of the soluble plutonium compounds and 0.001 % of the insoluble ones enter the blood stream (Voelz *et al.*, 2000).

Unlike in the case of inhalation and ingestion, in the case of incorporation of plutonium, like for example by absorption through skin cuts, up to 100% of the amount can be retained by the body (Hecker *et al.*, 2000).

Once in the blood stream, plutonium would deposit ≈ 50% in bones, ≈ 30% in the liver and ≈ 20% in other tissues (BfS, Internet site).

Longer exposure to plutonium is correlated with an increased risk for lung cancer (Tokarskaya *et al.*, 1997), (Koshurnikova *et al.*, 1998), liver cancer, bone cancer, and leukaemia (BfS, Internet site). The mortality rate was found to increase linearly with the dose of plutonium exposure and at a dose of 25 Sv, it has risen to 11 times the normal rate (Koshurnikova *et al.*, 1998).

However, in spite of the large number of cases investigated, in the case of persons exposed to high-level amounts of plutonium at the Mayak Plant in the former Soviet Union, the authors did not come to the same conclusions with respect to the dependency of the lung cancer risk on the exposure doses (Koshurnikova *et al.*, 1998), (Tokarskaya *et al.*, 1997).

2. 1. 4. Plutonium chemistry

The complex chemistry of plutonium is controlled by its electronic structure. As mentioned in the section above, the lowest energy configuration of the valence electrons is $5f^6 7s^2$, but the energy levels of the 6d and 5f orbital are very close, and a second electronic configuration, *i.e.* $5f^5 6d 7s^2$ can occur in competition to the first one.

Plutonium is an electropositive atom and therefore, it will lose easily between three to seven of its outer electrons, when in an aqueous solution, and will form positively charged cations.

Figure 9: The characteristic colours for the five oxidation states of plutonium

Five oxidation states are known for plutonium, each one of them with a characteristic colour in solution and each exhibits a distinctive spectral absorption (see Fig. 9).

Much of the chemical behaviour of plutonium depends on its oxidation state. Plutonium is the only element in the periodic table that can be present in aqueous solutions simultaneously in four oxidation states (Clark, 2000). The oxidation states from Pu(III) to Pu(VI) are the most common found in aqueous solutions.

Under noncomplexing acidic conditions (such as perchloric acid), both Pu(III) and Pu(IV) exist as the simple hydrated (or aquo) ions. Water molecules are coordinated around the metal ion, resulting in the molecular cations $Pu(H_2O)_n^{3+}$ and $Pu(H_2O)_n^{4+}$, where n varies depending on the concentration of other ions (the ionic strength). Common values for n are 8, 9, and 10. Pu(V) and Pu(VI) are so electropositive that they can strip in acid aqueous solutions oxygen from the water molecules to form PuO_2^+ and PuO_2^{2+} ions, respectively (Clark, 2000).The redox potentials that couple the four common oxidation states in acid solution (III, IV, V, and VI) are all remarkably similar, and approximately equal to 1.0 volt (Katz et al. 1986) as shown in Fig. 10.

As a result of the small differences in the redox potentials, the nature of the oxidation states can change very rapidly in aqueous solutions. Plutonium cations have a strong tendency to react with ions of their own kind. Disproportionation reactions, in which two or more ions in the same oxidation state are simultaneously oxidised and reduced, and reproportionation reactions when, under some conditions, two ions are simultaneously oxidized and reduced to form two ions of the same oxidation state, can take place in solutions. The reactions describing the processes are given in Fig. 11 (Clark, 2000). Lately there were discussed on the other hand, results that do not sustain the disproportionation of Pu(IV) to Pu(III) and Pu(V) (Walther, et al. 2005).

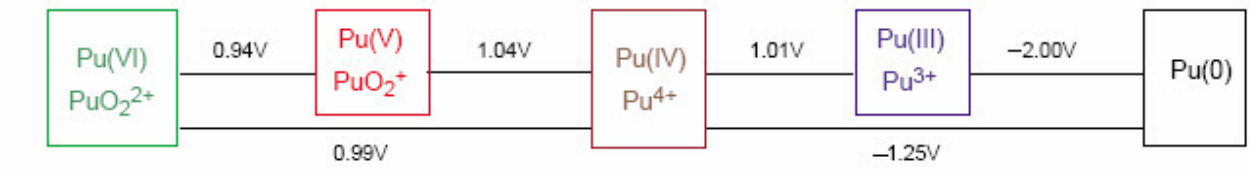

Figure 10: Redox potentials for plutonium aquo ions in 1 M $HClO_4$, and the potential difference between them and the metallic plutonium.

$$2Pu^{4+} + 2H_2O \Leftrightarrow Pu^{3+} + PuO_2^+ + 4H^+ (3)$$
$$Pu^{4+} + PuO_2^+ \Leftrightarrow 2Pu^{3+} + PuO_2^{2+} (4)$$
$$2PuO_2^+ + 4H^+ \Leftrightarrow Pu^{4+} + PuO_2^+ + 2H_2O (5)$$

Figure 11: The equations governing the redox behaviour of plutonium (after Clark, 2000).

Because there are H^+ ions involved in the equations, it is clear that the pH has a strong effect on the speciation. Moreover, the radiolytic decomposition of water, that could occur as a result of the radioactivity of plutonium, can produce short-lived radicals like $H\cdot$, $O\cdot$, and $HO\cdot$, and radical recombination products like H_2, O_2, and H_2O_2, that could influence further the equilibria (Clark, 2000).

With respect to the behaviour of plutonium under environmental conditions, its interactions with compounds found abundant in water, like carbonate, phosphate, sulphate, silicate, organic matter such as humic and fulvic acids, as well as hydroxides, and aluminates are of great interest. The transport of plutonium in the environment can be enhanced by its complexation with ligands.

The tendency of plutonium to form complexes depends on its charge-to-ionic-radius ratio and because the ionic radii of the four common oxidation states are very much similar, the stability of the complex will decrease in the order:

$$Pu^{4+} > Pu^{3+} \approx PuO_2^{2+} > PuO_2^+$$

(Clark, 2000).

The high charge of the Pu^{4+} ions allows them to easily hydrolyse and form multiple species simultaneously, even at low pH values (Walther, *et al.*, 2003), (Bitea, *et al.*, 2002). The generation of Pu(IV) colloids is one of the main processes that complicate the accurate determination of thermodynamic constants for plutonium solutions.

Because of their omnipresence, hydroxide and carbonate ions are the most important ligands that can form complexes with plutonium in the environment.

Carbonate ions are very strongly complexing ions for plutonium thus, by formation of anionic complexes, plutonium can become much more soluble in water. The environmental behaviour of plutonium carbonate complexes depends on their molecular structure and properties.

A schematic speciation of plutonium in natural water as a function of Eh and pH, is given in Runde (2000) (Fig. 12).

In many natural waters, plutonium will be in the Pu(III) and Pu(IV) state. However, redox reactions will allow

plutonium to assume any of the other oxidation states.

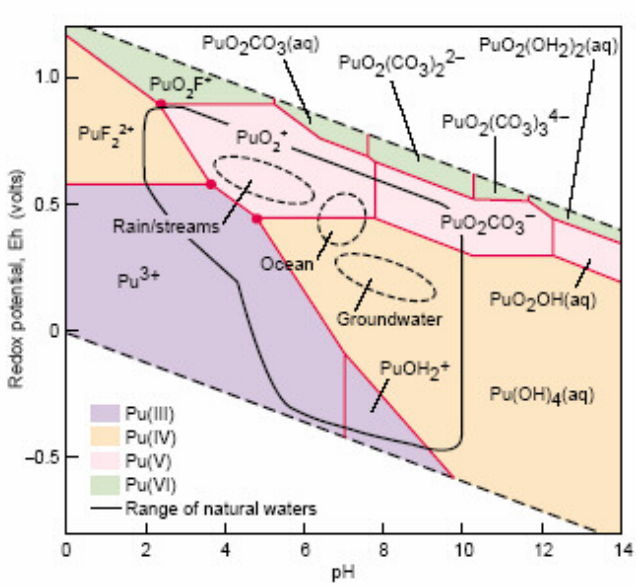

Figure 12: Speciation of plutonium in natural water containing carbonate, hydroxyl, and fluoride ions; [Pu] = 10^{-5} M, ligand concentrations are comparable to those found in natural waters (Runde, 2000).

The range of the Eh and pH values expected in nature are bounded by the solid black line. The red points on Fig. 12 mark conditions under which plutonium can coexist in three oxidation states.

Plutonium manifests a strong tendency to sorb to solid phase surfaces. In this way its transport in the environment could be hindered, by, *e.g.*, adsorption onto rock formations and fixation in this way. The sorption onto mineral surfaces depends on many factors, such as the speciation, the composition of the rock, pH, and others.

It can be concluded that the chemistry of plutonium is a very complex one, and intensive research must be still performed in order to understand and predict the behaviour of this element.

3. Environmental compounds

The most likely possibility for an environmental contamination with radioactive substances originating from a nuclear waste repository, is their disposal into the aquifer.

Ground waters are extremely complex systems containing a large variety of organic and inorganic matter dissolved or in suspension. To simplify matters in this study, only the influence of humic substances under aerobic and anaerobic conditions on the migration of plutonium in the aquifer, will be studied.

Clay minerals are taken as a geological barrier. These minerals are rather complex with respect to structural and chemical characteristics. In the frame of the project "*Migration von Actiniden im System Ton, Huminstoff, Aquifer*" (Migration of Actinides in the System Clay, Humic Substances, Aquifer), kaolinite was chosen as a model for the clay minerals due to its relative simplicity in comparison with other minerals and because its physical and chemical properties are very well characterised (Murray, *et al*., 1993), (Puukko, *et al*. 2003).

3.1. Humic substances

Humic substances are ubiquitous organic compounds in the aquifer. They are found in concentrations in orders of *(ppm)* in ground waters (Stevenson, 1982). Formed by the decomposition of the biomass, they have high molecular weight, and are heterogeneous organic materials. They are found typically in the size range of 1 nm to several hundred nm depending on their source and solution conditions (Lead, et al., 2000), (Bryan et al., 2001). No precise data are available concerning the structure of humic substances.

They are potentially important in the binding and bioavailability of trace metals and trace organic pollutants because of the large surface area and the strength of complexation and binding (Redwood, *et al.* 2005).

By humic coating the surface, electrostatic properties of minerals are affected, the biodegradability of the natural organic matter is decreased, and the partitioning behaviour of non-polar organic contaminants between the dissolved and adsorbed phase is affected (Barbot *et al*., 2002)

Humic substances are known to interact with metal ions, inorganic and organic species, affecting their speciation and their mobility in the environment. Because of their strong tendency towards forming complexes, and colloid generation, humic substances can enhance the mobility of radionuclides in water (Chopin, 1988).

The humic substances can be classified in three groups, based on their chemical and physical properties.

Humic acids consist of the fraction of humic substances that is not soluble in water under acidic conditions (pH < 3). They are the major extractable component of soil humic substances. *Fulvic acids* are the fraction of humic substances that is soluble in water over the entire pH range and the *humin* is the fraction that is not soluble in water at any pH value. Of course there are more differences between the three phases.

The main differences between humic acids and fulvic acids are explained by variations in molecular weight, number of functional groups (carboxylic groups, phenolic OH) and extent of polymerization (Stevenson, 1982).

The postulated relationships are depicted in Fig. 13, in which it can be seen that the carbon and the oxygen contents, the acidity, and the degree of polymerization change systematically with increasing molecular weight.

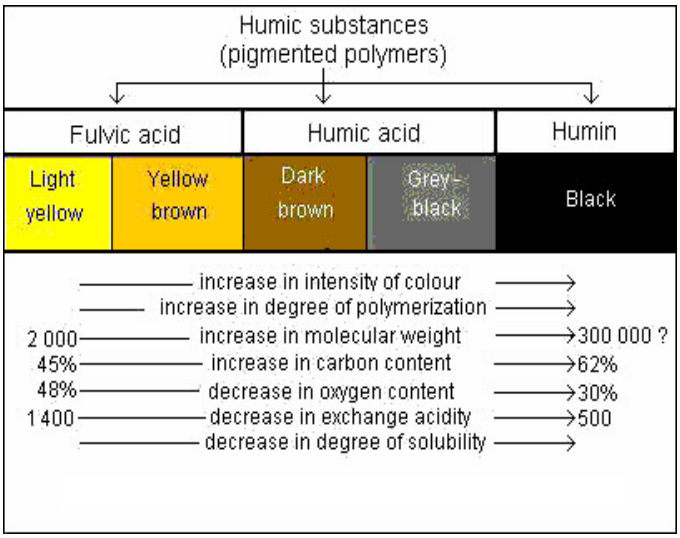

Figure 13: Chemical properties of humic substances (Stevenson, 1982)

The fulvic acids have higher oxygen and lower carbon contents than the high molecular weight humic acids. They also contain more functional groups of an acidic nature, particularly COOH. An important difference between humic and fulvic acids is the presence of oxygen. While in fulvic acids, oxygen can be more available, being accounted mainly by the functional groups like COOH, OH, C=O, in humic acids, a big part of the oxygen seems to take part in the structural composition of the molecule.

3.1.1. Humic acid

Humic acids are complex aromatic macromolecules with amino acids, amino sugars, peptides, and aliphatic compounds. The hypothetical structure for humic acid as postulated by Stevenson (1982) is shown in Fig. 14.

It can be observed that humic acid contains free and bound phenolic OH groups, quinine structures, nitrogen and oxygen as bridge units and COOH groups bounded to the aromatic rings.

Depending on their origin, the percentage distribution of the components in a humic acid molecule can vary. Tab. 6 presents some typical compositions of various humic acids (Kim *et al.*, 1988).

The functional groups found in humic acid are the carboxylic (-COOH), phenolic OH, ether bridges (R-O-R), methoxy ($-OCH_3$), and amino ($-NH_2$) groups, and heterocyclic nitrogen. The amount of carboxyl and carbonyl groups is about 20% higher compared to that of aliphatic and aromatic groups. This induces a high complexation affinity for metal ions.

The complexation of humic acids with a metal is considered by Kim *et al.* (1996) as a metal ion charge neutralization process. In this model, humic acids work like an ion exchanger. The metal ion occupies therefore the number of proton exchange sites equal to its charge. Therefore, a group of complexing sites is needed to neutralize the charge of a metal.

The redox potential of humic acid is very much dependent on the pH, it varies in the pH range 5.0 – 1.2 from 0.56 V to 0.66 V. The redox potential obtained by extrapolation to pH=0 is E_0 = 0.7 V (Marquardt, 1989).

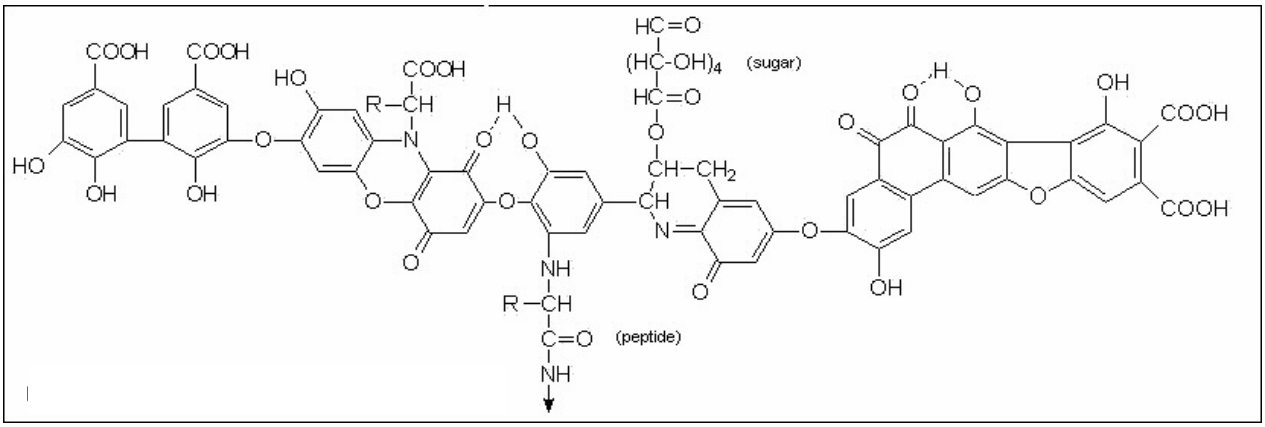

Figure 14: Model structure of humic acid (Stevenson, 1982)

Tabel 6: Elementary composition (in %) of various humic acids.

Element	*Aldrich-HA (Na^+) (1)*	*Aldrich-HA (H^+) (2)*	*Gohy–573-HA(H^+) I(3)*	*Gohy–573-HA(H^+)II (4)*	Boom-Clay *HA(H^+)II (5)*
C	48.93	55.23	56.25	57.32	62.36
H	5.13	4.48	4.52	4.76	6.05
N	0.29	0.32	1.69	1.77	2.94
O	43.4	37.64	35.8	35.72	26.98
S	2.2	2.33	1.73	0.43	1.66

Legend:

(1): original product from company Aldrich

(2): purified Na^+ form

(3): purified humic acid from Gorleben water

(4): a different fraction of purified humic acid from Gorleben water

(5): humic acid from Boom-Clay Belgium

This results in a reduction potential of humic acids for substances in aquatic solutions. Chopin and others have shown that humic substances cause reduction of plutonium or neptunium (Choppin, 1988) , (Jianxin *et al.,* 1993).

A variety of intermolecular forces such as electrostatic interactions, hydrogen bonding, hydrophobic interactions, and chelation with multivalent cations, influence the intermolecular association of humic acids leading to formation of aggregates. This aggregates might carry metals complexed by humic acids, in ground water over long distances.

Humic acids are easily sorbed in acid aquatic solutions on minerals surfaces. When sorbed to mineral surfaces, humic acids may bind and hence immobilize trace metals. They may also alter clay-mineral surface charge properties and the flocculation kinetics (Liang *et al*., 1990).

3. 2. Clay minerals

Clay minerals are basically large aluminosilicates with a layered structure. Each clay mineral has thus, its own unique chemical and physical properties which influence its interaction with species in the environment. A realistic scenario includes more sorts of clay minerals in one deposit, but for simplicity, one model clay mineral, namely kaolinite has been studied.

3.2.1. Kaolinite

Because of the unusual purity of the kaolin deposits from East and South Georgia, USA, large amounts of kaolinite were extracted in order to perform metal-mineral sorption studies, for the safety assessments of nuclear waste repositories. The deposits have very low content of sedimentary features and no fossils, thus a very low amount of organic matter (Moli, 2001).

The kaolinite lot to which the further will refer, was named KGa-1b. It has a white appearance , with a relatively soft hardness. Its chemical composition is $Al_2Si_2O_5(OH)_4$ and its structure is shown in Fig. 15.

The structure of kaolinite is composed of silicate sheets (Si_2O_5) bonded to aluminium oxide/hydroxide layers ($Al_2(OH)_4$) called gibbsite layers. The silicate and gibbsite layers are tighten together only through weak bindings between the silicate/gibbsite paired layers (s-g layers). The weak bonds between these s-g layers cause the cleavage and softness of this mineral.

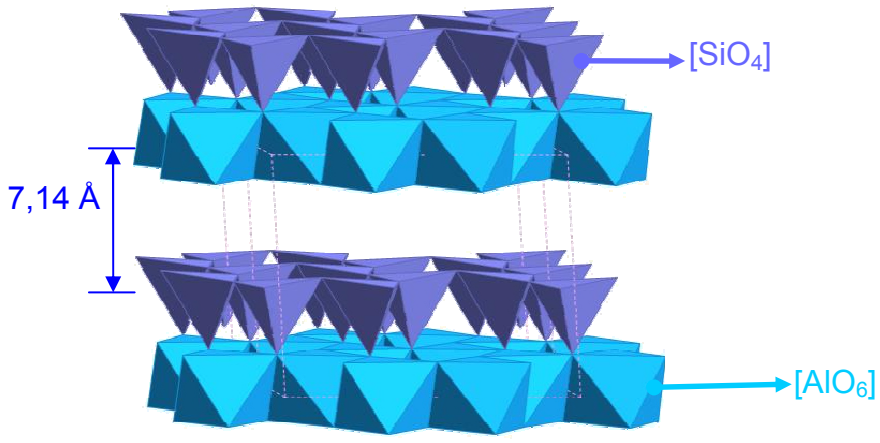

Figure 15: The chemical structure of KGa-1b kaolinite (picture from Amayri, (2006) based on (Drits *et al.*, 1960))

Tab. 7 presents the determined oxides composition of the KGa-1b kaolinite. The contents were determined by flame emission spectrometry and by atomic absorption spectrometry, respectively (Mermut *et al.*, 2001).

The kaolinite is found in large, euhedral, interlocking plates and vermiform crystals and 65 % of the particles are > 2 μm (Moli, 2001). The specific area determined by the BET-N_2 method, is ≈ 11.7 m^2/g (Prutt, 1993).

Tabel 7: Elemental composition of the source mineral kaolinite KGa-1b

Oxide	Amount %
SiO_2	43.36
Al_2O_3	38.58
TiO_2	1.67
P_2O_5	0.37
Fe_2O_3	0.35
Na_2O	0.05
MgO	0.04
CaO	0.04
Ignition loss 110-550 °C	13.60
Ignition loss 110-550 °C	1.45
Total	99.51

The surface properties of kaolinite are of great interest concerning the safety assessments for nuclear waste repositories. These properties affect the wettability, flocculation-dispersion characteristics, ion exchange, sorption capacities, and transport of inorganic substances. It has been proven that the surface properties like sorption or cation exchange capacity of colloidal hydrophilic minerals, can be affected by sorption of organic compounds usually found in water which could render the surface substantially more hydrophobic (Breiner *et al.*, 2006).

The surface of kaolinite presents two different types of charges, a permanent one which is not influenced by changes of the pH, and a nonpermanent one, which is pH dependent (Schoefield et al., 1954), (Cashen, 1959). The permanent one which accounts for the cation exchange capacity (CEC), is developed within the siloxane layer by the isomorphic substitution of Si(IV) with Al(III) or other trivalent cations, in tetrahedral positions (Huertas *et al.*, 1998). Compared to other clay minerals, the CEC for kaolinite is rather low (1-8 mEq/100 g), (Newman *et al.*, 1987). Some authors suggest that the size of the particles (both thickness and diameter) have a strong influence on the CEC (Ma *et al.*, 1999). The CEC for the KGa-1b mineral was established to be between 0.6 and 2.0 mEq/100 g (Schroth *et al.*, 1997).

The relatively low CEC value of kaolinite is attributed to the presence of small amounts of alumino-silicate gel coating (Huertas *et al.*, 1998). Experimental studies have revealed that the exchangeable cations occur mostly on the

edges and on the basal (OH) surfaces of the mineral (Ma *et al.,* 1999).

The permanent charge is minor in comparison to the nonpermanent one. The origin of the nonpermanent charge is the consequence of the acid-base properties of the surface groups located at the edges, and the reactions of these groups with ions present in aqueous solutions. At lower pH values the aluminol groups can undergo protonation contributing thus to the positive charge by formation of surface complexes $>AlOH_2^+$. At higher pH values, both the aluminol as well as the silanol groups can undertake deprotonation forming $>AlO^-$ and $>SiO^-$, respectively, and generating in this way a negative surface charge. In the absence of external ions or ligands sorbtion onto the surface of kaolinite, the only surface reactions are protonation/deprotonation of the surface groups, or H^+/cation exchange at the CEC sites.

At pH < 3 the kaolinite overall surface charge is positive due to deprotonation of aluminol groups or the weak acidic sites of internal hydroxo-aluminium groups, complemented by the strong acidic character of the external hydroxyl groups. From pH > 5.5 the silanol groups which are the least basic ones are becoming charged by deprotonation, inducing a negative surface charge. The aluminium groups deprotonate at higher pH values (pH > 9), complementing hence the negative surface charge.

By balancing the effects of these reactions, the KGa-1b kaolinite reaches the point of zero charge at pH ≈ 5.5 (Huertas *et al.*, 1998).

The point of zero charge (p.z.c.) is defined by IUPAC as a value of the negative logarithm of the activity in the bulk of the charge-determining ions, and it is the point when the surface charge density is zero (IUPAC, 1991).

The intention to use clay minerals as a geological barrier in the path of accidentally released radioactive contaminants from a deep geological formation nuclear waste repository, is being discussed, and arguments pro and contra have been brought into discussion. Further studies of the fixing potential of this materials are presented in this work.

4. Instruments and techniques

4.1. Detection methods for the analysis of plutonium.

Plutonium is found only in trace amounts in nature. Still, even in small concentrations this radionuclide can be dangerous to the biosphere, due to its high toxicity (see chapter 2). Therefore, as a precaution, its presence in the environment is constantly monitored. Extremely sensitive analyses are necessary for effective measurements of the Pu radionuclides.

Tabel 8: Analytical methods for the detection of plutonium, and their detection limits.

Method	Detection Limit [Atomes]	Detection Limit [g]
α- Spectrometry [a]		
^{239,240}Pu	10^{8}	10^{-14}
^{242}Pu	10^{9}	10^{-13}
^{244}Pu	10^{11}	10^{-11}
NAA/DNAA [b,c]		
^{239}Pu	10^{9}	10^{-13}
^{242}Pu	$10^{10} - 10^{11}$	$10^{-12} – 10^{-13}$
^{244}Pu	$10^{11} - 10^{12}$	$10^{-11} – 10^{-10}$
AMS [d]		
all isotopes	$10^{5} - 10^{6}$	$10^{-17} – 10^{-16}$
ICP-MS [e,f]		
all isotopes	$10^{7} - 10^{8}$	$10^{-15} – 10^{-14}$
TIMS [g]	10^{8}	10^{-14}
HEC-TIMS [h, i]	$10^{6} - 10^{7}$	$10^{-16} – 10^{-15}$
RIMS [j, k]	$10^{6} - 10^{7}$	$10^{-16} – 10^{-15}$
all isotopes		

NAA/DNAA – Neutron Activation Analysis/Delayed Neutron Activation Analysis

AMS – Accelerator Mass Spectrometry

ICP-MS – Inductively Coupled Plasma – Mass Spectrometry

TIMS – Thermal Ionization Mass Spectrometry

HEC-TIMS – High Efficiency Cavity Thermal Ionization Mass Spectrometry

RIMS – Resonance Ionization - Mass Spectrometry

[a] (Peuser *et al*., 1981), [b] (Perelygin *et al*., 1997), [c] (Hoffman *et al*., 1991), [d] (Winkler *et al*., 2004), [e] (Taylor *et al*., 2003), [f] (Truscott *et al*., 2001), [g] (Dai, *et al*., 2001), [h] (Riciputi *et al*., 2004), [i] (Buerger *et al*., 2006) [j](Grüning *et al*., 2004), [k] (Trautmann *et al*., 2004)

Over the time, radiometric methods and mass spectrometric techniques have mostly been applied for the analysis of radioisotopes. The most relevant techniques and their detection limits are presented in Tab. 8.

The main disadvantages of alpha spectroscopy are the long measuring times, the insufficient selectivity and the back ground problematic. For example the ratio $^{239}Pu/^{240}Pu$ can only be roughly determined, due to the fact that the α-decay energies of these two isotopes lie very close to each other (Tab. 4). The following chapter gives a more detailed description of the method.

4. 1. 1. α - Spectroscopy

Alpha emitting radioisotopes produce alpha particles (or ^4He nuclei) at characteristic energies. The monoenergetic nature of the emitted α-particles allows nuclear structure information to be deduced through spectroscopic measurements.

The α-decay process can be described as:

$$^{A}_{Z}M_{N} \rightarrow {}^{A-4}_{Z-2}D_{N-2} + \alpha \qquad (7)$$

M – mother nuclide

D – daughter nuclide

A particular isotope can emit α-particles of more than one energy channel, if excited states in the daughter nucleus are populated by the decay. The energies of α-decays of the most important plutonium isotopes are summarized in Tab. 4.

The alpha particles loose rapidly energy in materials, so they can be completely stopped by a piece of paper or by the human skin. Any physical medium found between the α-emitter and the detector will slow down the particles thus changing their energy. Therefore, the measurements are conducted in vacuum.

The thickness of a specific medium can be calculated by the shift of the α-energy. For example, the thickness of the titanium layer sputtered onto the RIMS filaments can be calculated with the Bethe–Bloch formula (Herforth *et al*., 1981).

$$-\frac{dE}{dx} = \frac{e^4 z^2}{4\pi\varepsilon_0 m_0 v^2} N_A \rho \frac{Z}{A} \ln\left(\frac{2m_0 v^2}{I}\right) \qquad (8)$$

$$= (0.307\, MeV \cdot cm^2/g)\rho \frac{Z}{A}\frac{c^2}{v^2} \ln\left(\frac{2m_0 v^2}{I}\right) \qquad (9)$$

z – atomic number of α-particle (z=2)

Z – atomic number of the absorber (titanium Z = 22)

A – nuclear mass of the absorber (titanium A = 47.867)

v – relative velocity

N_A – Avogadro number

ρ – density of the absorber (titanium ρ = 4.505 g/cm^3)

m_0 – rest mass of the electrons

I – the medium ionisation energy of the absorber

^{236}Pu is more suited for determining the titanium layer thickness as its decay energy is higher than the one of other plutonium isotopes. The loss of energy for alpha particles of ^{236}Pu (E_α = 5.768 MeV) through a titanium layer is ≈ 207 keV/μm.

The employed detectors are surface detectors from the company ORTEC with a specific surface of 450 mm^2, with an energy resolution < 25 keV at 5.5 MeV and a detection efficiency between 10-15 %.

4. 1. 2. Liquid Scintillation Counting

The (LSC) used in the experiments is a system constructed in our institute. It uses 10 ml of the scintillation cocktail Ultima Gold XR (Packard) for each sample, contained in 20 ml transparent glass vials purchased from Perkin Elmer Company.

The method is relatively fast; depending on the volume of the sample and the specific radioactivity of the nuclide, the typical measuring times can vary from 1 minute to one hour. The detection limit achieved with the method is ≈ 100 mBq.

The method cannot discriminate the energies of the emitted radiation; therefore, for precise determination of the concentration of the analysed solution, good knowledge of the isotopic composition of the samples is crucial.

4. 1. 3. RIMS

The classical mass spectrometric techniques such as TIMS, ICP-MS exhibit also some limitations like isobaric interferences as a result of their elemental unspecific ionization, which could lead to faulty results of the analysis. For example the ICP-MS cannot distinguish between isotopes like ^{238}U and ^{238}Pu or ^{241}Am and ^{241}Pu. In order to avoid this type of interferences, an elaborated sample preparation must be performed including good chemical separation of the elements.

AMS is better suited for this type of measurements. It provides high isotopic selectivity of up to 10^{15} and a good detection limit (10^4 atoms for some elements) (Tuniz *et al.*, 1998). However, this technique has high experimental costs.

Through the elemental selective ionization of RIMS, the isobaric interferences are avoided. Therefore, after it was first proposed in the eighth's decade of the last century by R. V. Ambartzumian and V. S. Letokhov (Ambartzumian and Letokhov, 1972), RIMS became one of the most versatile mass spectrometry methods for the analysis of ultra trace amounts of an element and for the determination of its isotopic ratio. The advantages offered by RIMS can be accounted as:

- high isobaric interference suppression obtained by highly element selective multistep resonant excitation
- high sensitivity obtained through the high ionization efficiency enabled by the high optical cross section, and the efficient ion detection in the mass spectrometer
- an outstanding isotopic selectivity achieved by the combination between the high elemental ionization selectivity with the high mass discrimination of the mass spectrometer

RIMS has found a large number of applications from measuring the ionization energy of actinides (Erdmann *et al.*, 1998), to ultra trace analysis of various elements/isotopes relevant in the nuclear fuel cycle, *i.e.* decay, fission, or activation products. ^{41}Ca (Wendt *et al.*, 2000), $^{89,90}Sr$, ^{99}Tc (Passler *et al.*, 1997) plutonium (Passler *et al.*, 1997) or uranium (Bürger, 2005) have been successfully measured at ultra-trace levels.

In this work the method was applied for trace analysis of plutonium and for the determination of its isotopic composition in environmental samples. In addition it has also been proposed as an alternative detection method for the development of a very sensitive speciation technique (the coupling CE-RIMS). The principle and the feasibility of the coupling technique are presented in chapter 4. 8.

4. 1. 3. 1 Principle of RIMS

The method is based on two main parts:

- the resonant ionization of the atoms
- the detection of the ions in a mass spectrometer

The element-selective ionisation is achieved by exciting the atoms via resonant absorption of laser light in several steps. Various excitation schemes, followed by ionization can be applied, as shown in Fig. 16.

First, the atoms are excited from the ground state or from a thermally populated low-lying state to a high-lying state by one or two resonant photon absorption.

In case (a) the electrons from the outer electronic levels (the valence electrons) are excited to a higher energetic level by absorption of a high energetic UV-photon.

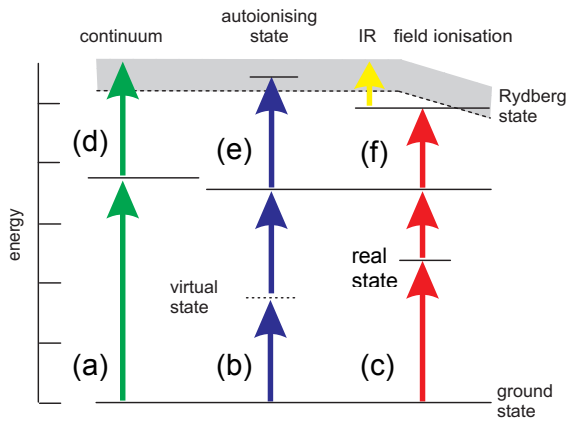

Figure 16: Various possible excitation schemes for resonance ionization of an element.

In case (b) the higher lying level is reached via a virtual intermediate state. In case (c) the high lying state is reached over a real state with the advantage that less laser power is sufficient for getting there and a higher selectivity which is improved by each additional excitation step. The experimental setup becomes however more complicated, as an additional laser must be installed.

Once the high lying state is reached, the atom can be ionized by absorption of an additional photon which can either non-resonantly raise the electron energy beyond the ionization limit to the continuum (d), or resonantly populates an autoionizing state (e). An autoionizing state is an unbound resonance state above the first ionization potential, which decays rapidly by forming an ion and emission of an electron.

An alternative to these ionization schemes is offered by case (f). Here, a high-lying Rydberg state is resonantly populated. The Rydberg state lies just below the ionization potential. From there, ionization can be attained by applying a non resonant IR laser or an electric field.

One of the decisive factors in choosing the ionization scheme are the cross sections of the processes, which can vary over orders of magnitude as shown in Tab. 9.

Tabel 9: Ionization steps of RIMS and their cross sections (Lethokov, 1983)

Type of ionisation	Cross section [cm^2]
Non-resonant	10^{-17} - 10^{-19}
Autoionizing state	$\approx 10^{-15}$
IR-ionization over a Rydberg state	$\approx 10^{-16}$
Electrical field ionization over a Rydberg state	$\approx 10^{-14}$

The extremely high elemental sensitivity of RIMS results from the fact that the density of levels which are accessible via electric dipole transitions in an atom is in the order of ≈ 1/1 eV for the low lying levels (n ≈ 20) with a typical line width of ≈ $7x10^{-8}$ eV (for 10 ns lifetime). Since the bandwidth of a common type of pulsed tunable laser is in the range of 10^{-4} eV, and even lower for a cw laser, the probability of ionising an undesired atomic species is negligible (Trautmann *et al.*, 2004). This probability decreases with increasing number of excitation steps.

Ionization of unwanted atoms or molecules can still occur as a result of non resonant photo-ionization.

The choice of an excitation scheme depends on the required selectivity and sensitivity.

The scheme chosen for the ultra trace analysis of plutonium in environmental samples uses a three step ionization via a Rydberg state with subsequent ionization in an electrical field.

The main advantages of this scheme are its high isotopic selectivity and high ionization efficiency.

The ions obtained by resonant ionization are analysed by a Time-of-Flight mass spectrometer. By optimizing the mass spectrometer, additional background suppression and mass selectivity are obtained.

4. 1. 3. 2. Experimental setup for RIMS

The arrangement of RIMS used in the following experiments is presented in Fig. 17.

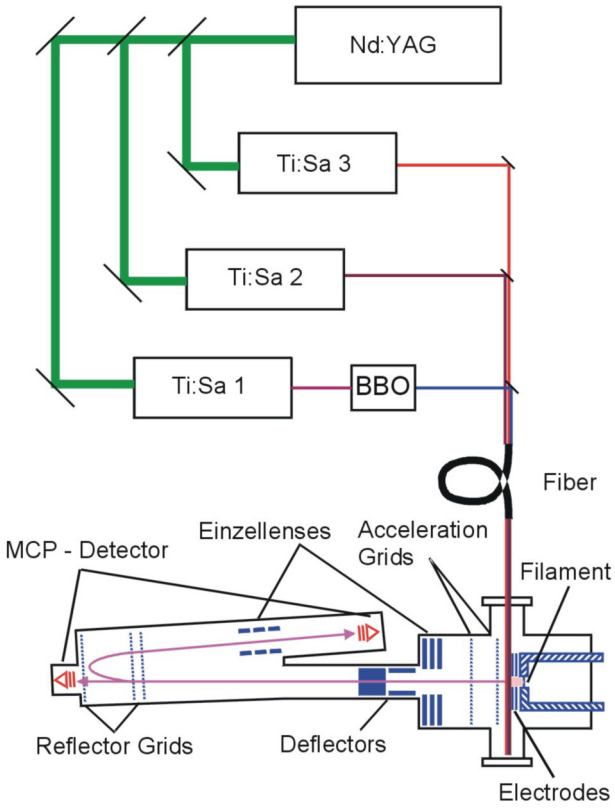

Figure 17: RIMS setup

Two main parts can be identified, namely, the solid state laser system and the mass spectrometer coupled to the ion source area.

The laser system is described in detail by C. Grüning (2001). The following factors were considered for developing the system: sufficient power for saturating all three ionization steps and high enough repetition rate of the pulsed lasers in order to ionize as many plutonium atoms emitted in a continuous mode, as possible.

The ionization energy of plutonium is 6.0258 eV ≡ 48601 cm^{-1} (Grüning, 2001). Therefore, ionization can be achieved in a three step scheme with laser wavelength in the visible range. A very efficient ionization scheme for plutonium is shown in Tab. 10.

Table 10: The wavelengths used in the three step ionization of plutonium

Ionization step	λ [nm]
1	420.76
2	847.28
3	767.53

Fig. 17 presents the setup of the laser system. A high repetition rate (1 – 25 kHz) Q switched and intracavity doubled Nd:YAG pump laser (Clark-MXR ORC-1000) is applied to pump simultaneously three titanium sapphire lasers.

The nominal power of the Nd:YAG laser is 50 W at 532 nm with a pulse length between 200-600 ns. For the typical pulse repetition rate used, 6.6 kHz, the pulse length is 400 ns. Thus , the pulse power is not sufficient for efficiently pumping a Dye laser. It is however, ideally suited for pumping Ti:Sa lasers like those described by Grünning (2001).

The three Ti:Sa lasers are pumped simultaneously by the same pump laser, and for this the pump laser beam is split in

a ratio 1.6:1:1 between the lasers 1, 2, and 3 in that order.

The typical Ti:Sa laser output under these conditions is 1.7 W for laser 1 and ≈ 1 W for lasers 2 and 3. Through a combination of birefringent filters and an etalon, the bandwidth is reduced to 2 – 3 GHz, and the tuneable wavelength range is between 725 nm and 895 nm with a pulse length of 60 -150 ns. The lasers are synchronized with intracavity Pockels cells used as Q-switches.

In order to reach the ionization energy, the frequency of laser 1 is doubled using an external single pass doubling setup with a BBO crystal (ß-BaB_2O_4). The first excitation step requires lower power than the 2nd and 3rd step, thus it can still be saturated despite the loss in power due to the frequency doubling.

For measuring the wavelength of each Ti:Sa laser, a small fraction of the beams is directed to a wave meter (ATOS LM007), and another fraction is sent to a photodiode to control the synchronization of the three lasers pulses by means of an oscilloscope.

The three laser beams are transported with an optical fibre to the interaction region between the laser beams and the sample atomic beam in the TOF apparatus. The overall efficiency of the transport through the optical fibre is > 60% for all three wavelengths.

The construction of the interaction region was carried out by F. J. Urban (1994). Special care was dedicated for designing the interaction region between the atomic beam and the laser beams.

The atomic beam is generated by heating up a filament containing the sample from 900 °C up to 1200 °C, by applying an electrical current of up to 40 A.

The interaction region ensures background suppression through a combination of electrodes. The electrons emitted from the filament are prevented to enter the mass spectrometer, where they could be accelerated and could ionize the rest gas molecules. The background can be produced also by thermally ionized atoms or molecules. For construction of the interaction region, these were also taken into account. The optimization of the parameters is described by Bürger (2005).

4. 1. 3. 3. Filament

A plutonium atomic beam is generated by electrically heating of a filament. Since the plutonium is not deposited in an elemental but rather in the oxide form, a special "sandwich-filament" was developed, which enables an efficient generation of an atomic beam, as shown in Fig. 18 (Eichler *et al*., 1996)

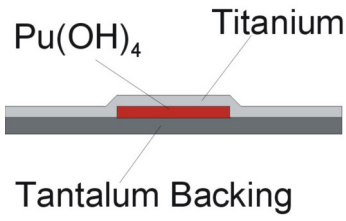

Figure 18: Schematic depiction of a RIMS filament

Plutonium is electrolytically deposited on a tantalum foil as ($Pu(OH)_4$). The filament is then covered by sputtering with a thin titanium layer. Tab. 11 summarizes the properties of the filament. When this filament is heated to 900 – 1200 °C, $Pu(OH)_4$ is deprotonated to plutonium oxide. The plutonium oxide then diffuses through the titanium layer, where it is reduced to the atomic form, and is evaporated from the surface.

Two sputter deposition systems were used for the preparation of Ti layers. The homogeneity, the right thickness, and the purity (titanium oxides on the filaments hinder the reduction of plutonium) of the titanium layer are factors with a strong influence on the overall efficiency of the analysis. A commercial sputtering machine (Baltec, SCD050 Sputter Coater) used for the measurements in the years 2003 and 2004 was replaced due to aging effects, by a home built sputtering system. The operational conditions of the commercial system and the construction and operation of a second home made system are described by Bürger (2005) and Wunderlich (2006).

Table 11: Dimensions of a RIMS filament

Entry	Characteristics
Ta foil	11 x 3.5 mm, 50 µm thick
Electrolysis spot	Ø 3 mm
Ti layer (overcoating)	1 µm thick

The advantage of the metal combination Ti/Ta is the efficient atomization of plutonium correlated with low emission of oxides by evaporation.

A minor part of plutonium is unspecifically ionized on the filament surface and only a small part is found in a thermally populated high-lying state as a result of the relatively low temperature applied (Grüning, 2001).

The thickness of the titanium layer was determined by alpha spectroscopy as described in chapter 4. 1.1.

4. 1. 3. 4. Mass spectrometer

The Time-Of-Flight (TOF) mass spectrometer used in this work was described in several papers, (Urban, 1994), (Erdmann, 1998).

A TOF is able to discriminate particles which are acclerated under the same conditions in vacuum. If the particles have all the same kinetic energy, their flight time through a given distance depends only on their mass, as deduced from equation (10) and (11).

$$E_{Kin} = \frac{1}{2} m v^2 \quad (10) \qquad v = \frac{d}{t} \quad (11)$$

For E_{kin} = const. and d = const.

$$t \cong \sqrt{m} \quad (12)$$

When a pulsed laser system is used for ionization, the ions are not formed continuously but with the frequency of the laser pulses. Therefore, each laser pulse can be considered as a flight start signal and the flight stop signal is given by the ions detection in the multichannel plate detectors (MCP). The synchronization of the laser system is thus very important.

The mass resolution of the TOF employed in our system was $m/\Delta m \approx 600$.

4. 1. 3. 5. Measurements and data processing

Data acquisition and measurement control is performed by a computer. Several steps like the lasers synchronization and wavelengths set up are, however, manually controlled.

In order to verify and quantify the presence of one or more isotopes of plutonium, a known amount of a tracer isotope which is not expected in the sample is introduced in the sample material before the chemical preparations. In the case of environmental sample analysis, the tracer was ^{244}Pu. For determining the plutonium isotopic ratio in the sample, the lasers are at first set on the resonance wavelengths necessary for the ionization of the tracer and the filament is slowly heated to the point when the first tracer ions are detected. Because the laser bandwiths are too narrow in order to equally excite all the isotopes at the same time, the lasers have to be tuned on each isotope individually. Therefore, with the use of a step motor, the wavelengths are changed in so called "jump scans" from the tracer ionization wavelength to the investigated isotope specific ionization wavelengths. The wavelengths for the important isotopes of plutonium are presented in Tab.12.

Table 12: Wavelengths used for the excitation and ionization of all relevant plutonium isotopes

Isotope	λ Laser 1 [cm^{-1}]	λ Laser 2 [cm^{-1}]	λ Laser 3 [cm^{-1}]
^{238}Pu	23766.40	11802.45	13028.80
^{239}Pu	23766.32	11802.52	13028.80
^{240}Pu	23766.16	11802.59	13028.81
^{241}Pu	23766.11	11802.64	13028.79
^{242}Pu	23765.98	11802.72	13028.81
^{244}Pu	23765.75	11802.84	13028.81

The jumps are repeated as long as necessary for obtaining a good counting statistics or until the filament is wasted by evaporating the entire amount of plutonium.

The periods for which the lasers are set on the resonance wavelengths necessary to ionize the tracer or the investigated isotopes respectively, are varied depending on the isotopic composition. For the environmental measurements, where the rate of the investigated isotopes ^{239}Pu and ^{240}Pu was considerably lower than that of ^{244}Pu as tracer, the lasers were set for 4 or 8 seconds on the resonance wavelength of the investigated isotope and 12 or 8 seconds on the resonance wavelength of the tracer. The jumps 4 s (investigated isotope)-12 s (tracer), were used for the water samples which had lower content of plutonium and the jumps 8 – 8 seconds for sludge and soil samples.

The efficiency of the method was calculated as the ratio between the detected ions (N) and the known number of deposited atoms (N_0) as described by eq. (13).

$$\varepsilon = \frac{N}{N_0} \qquad (13)$$

The detection limit is calculated with a 3σ error based on eq. (14).

$$LOD = \frac{3\sqrt{N_{BG}}}{\varepsilon} \qquad (14)$$

LOD –limit of detection

N_{BG} – background registered on the mass spectrum

The data received from the MCP are collected by an electronic system developed in our electronic workshop, and processed by a computer. The softwear sums the signals corresponding to each mass channel and displays them. The resulting peaks are directly proportional to the amount of the respective isotope in the sample. As a result, by calculating the peak areas, normalizing them to the different time periods used for resonant ionizing of the specific isotope, and comparing them to the tracer, the isotopic composition of the atoms in the sample is determined.

4. 1. 3. 6. RIMS for plutonium analysis in environmental samples

Various samples of groundwater, surface water, sludge, and soil were analysed with RIMS in order to determine the amount and the isotopic composition of plutonium. The work was commissioned in collaboration with the *Ministerium für Umwelt und Forsten Rheinland-Pfalz* (Ministry of Environment and Forests Rheinland-Pfalz).

The sampling was performed by workers from the *Landesamt für Wasserwirtschaft* (Regional Authorities for Water Management) and kept in PE vials at pH ≈ 2, in the case of the liquid samples, or as dry samples in PE containers in the case of the sludge and soil samples.

The samples were first chemically treated before production of RIMS filaments in order to remove as much as possible of the sample matrix.

In all cases, 1.4 x 10^{10} atoms of high purity ^{244}Pu were added as tracer to the sample before applying any type of chemical procedure. In order to verify the yield of the preparation process of the filament (chemical yield), a known amount of ^{236}Pu was added. This isotope has a shorter half-life than ^{239}Pu, ^{240}Pu, and ^{244}Pu (see Tab. 4) thus lower amounts can be detected.

For the case of water samples, 500 mL of sample material were mixed with 2 mg of iron ($FeCl_3$) and 5 ml of concentrated HCl. The iron was precipitated with NH_4OH and filtered over a membrane filter. The plutonium precipitated with iron hydroxide remained together with the iron on the filter.

This residue was then dissolved with 20 ml of 8 M HNO_3, reheated and precipitated again with NH_4OH. After the filtration, the residue was dissolved in 4 ml 8 M HNO_3. After adding 4 ml MilliQ water and 4 ml 4 M HNO_3, the solution was passed through a TEVA-SPEC column. Plutonium was fixed as Pu(IV)-nitrate complex while the iron passed through the column. After this, the column was rinsed three times with 4 M HNO_3. Plutonium was then eluted from the column by rinsing it three times with 4 ml 0.5 M HCl. The eluted fraction was concentrated by evaporation, dissolved in $(NH_4)_2SO_4$ and introduced into the electrolysing cell.

The sludge and soil samples are composed of a much more complex matrix; hence, their chemical preparation was more complicated.

Two grams of dried sample material were used for the preparation of a RIMS filament. They were fused with 10 g NaOH and 10 g Na_2O_2 in a Nickel crucible at 600 °C, and then boiled in 200 ml MilliQ water to dissolve the soluble components.

The suspension was then centrifuged and the precipitate was rinsed three times with 2 M NaOH in order to remove more of the soluble components. The residue was dissolved in 8 M HCl and 1.4 x 10^{10} atoms of high purity ^{244}Pu and a known amount of ^{236}Pu were added as tracers, and the iron existing in the probe was precipitated with NH_4OH together with the plutonium. In this way, the soluble Ni amounts from the Nickel crucible were removed by centrifugation for three times and the discarded supernatant was removed. The precipitate was rinsed three times with diluted NH_3, redisolved in 8 M HCl and reprecipitated with NH_4OH. The precipitate was filtered, rinsed three times with MilliQ water, and dissolved in 50 ml 10 M HCl. In order to reduce the unknown amount of iron from the sample, an ether extraction was performed as a next step. After separation, the aqueous solution containing plutonium was precipitated with a known amount of iron (2 mg) with NH_4OH. Plutonium precipitated and after filtration, remained as a hydroxide on the filter. The residue was dissolved in 10 ml 10 M HCl, and by adding ~ 5 drops of concentrated HNO_3 plutonium was oxidized to Pu(IV). This solution was passed through an anion exchange column (DOWEX 1X8 <400 mesh). Plutonium and iron were fixed as anionic chloride complexes. The column was rinsed afterwards four times with 2.5 ml 8 M HCl, and then plutonium was eluted together with iron with four times 5 ml 0.5 M HCl.

The procedure applied further on was similar with that applied for the water samples after the first filtration.

For the preparation of the filaments, the concentrated samples were introduced in a electrodepositing cell with ≈ 6 ml 20 % ammonium sulphate at pH = 1.5. Pu was then electrodeposited at a current of 300 – 360 mA and a voltage of 14-20 V for 90 minutes on a tantalum filament. The electrodeposited spot has a diameter of ≈ 3 millimetres.

The filaments prepared in this way were then measured by alpha spectroscopy for about 24 hours, in order to verify the chemical yield of the separation and deposition, by comparing the amount of ^{236}Pu atoms determined with the known amount that was added to the solution. The chemical yields were 15 – 50 %.

Afterwards, the filaments were covered by sputtering with a titanium layer (≈ 1 μm), as described in (chapter 4. 1. 3. 3).

Before starting the measurements of the environmental samples, the possible cross contamination in the system was verified. For this, a blank sample underwent all the chemical separation.

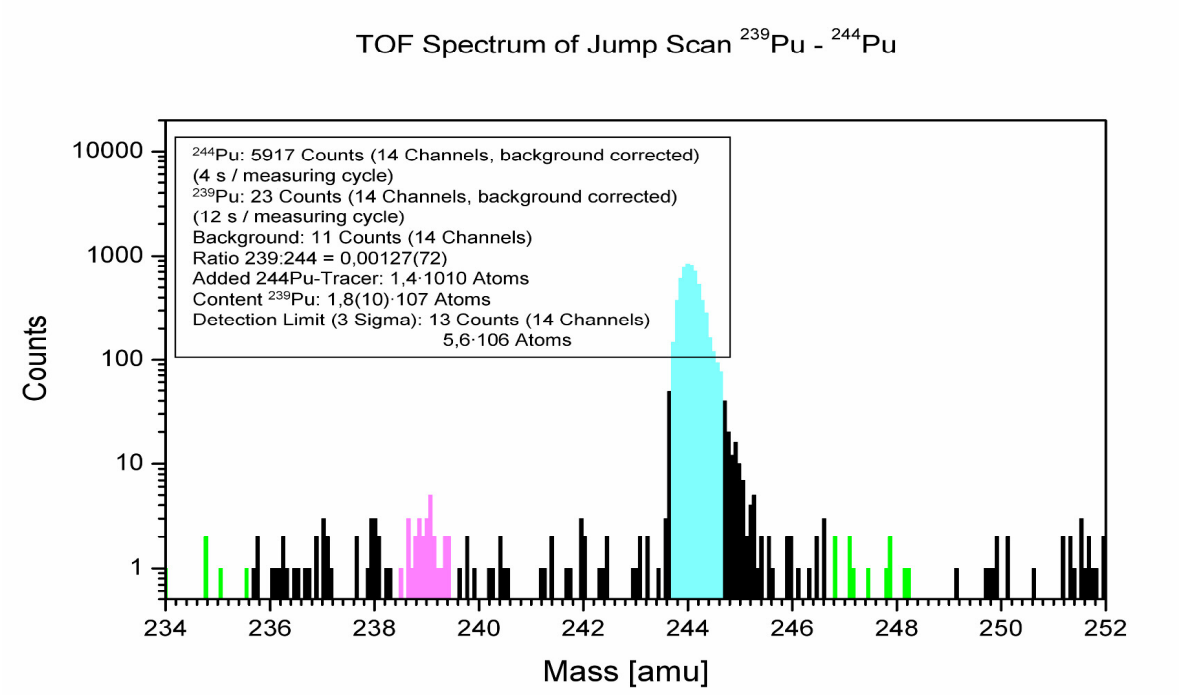

Figure 19: Graphic depiction of a jump scan analysis for plutonium in environmental samples; the blue peak corresponds to the tracer signal, the pink peak to the investigated isotope, and the green markers illustrate the regions used for calculating the background.

steps, in the same vials and using the same solutions which would later be used for the preparation of filaments. This filament was then measured by RIMS in order to detect any traces of contamination. If no contamination was found, the efficiency of the method for all the plutonium isotopes was verified by measuring a filament with known isotopic composition.

When the system was ready for analysis, the environmental samples were measured in duplicate or more. The scans were concentrated on the determination of ^{239}Pu and when it was possible ^{240}Pu, too. Fig. 19 presents an example of the data obtained for measuring an environmental sample. The data obtained for the measurements carried out in the years 2003 and 2004 are summarized by Bürger (2005). It was found that there was an enrichment of the plutonium amount in the sludge samples from big volumes of water.

Tab. 13 presents the data obtained for the measurements carried out in the year 2005 on sludge and soil samples.

The concentrations found for the water samples are presented in comparison with the permitted values after the German laws by Bürger (2005). There were found no limitations for the level of plutonium concentrations in soil samples. The results were compared with concentration permitted for plutonium in food products, by the European Council regulations (Euratom, 1989).

Table 13: The content of ^{239}Pu detected with RIMS in sludge and soil samples in 2005

Sample Form/Number	Chemical yield	Detection limit ^{239}Pu	Content ^{239}Pu/2g sample
Sludge/ 05-0019 I	13.7 %	$6 \cdot 10^6$ atoms	$5.6 \cdot 10^7$ atoms
Sludge/ 05-0019 III	15.1%	$1.2 \cdot 10^7$ atoms	$7.3 \cdot 10^7$ atoms
Sludge/ 05-0050 I	20.8%	$1 \cdot 10^7$ atoms	$9.6 \cdot 10^7$ atoms
Sludge/ 05-0050 II	18.3%	$8.2 \cdot 10^6$ atoms	$6.3 \cdot 10^7$ atoms
Sludge/ 05-0263 I	13.2%	$1.2 \cdot 10^6$ atoms	$6.9 \cdot 10^7$ atoms
Sludge/ 05-0263 II	32.2%	$8.4 \cdot 10^6$ atoms	$5.3 \cdot 10^7$ atoms
Sludge/ 05-0278 I	14.9%	$3.4 \cdot 10^7$ atoms	$5 \cdot 10^7$ atoms
Sludge/ 05-0278 II	22.6%	$7.2 \cdot 10^6$ atoms	$6 \cdot 10^7$ atoms
Soil/ U3040 I	28.3%	$1 \cdot 10^7$ atoms	$1.1 \cdot 10^8$ atoms
Soil/ U3040 II	14.6%	$4 \cdot 10^7$ atoms	$1.5 \cdot 10^8$ atoms
Soil/ U3041 I	25.8%	$8 \cdot 10^6$ atoms	$1.3 \cdot 10^8$ atoms
Soil/ U3075 I	29.6%	$6 \cdot 10^6$ atoms	$1 \cdot 10^8$ atoms
Soil/ U3129 I	19.3 %	$2 \cdot 10^7$ atoms	$4.9 \cdot 10^8$ atoms
Soil/ U3130 I	-	$2 \cdot 10^7$ atoms	$1.4 \cdot 10^8$ atoms

It can be observed that the concentration of plutonium found in soil is even lower than the concentration permitted by the European Council regulations in food products. The assimilation of plutonium by leaving beings from soil is less likely to be higher than from food, so it can be concluded that these concentrations of plutonium in soil are not dangerous.

Table 14: Content of ^{239}Pu determined by RIMS in environmental samples from Germany, compared with the legally permitted values

Entrance	Plutonium content	
	Atoms/g	µBq/g
Sludge samples 2003	$(3.7 – 28)\ 10^7$	34 – 260 (^{239}Pu)
Sludge samples 2004	$\leq 5.1\ 10^7$	≤ 47 (^{239}Pu)
Sludge samples 2005	$(2.5 – 4.8) \cdot 10^7$	23 – 44 (^{239}Pu)
Soil samples 2005	$(5 – 7.5) \cdot 10^7$	46 – 69 (^{239}Pu)
Permitted levels in food (Euratom, 1989)		≈ 80 000 (Pu)

4. 2. Preparation of plutonium oxidation states by electrolysis

For the preparation of the requested oxidation states of plutonium, electrolysis of plutonium solution in 1 M $HClO_4$ was applied. The arrangement is presented in Fig. 20.

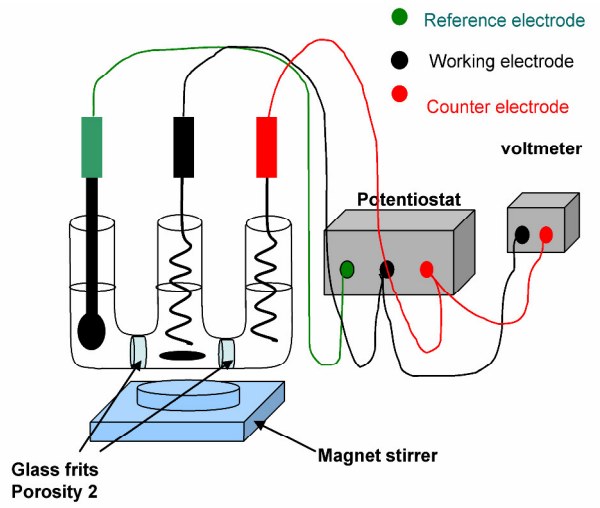

Figure 20: Setup of the electrolysing cell used for the preparation of different oxidation states of plutonium

The working and counter electrodes were constructed of a platinum spiral. Connecting an additional Pt net to the electrodes has substantially decreased the periods necessary for a complete electrolytic conversion to the desired oxidation state.

The cells were separated from each other by glass frits of porosity 2. The voltages were set by the power supply as described in Tab. 15, and the potentials monitored with a voltmeter.

The sample intended for electrolysis was introduced in the middle cell in concentrations relatively high, because the verification of the obtained species was performed afterwards with UV/VIS, which has relatively high detection limits for plutonium. Additionally, there was also observed a slight dilution of the solutions as a result of diffusion of plutonium through the glass frits.

The conditions for the electrolysis were selected from Cohen (1961) and are summarized in Tab.15.

Table 15: Conditions for the electrolytic preparation of the four oxidations states of plutonium

Intended ox. state	Starting ox. state	Working electrode	Potential (V)
Pu(III)	Pu(IV)	Cathode	*-0.1 - - 0.2*
Pu(III)	Pu(VI)	Cathode	*-0.6*
Pu(IV)	Pu(III)	Anode	*-1.3 - -1.4*
Pu(V)	Pu(VI)	Cathode	*-0.9*
Pu(VI)	Pu(III)	Anode	*-1.95*

4. 3. Speciation methods for plutonium

4. 3. 1. UV/VIS Spectroscopy

For the determination of the oxidation state of plutonium in the solutions that would be used later in the experiments, we made use of its spectral properties. UV/VIS spectroscopy was used in order to verify the composition of solutions with higher concentrations of plutonium. Fig. 21 presents the typical electronic absorption spectra for all known oxidation states of plutonium. The aquo ions were contained in a 1 M solution of perchlorate ($HClO_4$).

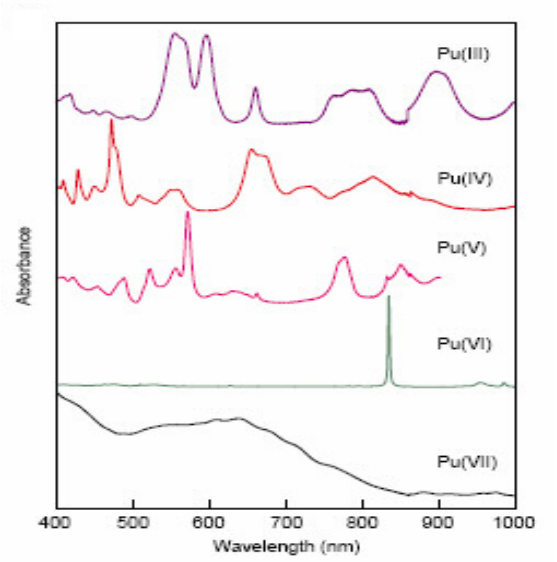

Figure 21: Electronic absorption spectra of plutonium aquo ions; Pu(VII) is a rare species but it can be formed under alkaline solutions (Clark, 2000).

It can be observed that each oxidation state can be identified by its characteristic absorption fingerprint. The advantages of this method are its fastness, the low operation costs, and the fact that all oxidation states can be determined.

The disadvantages of this method are the relatively high detection limit, and the fact that for solutions containing more than just one oxidation state, the absorption spectra can overlap and it can become unclear which species is responsible for the registered signal (*e.g.* Pu(III) overlapping traces of Pu(V)).

The UV/VIS spectroscopy was used as well for quantifying the humic and fulvic acids in aqueous solutions. Fig. 22 presents a typical absorption spectrum of Aldrich humic acid. The quantification is possible by comparing the light absorption at a certain wavelength (310 nm in this case), of the investigated solution with the one of solutions with known concentrations.

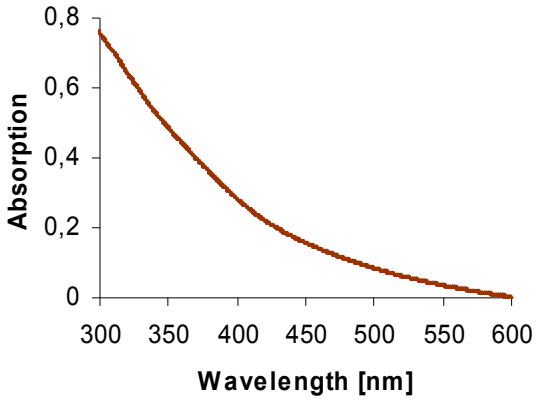

Figure 22: Absorption spectrum of Aldrich humic acid between 300 and 600 nm; [Aldrich humic acid] = 25 mg/L, in 0.1 M $NaClO_4$.

In this work, a high resolution UV/VIS spectrometer Cary 50 from Varian, USA was used. The samples were analysed using 10 mm thick, quartz or polystyrene cuvettes.

4. 3. 2. Liquid-liquid extraction

The extraction with different organic compounds hase been intensively used in the separation of actinides (Keller, 1971), (Nitsche, 1996). The speciation of plutonium is also possible by means of liquid-liquid extraction (Neu *et al.*, 1994). In this work, chemical extraction was used in combination with liquid scintillation counting (LSC) in order to monitor the redox behaviour of plutonium in aqueous solutions. Several extraction steps are needed for a complete characterization of the redox composition of a plutonium solution. In our work, we used as extracting agents a solution of 0.025 M 4-benzoyl-3-methyl-1-phenyl-2-pyrazolin-5-one (PMBP) (from Aldrich, in 99% purity) diluted in xylene and a solution of 0.5 M di(2-ethylhexyl) orthophosphoric acid (HDEHP) (Aldrich) diluted in toluene.

For the experiments, 1 M HCl was prepared by diluting analytical reagent grade concentrated HCl (Merck , Darmstadt, Germany). A solution of 0.02 M $K_2Cr_2O_7$ was prepared by dissolving the solid crystals (Aldrich, 99.5% purity) in 1 M HCl. The four extractions were carried out independently as indicated in Fig. 23. The extraction experiments were carried out in less than 30 minutes in order to avoid further redox reactions due to the acidic character of the solutions.

The extractions were performed using 400 µl of 1 M HCl and 400 µL 0.02 M $K_2Cr_2O_7$ disolved in 1 M HCl for the steps 1 and 3, respectively 2 and 4. This will be referred to further on as the aqueous phase. To each of these solutions, 200 µl of the samples to be analysed were added. Then, 100 µl of the mixture was taken out and transferred in individual vials containing 10 ml of LSC cocktail, and the activity was determined. These samples were used as reference. Afterwards the solutions were mixed with the extraction agents (solutions 1 and 2 with 0.025 M PMBP diluted in xylene, and solutions 3 and 4 with 0.5 M HDEHP diluted in toluene. This second phase will be referred to further on as the organic phase. Each biphasic solution was mixed vigorously for 2 minutes using a test tube shaker REAX top, (VWR International, Belgium), to allow for a good contact between phases. The solutions were then centrifuged for about 1 minute at 2500 rpm.

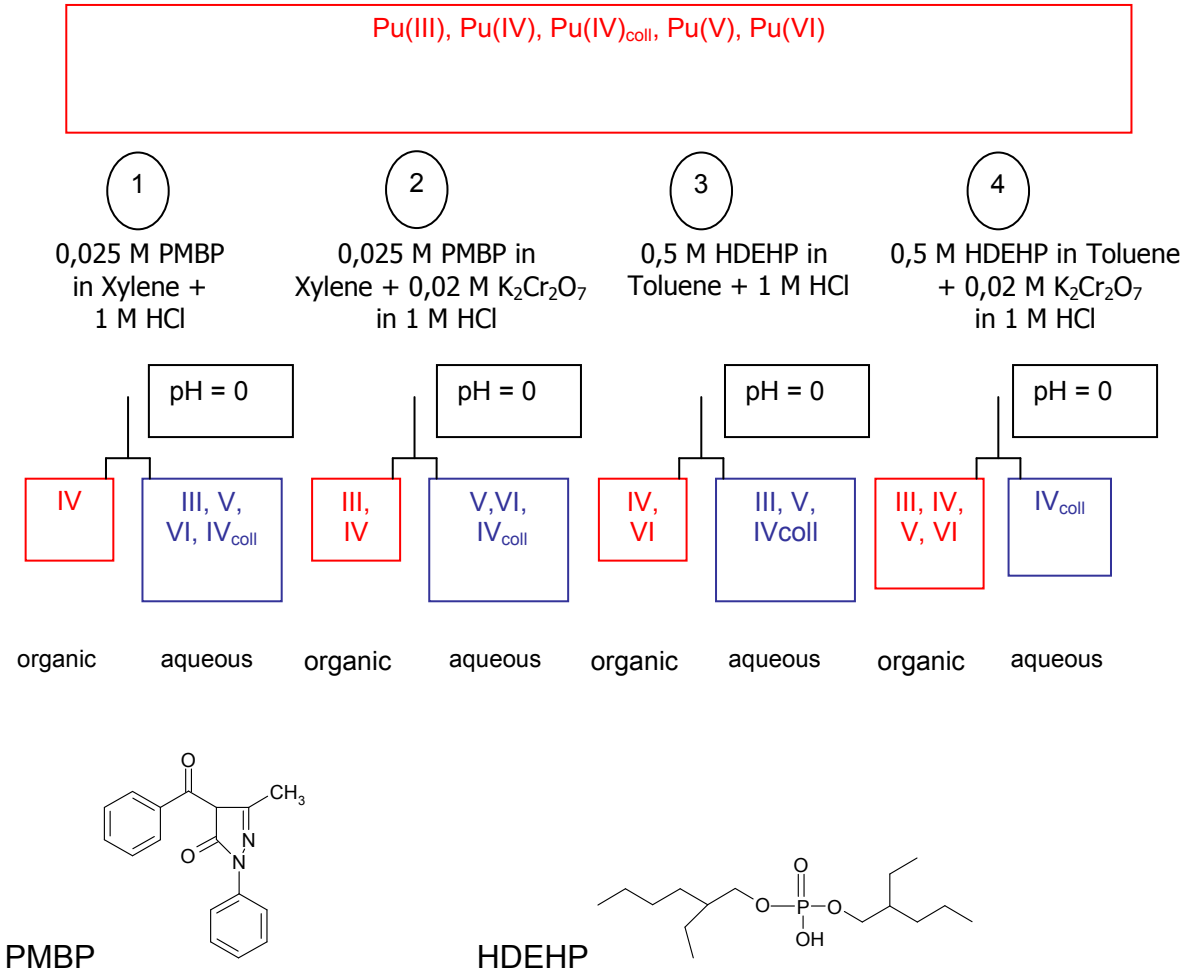

Figure 23: Liquid-Liquid extraction procedure, for speciation of plutonium; III, IV, V, and VI represent the plutonium oxidation states +3, +4, +5, and +6 respectively, and IV_{coll} represents Pu^{4+} polymeric materials (colloids) (Neu *et al.,* 1994); chemical structure of PMBP and HDEHP.

After separation, 200 µl from each organic and aqueous phase were transferred into separate vials and analysed by LSC. In the cases where the activity of the solutions was too low due to low concentration of plutonium, the same procedure was followed but using twice the amount of solution.

The precision of the work was verified by eq (15). The difference between the two terms can be accounted as experimental failure.

$$A_{reference} = \frac{A_{organic} + A_{aqueous}}{2} \quad (15)$$

$A_{reference}$ – activity of the reference sample

$A_{organic}$ – activity of the organic phase

$A_{aqueous}$ – activity of the aqueous phase

The error was between 5 – 8 %.

The composition of the analysed samples was determined in percentage relating half of each phase to the respective reference as 100% value. The speciation was determined as described in Fig. 24:

Pu^{3+} = (2) organic - Pu^{4+},

Pu^{3+} = (1) aqueous- (2) aqueous

Pu^{4+} = (1) organic

$Pu^{4+}_{colloids}$ = (4) aqueous

$Pu^{5+} = Pu_{total} - Pu^{6+} - Pu^{4+} - Pu^{4+}_{colloids} - Pu^{3+}$,

Pu^{6+} = (3) organic - Pu^{4+}

Figure 24: Calculation of the composition of plutonium solutions in percentage.

The advantages of the Liquid-Liquiud extraction are its low detection limits (down to [Pu] = 10^{-9} -10^{-10} M for ^{238}Pu), and the applicability for aqueous solutions without preliminary preparations. The main disadvantages are its relatively high error, and the laborious procedure (each sample can take up to one hour for measuring). The method is also hindered in the case when strongly reducing agents are present in solutions to be analysed, as step 2 and 4 are based on the oxidation of Pu^{3+} to Pu^{4+} in step 2, and Pu^{3+} and Pu^{5+} to $Pu4^{+}$ and Pu^{6+} respectively, in step 4, due to the oxidising effect of $K_2Cr_2O_7$.

4. 3. 3. CE-ICP-MS

4. 3. 3. 1. **Capillary Electrophoresis**

Since its first use as a separation technique in 1909 by L. Michaelis, the capillary electrophoresis (CE) has been applied successfully to a large variety of samples from bio-molecules to inorganic compounds (Landers, 1996). Today, it has become one of the most competitive methods for the separation of liquid samples (Cornelis *et al.,* 2003). The main advantages of CE are the low amounts of sample material needed, the relatively low operational costs and duration of the investigation, and minor interferences with the original sample chemical state (Li, 1993).

CE uses the dissimilarity in the mobility of different charged particles in an electrolyte when an external electrical field is applied. The species are contained in a small capillary filled with electrolyte and their mobility is dependent on the size to charge ratio.

On a charged particle (in our case metal ions) situated in an electrical field $\vec{E}$, acts a force $\vec{F}$ proportional to the charge:

$$\vec{F} = z_{ion} \cdot e \cdot \vec{E} \qquad (16)$$

z_{ion} – Ionic charge

e – Elementary charge [1.6 x 10^{-19} C]

$\vec{E}$ - Electric field strength [V/M]

The friction force $\vec{F}_R$ for spherical particles can be calculated according to Stokes:

$$\vec{F_R} = 6\pi \cdot r_i \cdot \eta \cdot \vec{\upsilon}_i \qquad (17)$$

r_i - Particles radius [m]

η – Dynamic viscosity of the solution [Pa s]

$\vec{\upsilon}_i$ - Electrophoretic velocity of the particle

The electrophoretic mobility μ_i of the ions is defined as the ratio $\frac{\vec{\upsilon}_i}{\vec{E}}$; if an equilibrium between the motion and the friction forces is formed, the mobility μ_i can be defined from the equation (16) and (17) as:

$$\mu_i = \frac{\vec{\upsilon}_i}{\vec{E}} = \frac{z_{ion}}{r_i} \cdot \frac{e}{6\pi\eta} \qquad (18)$$

It can be observed from the equation (17) that the ionic charge and the radius of the ion are the factors that influence the mobility of the ion in solution. So, if two species in a sample have different charges or different radii, they will migrate with different velocities through the capillary.

The electrophoretic mobility of one species can be determined experimentally,

dependent on the field strength and the migration time:

$$\mu_i = \left(\frac{L}{t_r}\right)\left(\frac{L_t}{V}\right) \qquad (19)$$

L – distance from the inlet to the detection point [m]

L_t – total length of the capillary

t_r – time needed for the species to reach the detection point [s]

V – applied voltage on the electrodes [V]

In addition to these parameters, the velocity of the migration of the species through the capillary will depend also on the so called electroosmotic flow (EOF) of the buffer solution. An EOF is observed when an electric field is applied to a solution contained in a fused-silica capillary as an effect of the mobilisation of the positive charges found on the inner surface. Most of the CE capillaries are produced from fused-silica. The walls of these capillaries consist of silanol (Si-OH) groups. Depending on the pH of the solution contained inside, the silanol groups are ionized to negatively charged silanoate ($Si\text{-}O^-$) groups, and consequently, positively charged ions will be found in the buffer solution. Attracted by the negatively charged cathode, the positive ions will move towards it, forming the EOF. Fig. 25 shows the formation of the EOF schematically.

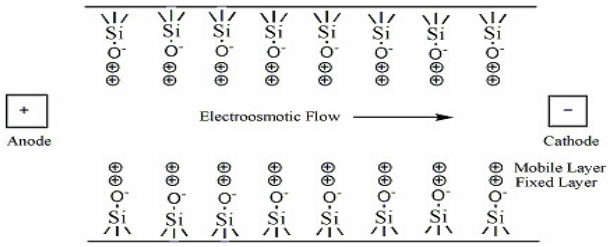

Figure 25: Schematic description of the interior of a fused-silica capillary, and the EOF formation (Terabe et al., 1984).

The EOF velocity is also dependent on the strength of the electric field $\vec{E}$. It can be written:

$$\vec{\upsilon}_{EOF} = \mu_{EOF} \cdot \vec{E} \qquad (20)$$

υ_{EOF} - *Velocity of EOF*

μ_{EOF} - *Electroosmotic mobility*

The EOF can sometimes be greater than the electrophoretic flow, so all species (positively charged followed by neutral and negatively charged species) can be carried towards the cathode, if no external forces are applied.

The overall velocity can be written as the sum of the two velocities, the electrophoretic and the electroosmotic.

$$\vec{\upsilon}_{tot} = \vec{\upsilon}_i + \vec{\upsilon}_{EOF} \qquad (21)$$

$$\vec{\upsilon}_{tot} = \left(\mu_i + \mu_{EOF}\right) \cdot \vec{E} \qquad (22)$$

Equation (22) suggests that the strength of the electric field is a decisive parameter, with respect to the mobility of the species. The electric field is directly proportional to the voltage applied on the

capillary, so the choice of voltage is crucial for a good separation. Typically, values between 20-30 kV are chosen. When less than 20 KV are applied, the separation could be too ineffective, and at voltages above 30 kV changes in the structure of the investigated species can occur (Cornelis. *et al.*, 2003)

Unlike High-Performance Liquid Chromatography (HPLC) where the mobility is ensured by pressure driven flow, the flow profile in a capillary is linear, if no other forces are applied (pressure at the inlet or vacuum at outlet of the capillary). However, for some applications it is necessary to apply a slight pressure at the inlet, in order to drive both positively and negatively charged particles to the end of the capillary (see chapter 4. 3. 5).

The sample introduction is achieved by a hydrodynamic mode. Applying an increased pressure on the vessel containing the sample, various volumes of liquid can be injected according to Poiseuille's law (Kok, 2000):

$$V = \frac{r^4_{cap} \; t_{inj} \; \Delta P \; \pi}{8 \eta L_{cap}} \qquad (23)$$

V – Injected volume [L]

r^4_{cap} *– Inner radius of the capillary*

t_{inj} *– Injection time [s]*

ΔP *– Difference of pressure [Pa]*

η *- Dynamic viscosity of the solution [Pas]*

L – Total length of the capillary [m]

The difference of pressure can be calculated as a function of the differences in the height of the inlet, respectively outlet of the capillary, the density of the injected fluid, and the externally applied pressure.

$$\Delta P = P_{ext} + \rho \cdot g \cdot \Delta h \qquad (24)$$

P_{ext} *– External pressure [Pa]*

ρ *- Density of the injected fluid [kg/m³]*

g *– Gravity acceleration [m/s²]*

Δh *– Height difference [m]*

Many parameters can be varied in order to optimize the method for the desired applications.

The typical sample injection volume is between 5 – 50 nl (Cornelis et al., 2003). It is varied depending on the concentration of plutonium in our case, and on the setup of the system.

Because the liquid column acts like an electric resistance when an electric current is applied, it can generate heat leading to the warming of the sample. This is one of the parameters that must be taken into account when the inner diameter of the capillary is chosen. It is typically between 25-150 µm.

For the detection of the species, several methods can be used. Most common UV/VIS spectroscopy is used,

but methods like laser induced fluorescence (LIF), amperometry, conductivity, or mass spectrometry (Agilent Technologies, web site) are also applied. A comprehensive description of the detection methods for CE is presented by Landers (Landers et al., 1998).

For the speciation of plutonium in environmental samples, very sensitive and isotope selective methods are needed. This can be achieved by coupling the CE online or off-line to mass spectrometry. In the following section, the coupling of CE to Inductively Coupled Plasma-Mass Spectrometry (ICP-MS) and to RIMS will be described.

4. 3. 3. 2. ICP-MS

ICP-MS uses the high energetic potential of radio frequency generated plasma in order to ionize the investigated elements. The temperatures reached inside the plasma are about 6000-8000 K. Because of the high temperature, the samples are atomized and then non selectively ionized.

The resulting ions are separated in a mass discriminator and detected via a multi channeltron electron multiplier in most cases (Jarvis et al., 1992).

The most common mass separator is the quadropole. Using a combination of DC and AC electric potentials applied to four parallel metal rods, this robust and simple system discriminates the different ions based on their mass to charge ratio. Thus, the paths of the ions towards the detectors are influenced, allowing only the desired masses to arrive at the electron multipliers. The quadropoles have a relatively low resolution for the ions with similar mass to charge ratios. For better resolutions, doubly focusing sector field analysers can be employed.

The ICP-MS system that was used for the experiments performed within this work, was a HP 4500 quadropole mass spectrometer (Agilent, Waldbronn, Germany) at the Institut für Kernchemie in Mainz, or an Elan 5000 quadropole (Perkin Elmer, Rodgau-Jügesheim, Germany) at the Institut für Nukleare Entsorgung in Karlsruhe.

4 .3 .3. 3. CE-ICP-MS

The coupling of CE to ICP-MS (CE-ICP-MS) was first reported by Olesik in 1995, as an alternative to other separations techniques like (HPLC) or Gas Chromatography (GC) coupled to a variety of other techniques like Optical Emission Spectrometry (OES), ICP-MS etc. (Olesik et al., 1995). It has turned out to be a powerful tool also for the speciation of plutonium because of its relatively low detection limits (Kuczewski et al., 2003), (Ambard et al., 2005).

In the PhD work of B. Kuczewski, a detailed description of the CE-ICP-MS system used in the present work is provided (Kuczewski, 2004).

The computer controlled sample changer was built in our workshops. A software controls the pressure injection system, the voltage that can be applied and the succession of the samples.

Up to 16 samples can be loaded in 20 ml vials, and the system can be programmed. For reduced sample volumes smaller vials can be used (2 ml).

The sample injection into the capillary is achieved by applying an increased pressure on the vial containing the sample. This is attained by allowing a pressure controlled flow of argon to enter the hermetically sealed vial, as outlined in Fig. 26. The pressure of the argon flow can be varied between 50 – 1000 mbar.

The high voltage source was also built in our electronic workshop. It can deliver voltages between 0 and ± 30 kV.

Fused-silica capillaries were used, with inner diameters of 50 or 75 µm, and outer diameters of 150 or 350 µm. The length was varied depending on the application (CE-ICP-MS or CE-DAD-ICP-MS) between 60 and 75 cm.

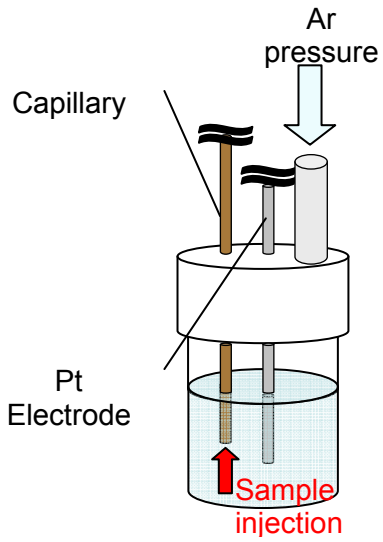

Figure 26: The hydrodynamic injection of the sample into the CE capillary

The online coupling of the CE to the ICP-MS is based on the technique described by Prange and Schaumlöffel (Prange *et al.*, 1999). It has been performed using a four path interface like that patented by Schaumlöffel and Prange (Schaumlöffel, 1998). The interface was made of polyetheretherketone (PEEK) and had the role to provide an electrical contact, to fulfil the flow from the CE to the flow necessary in the nebuliser, and to

prevent possible suction effects from the nebuliser on the capillary. A schematic depiction of the interface and a photo of the real interface are shown in Fig.27.

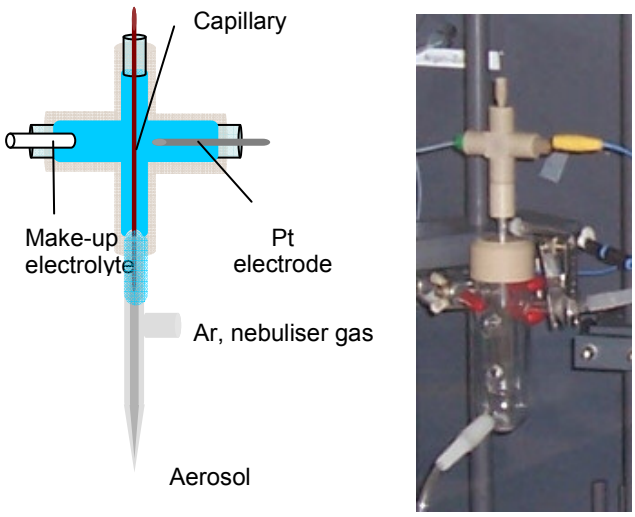

(a) (b)

Figure 27: Schematic depiction of the CE-ICP-MS interface (a) photo of the actual interface (b).

It can be observed in both pictures that on the upper part, the capillary enters the interface through a sealed inlet and it comes in contact with the make-up electrolyte just some millimetres from the intake of the nebuliser. This is a parameter of great importance, as it influences very strongly the results of the analysis. If the distance is too large, the electrolyte coming out of the capillary will dissolve in the make-up solution, resulting in too broad peaks.

The edges of the capillary end must be also straight at an angle of 90° in order to prevent the same effect. Therefore, the cutting of the capillary must be carried out with much caution. The edges were verified with a microscope. Fig.28 exemplifies the correct and the incorrect manner a capillary can be cut.

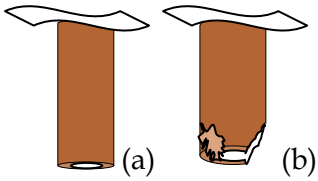

Figure 28: The correct cut of the capillary end (a), problematic end of a capillary (b)

If the distance is too short, suction effects can occur, influencing the migration times of the species through the capillary. The optimal distance was found to be between one and three millimetres.

Because the flow through the capillary (some nl/min) is much lower then the liquid consumption of the nebuliser (between 50 – 200 µl/min for the nebulisers used in this work), the volume is adapted using a make-up solution. This is added through the left side intake represented in Fig. 27, based on the suction effect of the nebuliser.

The nature of the buffer used for the electrophoresis varies with the type of application. For the speciation of actinides in environmental samples, the most suited buffer found was 1 M AcOH at a pH ≈ 2.4 (Kuczewski, 2004). The make-up solution consisted of 2% HNO_3.

The make-up solution has also the task to enable the contact between the

buffer and the high voltage conection. The voltage is introduced with the use of a Pt electrode situated on the right side of the pictures in Fig. 27.

Another factor with major influence on the results of the analyses is the capacity to transport the complete species fractions to the analyser, in our case the ICP-MS.

The nebuliser creates an aerosol stream that has to be separated from the big liquid drops as they could obstruct the proper functioning of the plasma.

The nebulisers used in this work were MicroMist 200 and MicroMist 50 (GlassExpansion, West Melbourne, Australia).

Different types of spray chambers were also tested. The best results were obtained with a cyclonic spray chamber with cooling/warming mantle (Cinnebar Cyclonic Small Volume) and with a double pass spray chamber (Scott-type).

Attempts to optimize the transfer of the aerosols into the plasma were performed, making use of the warming/cooling mantle of the cyclonic spray chamber. While warming, the liquid drops condensed on the walls of the spray chamber are evaporated and found in the aerosol stream. This is a desired situation because it means that a higher amount of sample is transported to the ICP-MS. Unfortunately the CE system has to be operated in a closed, aspirated box, for health safety reasons (the system produces plutonium aerosols, which can be extremely hazardous). This means that the coupling to the ICP-MS is achieved through a polyethylene (PE) or Teflon tube. The steam formed by evaporating the drops condensed on the tube walls, and after longer periods of operating bigger liquid drops were formed, which had a very negative influence on the plasma. It was attempted also to heat the entire tube, but a complete heating of all the junctions was not possible, with the result that the non heated parts seemed to accumulate much faster liquid drops, hindering even stronger the functioning of the plasma.

While cooling the spray chambers big drops of liquid are found on the walls. They are removed using a rotary pump at the bottom of the spray chamber. The cooling impairs accordingly the volume of sample transferred to the ICP-MS in our case.

4. 3. 3. 4. Applications of CE-ICP-MS

The coupling of CE to ICP-MS was routinely used for speciation of plutonium in aqueous solutions. The method is relatively fast, and as shown in the work of Kuczewski (2004), has a good reproducibility.

Before a capillary is used for the first time, it needs a preconditioning of the silan surface (Ehmann *et al.*, 1998). The applied preconditioning procedure included the rinsing of the capillary with acetone in the first step. This was carried out for a period of five minutes applying a pressure of 1000 mbar, in order to remove organic impurities. Subsequently, 0.1 M NaOH and 0.1 M HCl, respectively, were injected with a pressure of 1000 mbar for five minutes each. This step was repeated for two times. The acid was then washed away with MilliQ water for ten minutes with a pressure of 1000 mbar. For rinsing the capillary after use (*e.g.* for preventing cross contamination), the same procedure was applied with the specification that the rinsing periods were reduced from five to two minutes.

Before starting the experiments, the capillary was filled with AcOH 1 M, by injecting it with a pressure of 800-1000 mbar for a short period (about one minute) to make sure that the dilution with the water column is not affecting the liquid column used for electrophoresis.

After the experiments, the capillaries were washed using the above described method, and they were dried by allowing an argon flow to pass through, for a period of about five minutes.

For the separation of species, in all the experiments (unless otherwise stated), a 30 kV voltage was applied. The current changed with the time between 0 -50 μA.

The nebuliser was operated with an argon flow between 0.9 - 1.2 L/min. A lower argon flow would reduce the amount of sample transported to the ICP-MS and a higher amount blocks completely the nebulising, by inducing a back pressure effect.

In the make-up solution, rhodium was introduced as marker with a concentration [Rh] ≈ 10 ppb. By constantly monitoring the rhodium signal, it was possible to eliminate the effects of the fluctuations in detection efficiency, by normalising the plutonium signal to the rhodium signal.

These fluctuations can be the result of instability in the nebulising process, aerosol transport, or efficiency of the detection of ICP-MS.

The conditions under which the system was operated are summarized in Tab. 16.

Tabel 16: Operating conditions of the CE-ICP-MS

Entry	Conditions
CE	
Capillary	Fused silca, inner diameter 50 µm, length 60 – 70 cm
Sample injection	5-10 s at 50 – 150 mbar
Electrolyte	1 M AcOH
Voltage, current	30 kV, 0 - 50 µA
Sample transfer	
Make-up solution	2 % HNO_3 with 10 ppb Rh as marker
Nebuliser	MicroMist 50, MicroMist 200
Spray chamber	Heated/Cooled Cinnebar Cyclonic, Scott-type
Tube	PE, Teflon, heated/not heated, length 1 -1.5 m
Argon flow	0.9 – 1.2 L/min
ICP-MS	
RF power	1100 – 1300 W
Analyser set	100 ms on Rh, 800 ms on Pu for plutonium measurements 100 ms on Rh , 100 ms on every other element for calibration measurements

Before the measurements, the ICP-MS was calibrated, using tuning solution standards for ICP-MS (Merck, Darmstadt, Germany).

A solution containing Li(I), Cs(I), Sr(II), La(III), Th(IV), and U(VI) in 2% HNO_3 was prepared and measured before analysing the actual samples in order to find the optimum performance of the separation and detection. This is necessary because the system is very sensible and the accurate adjustments can be very rapidly disturbed.

The technique is able to separate all the ions listed above, and well defined individual peaks are obtained for diverse species.

The complexation between the acetate groups from the acetic acid and the metal ions influences the migration of the species in the capillary as this depends on the ions effective charge/ion radius ratio. The succession of elution peaks is presented in Fig. 29. After verifying the accuracy of the separation and detection, the real plutonium samples were analysed.

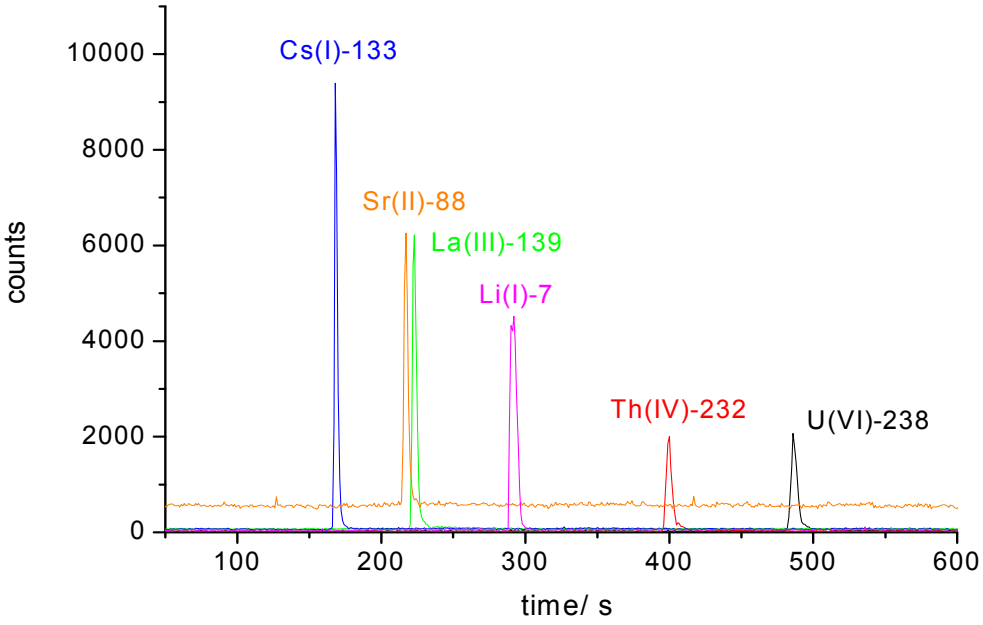

Figure 29: Separation of ions with oxidation states from I to VI. The concentrations were between 10 - 100 ppb.

The aqueous samples didn't require special preconditioning; the method is able to separate plutonium species dissolved in organic and inorganic acids, as well as directly in aqueous solutions.

Fig. 30 displays the separation of all four oxidation states of plutonium, found usually in aqueous solutions. The results obtained for analysing the solutions containing the different plutonium species with CE-ICP-MS, were compared with the results for the same solution but higher concentrations, determined with UV/VIS spectroscopy. A good agreement was found between the results obtained with the two methods. Hence, it was demonstrated that the redox equilibrium formed in solutions is not disturbed by applying the high voltage needed for the separation of the species.

The reproducibility of the measurements was ≥ 95% for the peaks area and ≥ 99 % for the retention times of the species in the capillary. The detection limits were as low as 20 ppb for plutonium (Kuczewski, 2004). The method was successfully applied for speciation studies of plutonium in contact with humic and fulvic acids. Further details are presented in chapter 5. 1. of this work.

For the studies of the complexation constants of plutonium with humic and fulvic acid, the method can be applied in order to monitor the concentrations of free (not complexed) plutonium ions in solutions, but unfortunately the humic substances can not be detected and quantified directly with this set-up. Adding a second detector to the system, which would be sensitive

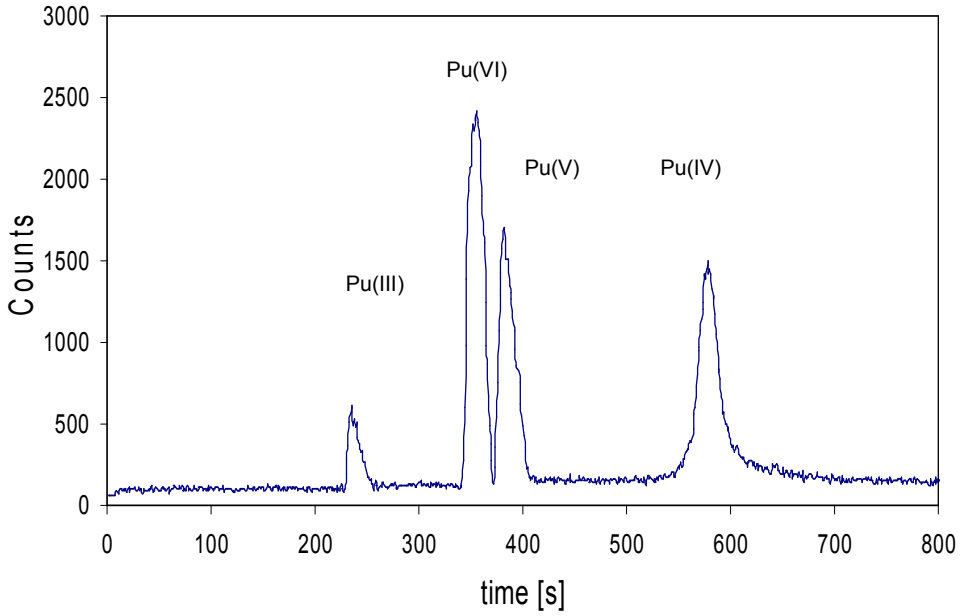

Figure 30: Separation of all four oxidations states of plutonium found in aqueous samples

enough for detecting humic substances, could enable the detection of the free plutonium, complexed plutonium and humic substances, and free humic substances.

For this, a Diode Array Detector (DAD) can be employed. It can detect the humic substances making use of their spectroscopic properties (see chapter 3. 1).

The first steps in developing the coupling CE-DAD-ICP-MS are presented in the chapter CE-DAD-ICP-MS.

Although the detection limits of CE-ICP-MS are lower than the ones of other methods used for the speciation of plutonium (*e.g.* UV/VIS spectroscopy), they are not sufficient for analysing environmental samples. The concentration of plutonium in environmental samples is expected to be much lower (see chapter 2. 1) so more sensitive detectors are needed for investigating the speciation of plutonium under these conditions.

One possibility to decrease the detection limits would be the use of a more sensitive detection system, for example a sector field ICP-MS that could enable the detection of one or two orders of magnitude less plutonium. These machines are, however, very expensive.

Another possibility would be the off-line coupling of CE to RIMS. RIMS has a detection limit of 10^6 – 10^7 atoms (see chapter 4. 1. 3), and has a very good element and isotopic selectivity.

The off-line coupling CE – RIMS will be discussed in the next paragraph.

4. 3. 4. CE – RIMS

RIMS can offer very useful information on the isotopic composition and on the amount of plutonium in the environment, but unfortunately, alone, it can provide no information on the speciation of the element in the analysed samples.

The speciation of plutonium is of great interest, as its behaviour with respect to the possible migration in the environment after accidental release from nuclear waste repositories, is significantly influenced by the oxidation state and the species in which it is found. Several speciation methods have been developed for the study of plutonium throughout the years. They are summarized in Tab. 17 together with their detection limits.

Tabel 17: Speciation methods applied for the determination of plutonium species, and their detection limits

Speciation method	Detection limit Pu [mol/L]
UV/Vis Spectroscopy [a]	10^{-5} – 10^{-6} dependent on the oxidation state
Liquid-Liquid extraction [b]	10^{-6} – 10^{-10} dependent on the isotope
EXAFS [c]	10^{-5} – 10^{-6}
LIBD [d]	10^{-7} – 10^{-8} (for Pu(IV) colloids)
LIPAS [e]	10^{-8}
(TL) [f]	10^{-7}
CE-ICP-MS [g]	10^{-7} – 10^{-8}

[a] (Choppin, 2004)
[b] (Nitsche *et al*., 1988)
[c] (Reich *et al*., 2005)
[d] (Bitea, 2005)
[e] (Stumpe *et al*., 1984)
[f] (Moulin et al., 2001)
[g] (Kuczewski *et al*., 2003)

UV/Vis – UV and visible spectroscopy
EXAFS- extended x-ray absorption fine structure
LIBD – laser induced breakdown detection
LIPAS- laser induced photoacustic spectroscopy
TL - Thermal Lensing
CE-ICP-MS – capillary electrophoresis – inductively coupled plasma-mass spectrometry

The methods mentioned above have insufficient sensitivity for speciation studies of plutonium under naturally relevant conditions.

The detection limit of RIMS is usually lower than that of ICP-MS. By combining the good separation capability of CE with the sensitivity of RIMS, a good speciation tool can be established. In this way, the oxidation state and the isotopic composition of natural samples could be determined at the same time.

4. 3. 4. 1. Principle of coupling CE-RIMS

The coupling of CE to RIMS can only be realised off line. Fractions of plutonium separated by the CE are collected in different vials. The electrolyte containing the plutonium fraction is then used to prepare RIMS filaments by introducing it directly into the electrodepositing cell. The filaments are measured by RIMS afterwards. In this way, the contribution of each fraction to the composition of the initial solution can be determined.

The main disadvantage of the method is the time consuming preparation of the filaments and the subsequent measurements by RIMS.

In the work conducted so far, just the first steps demonstrating the applicability of the method were performed.

As a first step, the elution times of each one of the plutonium species from the capillary were determined using CE-ICP, with concentrations of plutonium higher than the ones used later for CE-RIMS.

Next, based on the obtained electropherograms, the times when each fraction would be collected were defined. For separating the different fractions, it is necessary to change the collection vials. To do this, the high voltage must be interrupted. The approximate time necessary to change the vials was thirty seconds.

The time windows were defined and several runs were performed interrupting the high voltage for 30 seconds at the desired points. The possible diffusion of the species in the capillary during the time when the high voltage is interrupted was monitored and it was determined that these effects are minimal as shown in Fig. 31.

Because of the close vicinity of their peaks, Pu(VI) and Pu(V) could not be separated into two fractions under the conditions used in these experiments. This could be, however, possible by using a longer capillary which would allow a longer time for the separation of the species. The reproducibility was verified in several consecutive runs. Once the location of the high voltage breaks was well defined on the time scale, the setup of the system had to be modified, to enable the positioning of the collecting vials.

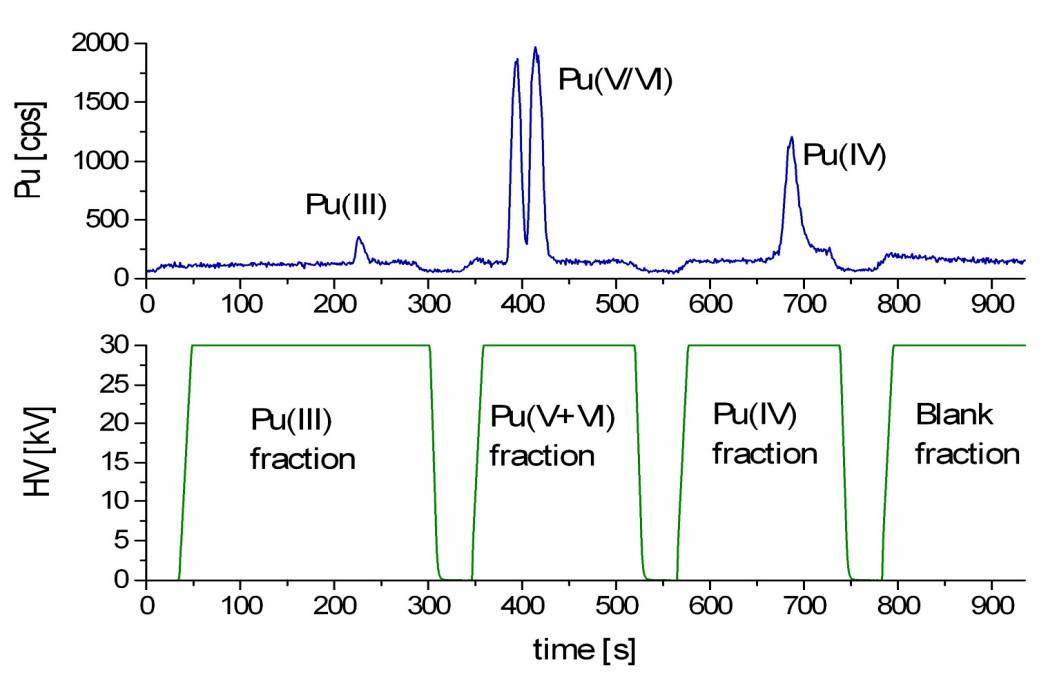

Figure 31: The definition of the high voltage breaks for the collection of different plutonium fractions for coupling off-line CE-RIMS

In this sense, the interface used for the ICP-MS coupling was replaced by a glass vessel containing 1 M AcOH as electrolyte. All the other parameters such as high voltage, length and positioning of the capillary, pressure applied, and the argon flow in the nebuliser, must remain unchanged, as they can influence the migration times.

In order to validate the applicability of the method, several experiments were performed, analysing the collected fractions with α- spectroscopy which is a much simpler method than RIMS. For this, collecting vials containing 1000 µl 1M AcOH were placed at the end of the capillary. After the collection of the different fractions, 500 µl of each of the solutions were evaporated on a titanium filament. The filaments were measured for 24 hours in an α- spectrometer. The mean values of the experiments corresponding to each fraction were compared with those obtained with CE-ICP-MS and they are presented in Tab. 18.

The fraction containing Pu(V)+Pu(VI) has a significantly higher rate in the results obtained by α-spectroscopy. This could be explained by a contamination in the capillary, due to the fact that the same capillary has been used in runs with much higher concentration of plutonium before, in order to determine the collection times of the fractions. The capillary was washed, but the contamination could not be removed completely.

Table 18: Comparison between the plutonium fractions detected by α- spectroscopy and ICP-MS after separation by CE

	Pu(III) %	Pu(V+VI) %	Pu(IV) %
CE-ICP-MS	30.9(5.2)	5.5(1.0)	63.6(4.5)
α- spectroscopy	31.9(4.8)	10.8(1.6)	57.2(8.6)

In order to simplify matters, for a first test of the CE-RIMS coupling, a solution containing just two collection fractions was prepared. First, a solution with ≈ $1x10^{11}$ atoms/sample volume injected into the capillary, was analysed by ICP-MS. The oxidation state ratio of the solution was determined, as well as the time scale location for the high voltage breaks.

The same solution was subsequently diluted to a concentration of ≈$1x10^{9}$ atoms/sample and separated by CE. The fractions were eluted in the same way as described above for α- spectroscopy. 500 µl of electrolyte were introduced directly into the electrodepositing cell used for preparing RIMS filaments. The filaments were then measured by RIMS and the plutonium oxidation state composition was determined. Tab. 19 presents a comparison between the results obtained with the two methods. A rather good agreement between the two methods was found. The high sensitivity of RIMS was not completely exploited in the frame of these first experiments. The detection limits of this method could be theoretically reduced by 2 or 3 orders of magnitude, as the sensitivity of RIMS goes as low as 10^{6} – 10^{7} atoms.

One of the problems encountered while working with CE-RIMS was the contamination with plutonium sorbed on the capillary on the preceding runs, used for the calibrating of the elution times, when higher concentrations of plutonium are necessary. This could be avoided by the use of a different isotope of plutonium in the calibrating runs than in the actual sample. As the RIMS is isotope selective, by measuring just the isotope of interest, the contamination problem could be solved. This was however not yet done.

Table 19: Comparison between plutonium speciation results obtained with CE-ICP-MS and CE-RIMS

Method	Pu(V+VI) %	Pu(IV) %
CE-RIMS (off-line)	19.2(2.0)	80.3 (3.0)
CE-ICP-MS	15.2(5.0)	84.8 (5.0)

The main disadvantage of CE-RIMS are the relatively time consuming preparations, necessary for RIMS measurements.

It could be however demonstrated that CE-RIMS might become a powerful tool for the speciation of plutonium in trace amounts in environmental samples. Further experiments are needed in order to determine the absolute detection limits and the applicability of this method for authentic samples. This should be followed up in a subsequent doctoral thesis.

4. 3. 5 Ultrafiltration

For the determination of the complexation constant of humic acid with plutonium (logß), the ultrafiltration technique was applied. The concept is to make use of the higher molecular size of humic acids, in order to retain them on a membrane filter. The smaller plutonium species which are not attached to humic acid molecules are able to pass through the filters. In this way, the free plutonium is separated from the complexed part and is detected by means of LSC in the filtrate.

Microsep 1kOmega membrane filters (Pall Life Sciences, USA) with 1 kDalton pore sizes were used. With the help of UV/VIS spectroscopy it was determined that about 85 % to 95 % of the humic acids are retained by the filters depending on their concentrations. By adding metal ions, the retention of humic acid increases even more (Bürger, 2005).

The fulvic acids are retained in a much lower rate, 60 -40 %, so the method cannot be applied for the investigation of complexation of fulvic acids with actinides.

After passing through the filter, plutonium is quantified by LSC. > 95% is recovered if the solution is colloid free.

Due to the small dimension of the pores in the membrane filters, the filtration takes much too long if it is conducted in a gravimetric way. Therefore, the solutions were filtered under centrifugation. The centrifuges (Fritz Bayet OHG, Frankfurt M., Germany), were operated at around 2500 rpm. About 20 minutes were necessary for the filtration of ~ 500 µL solution.

The technique was used in this work for determining the logß constant for the complexation of Pu(III) with humic acids. It is a simple and relatively fast technique, but the drawback is that it has a relatively high error (fluctuation in filtering capacities) and that it is not suitable for studies involving fulvic acid.

An alternative technique is under development, specifically the online coupling of capillary electrophoresis to a diode array detector and inductively coupled plasma mass spectrometry (CE-DAD-ICP-MS).

4. 3. 6 CE-DAD-ICP-MS

4. 3. 6. 1 Diode Array Detector

Like the UV/VIS spectrometer described earlier, a diode array detector (DAD) makes use of the spectral properties of substances such as light absorption, in order to detect them in liquid solutions.

It practically monitors the light that passes through a liquid sensor cell, and displays the changes that might appear when the composition of the monitored solution changes.

The light source is usually polychromatic, and after passing through the cell, it is dispersed by a prism or a diffraction grating onto the surface of the analysing sensors. These sensors are a high number of photosensitive diodes placed side by side and insulated from one another, in the form of a multi-layer sandwich. Thus, each diode will receive light of a slightly different wavelength compared to that received by its neighbour. As the wavelength range can be very broad, a sufficient number of diodes must be incorporated into the array to cover the entire wavelength range. Hence, the outputs of all the sensors can be acquired and assembled to construct an absorption spectrum that can be compared with standard spectra for the identification of the compound.

The DAD system used in the following experiments was a Knauer DAD K-2800 (Knauer ASI, Germany). This is a top performance UV/VIS/NIR-detector based on highly advanced fibre optical technology.

It covers the wavelength range between 190 – 1024 nm, with a D_2-lamp and a halogen lamp installed. The light is transported through an optical fibre to the detection cell, focused on the sample, and then, after passing through it, is recaptured in a new optical fibre and transported to the diode array.

By simply connecting longer fibre optical cables, the flow cell can be moved from inside the instrument to any other place, enabling thus the coupling to CE.

The diode array detector can be used to record up to four chromatograms at the same time, with a frequency of 10 spectra per second. In this way, by selecting the appropriate diode alternatively, the wavelength with the maximum light absorption can be selectively monitored to provide maximum detector sensitivity for the investigated substance. It provides also 2D and 3D (time, absorption intensity, and wavelength) chromatograms over the entire wavelength range.

Together with the hardware, the ChromGate software was delivered. This

was used for the operation of the system and for the analysis of the data. Further details on the applications are given in the chapter CE-DAD-ICP-MS.

4. 3. 6. 2. Principle of coupling CE-DAD-ICP-MS

The ultrafiltration method (see chapter 4. 3. 5) can exhibit unwanted fluctuations of the results for the complexation studies of plutonium with humic acids. It was also demonstrated that ultrafiltration is not suitable for investigating the complexation of plutonium with fulvic acids.

Therefore, an alternative method was proposed, specifically the coupling CE-DAD-ICP-MS. The concept of this method is to detect and quantify the three compounds individually, free humic substances, the complex humate-plutonium, and free plutonium ions, and to process the data in a similar way as for the ultrafiltration method.

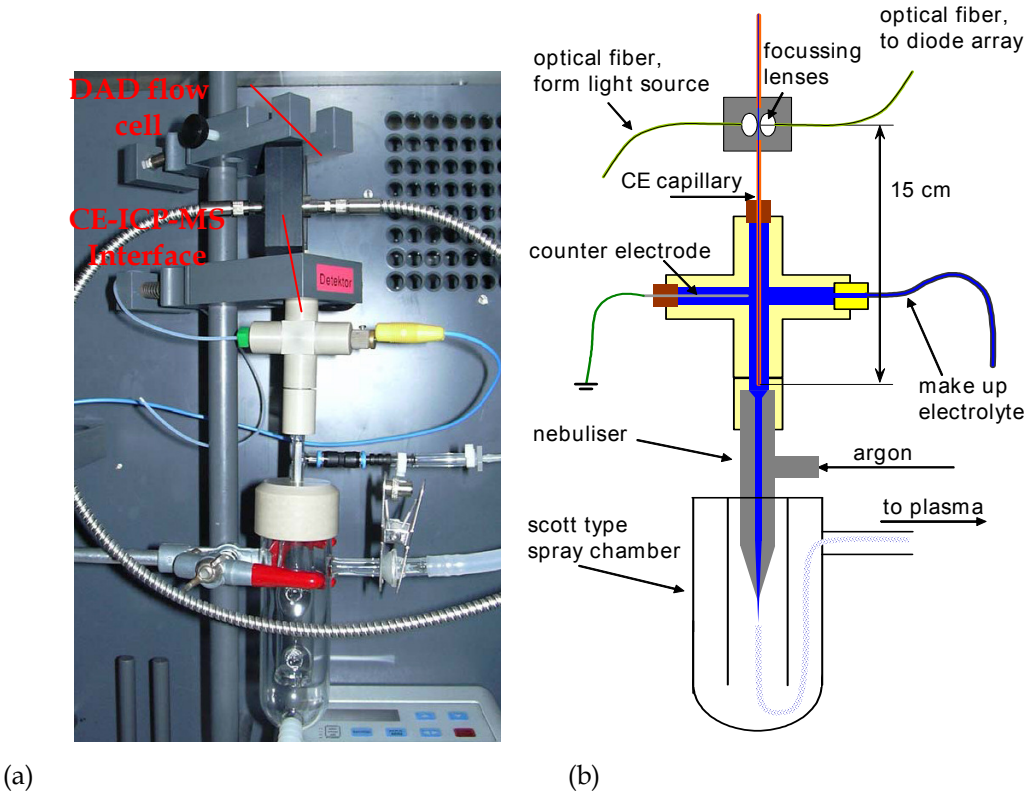

(a) (b)

Figure 32: Photo of the coupling CE-DAD-ICP-MS (a) and schematic illustration of the setup of the system (b).

The two detectors can be coupled on-line so that the DAD can detect the humic substances and the ICP-MS the plutonium species. The concentration of plutonium is too low for the detection with DAD, but a solution with concentrations of plutonium down to [Pu] = 10^{-6} - 10^{-7} M can be still detected with ICP-MS (Kuczewski, 2004)

Fig. 32 presents the experimental arrangement. It can be seen that the detection of the humic substances is achieved in the capillary, at a few centimetres in front of the interface used for the coupling of the CE to ICP-MS.

The light transported with the optical fibres is focused onto the capillary and the changes in the light absorption of the electrolyte passing in front of the detector are monitored.

Concerning the coupling interface for CE-ICP-MS, practically the same setup as earlier described (see chapter 4. 3. 3. 2) can be maintained with the specification that the capillary has to pass through the DAD flow cell first.

The capillaries used can be the same as used for the CE-ICP-MS coupling. They are normally coated with a brown coloured polyimide coating of about 5 µm thickness. This grants flexibility to the capillary that would be otherwise very fragile (Landers, 1996).

In order to enable the detection of the smallest changes in the light absorption of the solution that passes through the capillary, the polyimide coating has to be removed, thus creating a window that will allow the light to pass undisturbed through the capillary. This is achieved by heating up the surface, usually with a gas lighter and wiping the surface with an ethanol or acetone soaked lens tissue. This process is delicate because the thin silica capillary can melt and block if too much heat is conferred and too high temperatures are reached.

Caution must be taken when handling the capillary once the window was created since this area is extremely fragile, and can break very fast. The window width is between 3 – 5 mm.

The window must be then fixed precisely in the light focusing area of the DAD. This step is carried out by monitoring the light absorption while slowly sliding the capillary in the DAD cell. When the point with the lowest light absorption is encountered, it is assumed that the window has reached the desired position in the light focussing area. It is necessary to make sure that the window is clean, and that the light focusing does not occur at the side of the window, but precisely in the centre of it.

It has been explained in the chapter 4. 3. 3 that the precise positioning of the end of the capillary in the CE-ICP-MS interface is very important for the optimum functioning of the technique. Therefore, the DAD cell as well as the CE-

ICP-MS interface was fixed using adaptors that could slide up and down, for fine tuning of the vertical position of the components as presented in the Fig. 32.

The system has the potential to detect thus the humic substances by DAD as well as plutonium by ICP-MS as described in the earlier chapters.

4. 3. 6. 3. Applications of CE-DAD-ICP-MS

The aim of coupling the three methods is to study the interactions of low amounts of actinides with humic substances. The complexation constants between the two compounds could be calculated, if quantitative information on the free rmetal-ion as well as on the humate-metal complexes is available.

This can be principally achieved if a solution containing both species is separated with the CE and then the separated components are detected with the DAD and ICP-MS, respectively.

For the study of the complexation constants of plutonium with humic substances, the reactants can be contacted in an aqueous solution and the solution can be afterwards analysed.

The humate-plutonium complex can be negatively charged as the humic substances do not have usually all the complexing sites neutralised by metal ions. However, the charge will be less negative compared with that of the free humic substances, resulting in another mobility of the species in the CE. If the Loading capacity of the humic substances is reached, all the available complexing sites would be occupied and the complex will be neutrally charged according to the metal ion charge neutralization model of Kim (Kim *et al*., 1996). Thus, once injected into the capillary, the humic substances and the humate complexes will migrate in different directions as plutonium when a voltage is applied, due to their opposite electric charge. In this way, the three species will be separated because of their different charges.

In order to detect the species, they must be all found at the end of the capillary after the separation. This can be achieved by applying a slight pressure on the buffer from the beginning of the capillary. This will induce a laminar flow of electrolyte in the capillary. If the flow is fast enough, it could counteract the electrophoretic motion of the species towards the starting point of the liquid column. The pressure must not exceed certain values in order to allow enough time for the separation to take place.Thus, it would be possible to detect the separated species at the same end of the capillary.

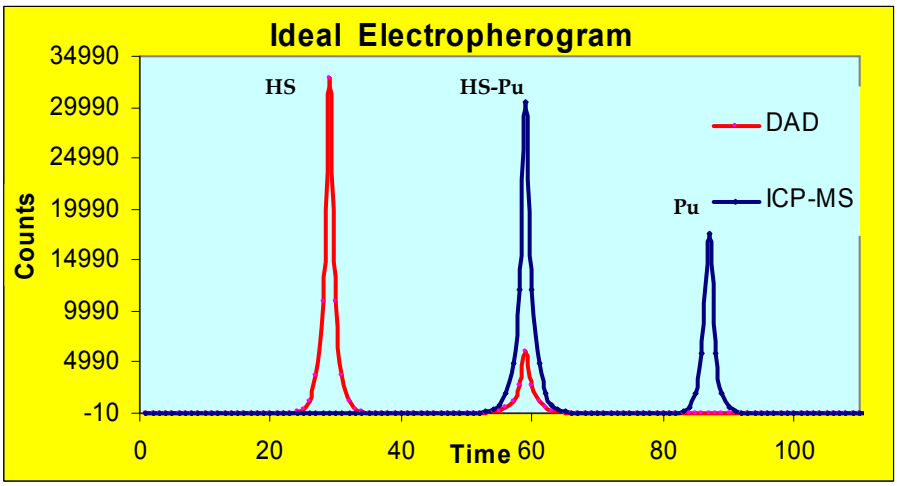

Figure 33: Schematic, hypothetic description of the analysis performed with CE-DAD-ICP-MS for determining the ratio humic substances/humat-plutonium complexes/free plutonium ions.

Fig. 33 is a hypothetical representation of the detection of the three possible species (uncomplexed humic substances (HS), humate-plutonium complexes (HS-Pu), and free plutonium (Pu)).

If a positive voltage is set on the pole corresponding to the end of the capillary, the negatively charged humic substances migrate towards it, passing through the detection window. In this moment they are recorded by the DAD. The ICP-MS is set on the mass of plutonium, so it will not sense the presence of humic substances

After a certain time, the less negative/neutral complexes are carried by the electrophoretic/EOF and the laminar flow in the capillary through the light focus on the window. The humic substances are detected by DAD. This corresponds to the second peak acquired with the DAD on the specific light absorption wavelength of the investigated humic substances. The DAD senses no difference between the free and complexed humic substances. Therefore, the absorption spectra depend only on the amount of humic substances that are found in the pathway of the light. Consequently, after a short time necessary for the complexes to reach the plasma, a plutonium signal corresponding to the metal bound in the complex, is received from the ICP-MS. The presence of plutonium correlated with a signal for humic substances, implies the presence of a humate-plutonium complex.

For this step, a calibration of the time necessary for the species to reach the plasma after passing the DAD cell is necessary. This period is around one to two minutes depending on the length of the last part of the capillary and of the tube that transports the aerosols from the

spray chamber to the inlet of the ICP-MS. The calibration and correlation between the two detectors will be discussed more detailed in the following paragraphs.

Plutonium is carried by the laminar flow of the electrolyte induced by the applied pressure at the start of the capillary, counteracting its tendency to migrate in the other direction, through the capillary and then it is eluted into the nebuliser.

The concentration of plutonium is too low for the detection with DAD so it is not detected as it passes through the light focused on the capillary window. Only the ICP-MS is able to detect it and based on the results obtained with this detector the quotient between complexed and uncomplexed metal can be determined. Parallel to this, a run with a similar solution containing plutonium in the same oxidation states and with the same concentration and no humic substances will be performed. Comparing the plutonium peaks areas obtained for this, with the ones from the preceeding experiment, it can be determined the ratio free/complexed plutonium and these data can be used similar as in the case of the ultrafiltration for determining the complexation constants.

It can be thus concluded that the information that can be acquired by CE-DAD-ICP-MS is sufficient for the calculation of the complexation constants.

4. 3. 6. 4. Humic substances detection

As a first step, the sensitivity of the DAD technique for the detection of humic substances was explored. For humic substances, the main limitation is the short cross path of the light through the solution.

The capillary inner diameter is 50 or 75 μm. Larger diameters would influence negatively the separation in the CE (Landers, 1998). The pathway of the light is therefore extremely limited in comparison with that of a UV/VIS spectroscopy cell (10 mm).

Two types of analysing cells were delivered by the Knauer company and tested for their suitability. The main difference between them was the focusing of the light. Fig. 34 presents a schematic description of the two cells.

It can be observed that the first cell has the focusing lenses further from the capillary than the second one. In this case it was possible to work with thicker capillaries, as this cell is intended for the detection in HPLC capillaries which are considerably thicker than the ones used for electrophoresis. The diameter of the

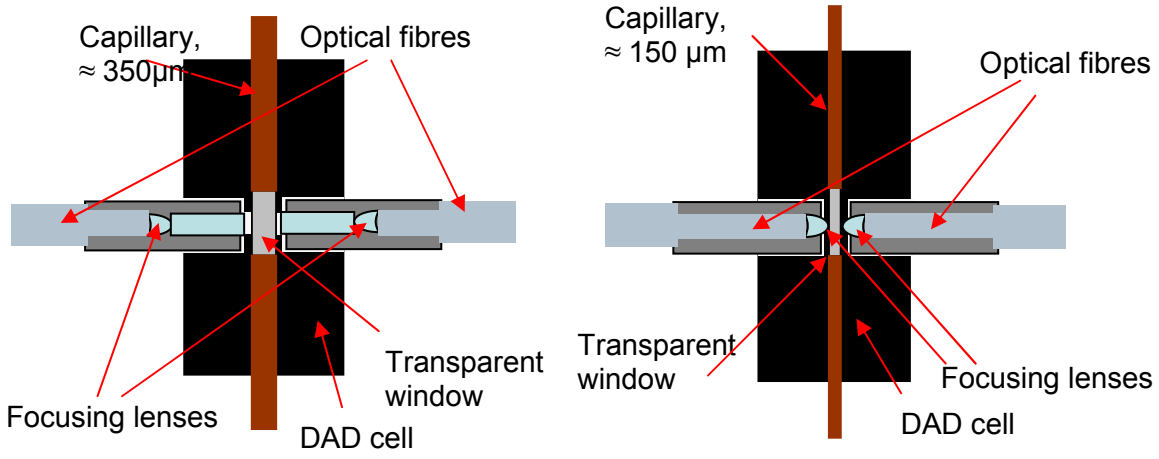

(a) (b)

Figure 34: Schematic depiction of the two employed DAD cells. In the case (a) the outer diameter of the capillary was 350 µm; in case (b) only a thinner capillary can be used;

focusing spot in the first case is also larger than the outer diameter of the capillary (around 2 mm for the focussing spot, in comparison with ≈ 350 µm for the capillary outer diameter). This affects the sensitivity of the technique, as the light is not solely focused onto the sample, hence the signal on the detectors is dominated by the light that does not interact with the sample.

This leads to a loss in sensitivity, as small modifications of the absorbed light are not detected above the high background. The second cell is designed for thinner capillaries. The capillaries with ≈ 350 µm outer diameters do not fit in this cell, only those with ≈ 150 µm outer diameter do. The drawback of this cell is that its inner space is too broad, so the capillary can bend inside the cell.

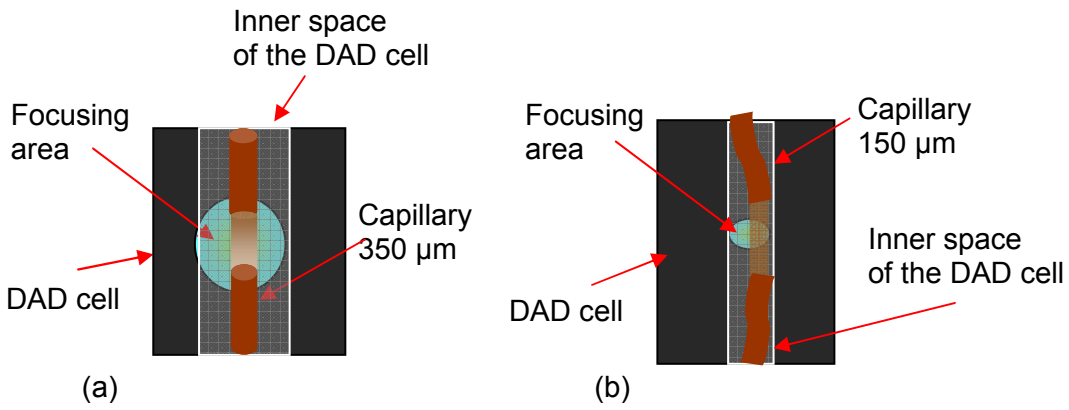

Figure 35: Cut through two DAD cell, (a) a HPLC cell with larger inner space, and larger focusing area; (b) a cell with smaller focusing area (lenses closer to the capillary) and smaller inner space

This can complicate the positioning of the transparent window in the focusing area even more as presented in the Fig. 35, as the focusing spot is much smaller.

As a first step for the studies of the complexation of plutonium by humic substances, the migration of Aldrich humic acid through CE and the possibility to detect it was investigated. Both cells were tested for the investigation of samples containing Aldrich humic acid. The conditions for the experiments were selected similarly to those which will be used for the experiments including the metal species later. They are summarized in Tab. 20.

Tabel 20: Experimental conditions for the detection of Aldrich humic acid with CE-DAD

Parameter	Conditions
Electrolyte	1 M AcOH, pH ≈ 2,4
Separation conditions	30 kV, 0 - 75 mbar, 15 – 32 µA
Capillary	Fused silica, 75 µm inner diameter, ≈ 58 cm length from start to the transparent window
Sample introduction	5 – 10 s, at 50 – 100 mbar.
EOF marker	Acetone, Water

The DAD cell with the larger inner diameter was found more suited with respect to the stability of the signal. In the case of the other one, very small vibrations were enough to induce high deviation of the standard signal. With other words, the capillary could move very easily in and out of the focusing area of the light.

A specific signal was obtained for the Aldrich humic substances as presented in the 3D plot in Fig. 36. By changing the polarity of the electrical field and applying a slight pressure (75 mbar) at the start of the capillary, it was demonstrated that it is possible to obtain a negatively charged species at the end of the capillary even if a negative voltage is applied.

The reproducibility of the migration times through the capillary was > 95%. Using this arrangement it was possible to detect a solution of Aldrich humic acid with a minimum concentration of 500 mg/L.

The DAD software permits the online monitoring of just the temporal variation for up to 4 specific wavelengths simultaneously. In this way, different species that are found in front of the detector at the same time can be differentiated, if their light absorption occurs at different wavelengths. The temporal variation of the signal over the entire wavelength range is stored and after the run is finished, a 3D plot can be reconstructed. Thus, by analysing the 3D

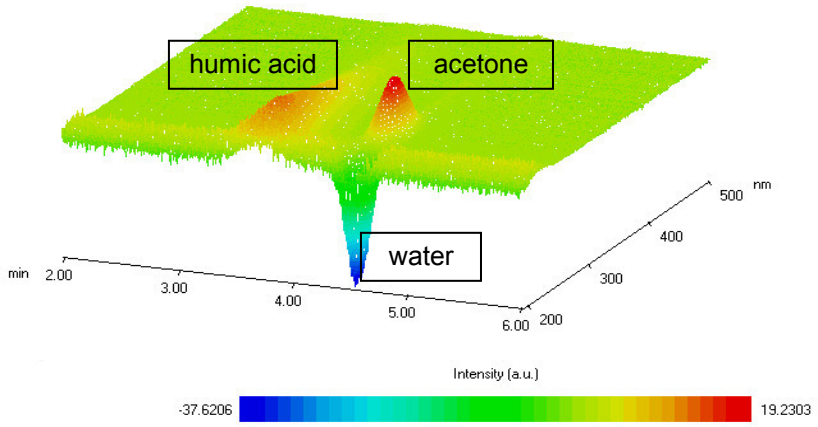

Figure 36: Electropherogram of Aldrich humic acid separation with CE.

plot, the wavelength at which the investigated species shows the maximum light absorption can be selected, and its presence in front of the detector can be easier observed online. Fig. 36 presents the 3D plot of the separation of Aldrich humic acid from the neutrally charged water and acetone. Fig. 37 presents the same run, monitored for two different wavelengths (207 nm and 249 nm). The detection limits achieved with this setup are not low enough for the studies of the interaction of plutonium with humic substances under environmentally relevant conditions.

Because the DAD relies on sensing the differences in light transmission from the light source to the detectors, one possibility to reduce the detection limit is to eliminate the background light in the case of the DAD cell with larger inner space (Fig.38 (a)).

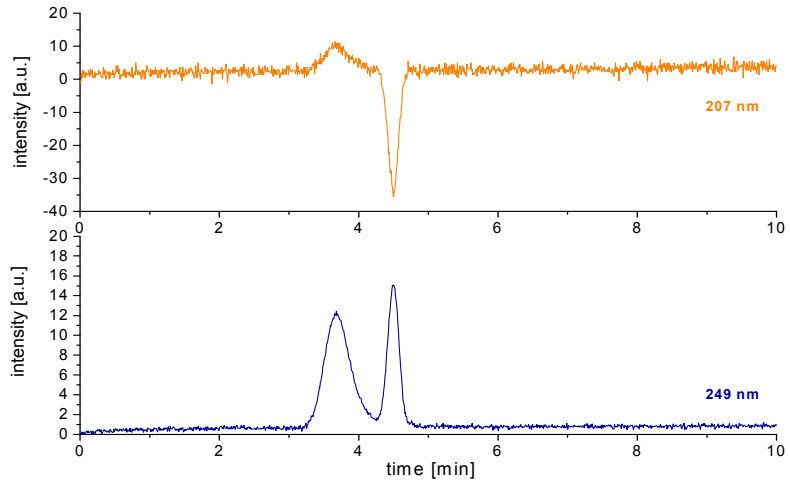

Figure 37: Electropherograms of Aldrich humic acid recorded at different wavelengths; the EOF markers were water and acetone

Due to the fact that the focus spot is much larger than the effective analysing area, light changes in the smaller area will not produce a significant alteration of the entire light transmission sensed by the detectors.

By blocking the transmission of the background light, the changes in light absorption in the capillary have a much higher significance. This effect is presented in Fig.38. A piece capable to block the background light was designed and constructed in our workshop. Its role in addition to blocking the unexploited light, was to centre the capillary in the right position. The distinctive feature at constructing this adaptor was its extremely small dimension as seen in Fig. 39. Using the designed adaptor, the detection limit for Aldrich humic acid could be lowered to 20 mg/L. This is a concentration that is relevant for environmental samples.

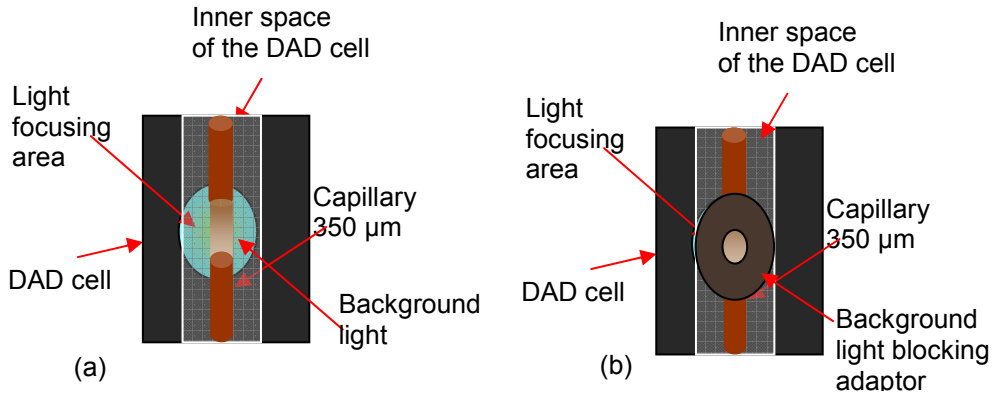

Figure 38: The effect of a light blocking adaptor on the sensitivity of DAD.

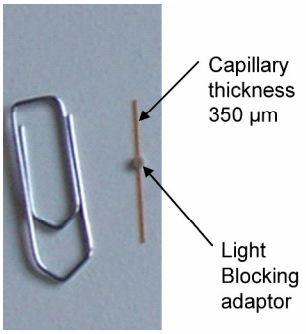

Figure 39: The light blocking adaptor in comparison with a usual size paper clip

4. 3. 6. 5. Feasibility of CE-DAD-ICP-MS

After the individual testing of both detection systems, the coordination between the two detectors was assessed.

First tests were performed with a highly concentrated solution of iodine and iodide, as it can be easily detected by both detectors. The separation was performed under the conditions summarized in Tab. 21. Two separate peaks were obtained with the DAD, as shown in Fig. 40.

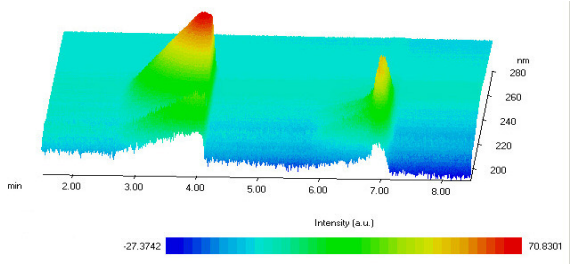

Figure 40: Detection of two species of ^{127}I by DAD after separation with CE.

The same separation was monitored at the same time by ICP-MS set on mass 127. Two different peaks corresponding to iodine carrying species were obtained with this method, too.

The electropherogram obtained on the optimal wavelength channel, with the DAD was compared with the one obtained with the ICP-MS in order to evaluate their resemblance as presented in Fig. 41. It can be observed that there is a time scale shifting between the two detectors. This can be explained by the experimental arrangements.

Tabel 21.: Experimental conditions for the separation of the iodine species.

Parameter	Conditions
Electrolyte	1 M AcOH, pH ≈ 2,4
Separation conditions	-30 kV, 75 mbar, 15 – 32 µA
Capillary	Fused silica, 75 µm inner diameter, ≈ 58 cm length from start to the transparent window
Sample introduction	5 – 10 s, at 50 – 100 mbar.

Since the species are detected by the DAD at ≈ 15 cm apart from the end of the capillary, they still have to undergo the entire length of the column before they can be transferred into the nebuliser, nebulised and eventually transported to the plasma. The cumulated effect is expressed as a delay of about two minutes between the signals of the two detectors.

The differences in peak areas are caused by the different properties used for detection. While the ICP-MS counts ions, the DAD measures light absorption. If the two species have different extinction coefficients, a smaller amount of the

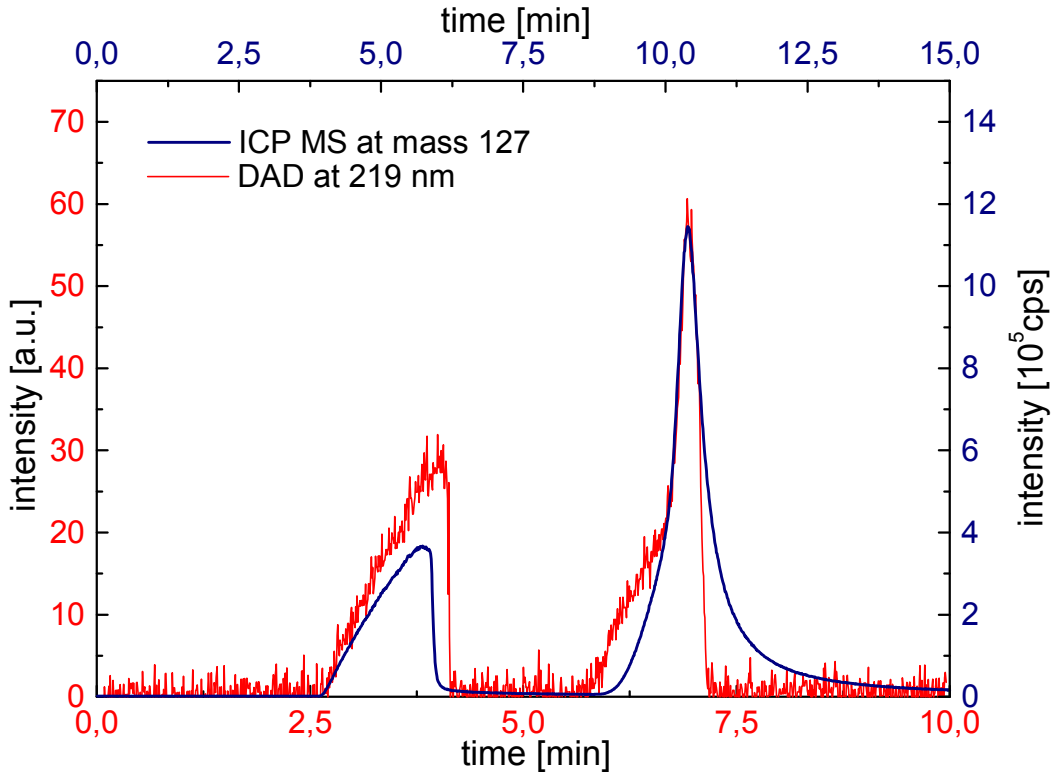

Figure 41: Equivalence of the DAD with ICP-MS. The peaks are obtained by monitoring concomitant the separation of the iodine/iodide solution with the DAD set on wavelength 219 nm and the ICP-MS on mass 127. The tailing of the peaks is caused by the high concentration of the solution

substance with high extinction coefficient could lead to the same signal intensity as the substance present in higher concentration, but with lower extinction coefficient.

In conclusion, a good agreement was found between the results for the separation of the iodine and iodide species obtained with the two detectors.

The step described above can be used for the calibration of the delay time between the DAD and ICP-MS.

The separation of different species of plutonium and humic substances by CE, and the detection of both (metal and humic substances) was performed only separately so far.

Unfortunately, the ICP-MS used in this work has become inoperable because of a series of technical failures and aging effects. It was thus impossible to investigate solutions containing free plutonium ions, plutonium/humat complexes, and free humic substances. The acquisition of a new ICP-MS is planned for the autumn of 2006.

The separation of free metal ions from complexed ions and humic substances, respectively, was applied successfully for the investigation of the

complexation behaviour of lanthanides with humic acid by Kautenburger *et al.* (2006), co-workers in the project "Migration von Actiniden im System Ton, Huminstoff, Aquifer". They used a similar setup for the separation, with detection of both positively as well as negatively charged species at the end of the capillary by applying a slight argon pressure at the starting point.

The main modification of this method is the detection of the humic species as they did not use a DAD. Instead, they use iodine spiked humic acid, which is detected by the ICP-MS set on the mass 127. The results obtained for the complexation constants were in good agreement with the literature.

Therefore, there is a good chance that the CE-DAD-ICP-MS will turn out to be a suitable method for the determination of the complexation constants of plutonium and other actinides with humic and fulvic acid. Further experiments are presently conducted (Diploma thesis of D. Kutscher) in collaboration with the Institute of Inorganic and Analytical Chemistry from Johannes Gutenberg-Universität Mainz, for developing the method. These experiments are, however, carried out with non radioactive metals for safety reasons. The adaption of the method to plutonium species is anticipated as soon as the new ICP-MS is available.

4. 3. 7. X-ray Absorption Fine Structure

X-ray absorption spectroscopy (XAS) measures the absorption of X-rays by a sample, as a function of X-ray energy.

The phenomenon was observed about 70 years ago, but the development of this method as a source for accurate structural information was a much sustained process (Rehr, 2000).

X-ray absorption fine structure (XAFS) is the modulation of the X-ray absorption coefficient at beam energies near and above the so called X-ray absorption edge. The intensity of the X-ray absorption varies with the thickness of the sample and the absorption coefficient as described below. We have

$$I = I_0 e^{-\mu x} \qquad (25)$$

where x is the thickness of the sample, I_0 and I the intensity of the incoming and outgoing X-ray beam, respectively, and μ the absorption coefficient.

The absorption coefficient μ depends strongly on X-ray energy (E) and atomic number of the sample (Z), and on the density (ρ) and Atomic mass (A).

$$\mu \approx \frac{\rho Z^4}{AE^3} \qquad (26)$$

In addition, μ has sharp absorption edges corresponding to the characteristic core-level energies of each specific atom. The photon energy of the X-rays is gradually increased such that it traverses one of the absorption edges of the elements contained within the sample. Below the absorption edge, the photons cannot excite the electrons of the relevant atomic level and thus absorption is low. However, when the photon energy is just sufficient to excite the electrons, then a large increase in absorption occurs, known as the absorption edge.

All elements with Z > 18 have a K- or an L-edge between 3 and 35 keV, which can be achieved by many synchrotron sources.

The electrons receive energy from the photons, and are ejected leaving behind a core hole. The excited core-hole will relax back to a ground state of the atom, by dropping of an electron from a higher level core, and a fluorescent X-ray or an Auger electron is emitted.

The energy of the photoelectrons so formed is equal to the energy of the photon minus the binding energy. The photoelectron interacts with electrons from the surrounding non-excited atoms. If the photoelectron is compared to a wave and the surrounding atoms are considered as point scatterers, then it is possible to imagine that the back scattered

photoelectron waves will interfere with the outgoing waves as presented in Fig.42.

The resulting interferences from a single scattering are generally weak oscillations at about 30eV beyond the absorption edge and are monitored by EXAFS (extended X-ray absorption fine structure). The region closer to an edge is characterized by stronger scattering processes (multi-scattering and local atomic resonances) and is referred as the X-ray absorption near-edge structure, or XANES (Rehr, 2000).

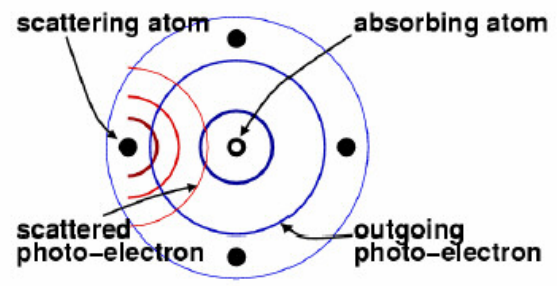

Figure 42: Pictorial view of the back scattering of an outgoing wave off neighbouring atoms (picture from Newville, 2004)

The data interpretation of EXAFS contains precise information about the atomic structure around the photon absorbing atom. XANES spectra are more complicated but they can help to explain what bonding orbitals and structural characteristic give rise to certain spectral features.

The X-ray absorption spectroscopy can measure individually the *Transmission* when the loss in beam intensity is determined directly by measuring what is transmitted through the sample, or the *Fluorescence*, when the fluorescent X-rays emitted by the re-filling of a deep core hole is detected.

With the help of XAS, important knowledge on the speciation and the vicinity of the absorbing atoms can be achieved.

Since the method requires a tunable X-ray source, the experiments are performed at synchrotrons, on beamlines specially adapted for this purpose.

The experiments conducted in the frame of this work, took place at the beamline of the Institut für Nukleare Entsorgung (INE) at the ANKA Synchrotron Light Source FZK. The energy range at this beam line is 2.3 - 23 keV and it has a resolution of 2×10^{-4} $\Delta E/E$ (ANKA website).

5. Investigations on the interaction of plutonium with humic substances and kaolinite in aqueous solutions

The study of plutonium under conditions similar to those expected in nature is a very complex task. This element is found in very low concentrations and it can coexist in four oxidation states at the same time in solution (see chapter 2. 1).

The natural groundwater is also a complex matrix which contains a large variety of organic and inorganic substances, micro organisms, and minerals dissolved or suspended over a pH range that can vary from acidic to basic.

In order to facilitate the understanding of the influence of some important components of the groundwater and of the surrounding rock formations on the migration behaviour of plutonium with respect to the safety assessments of the deep geological nuclear waste repositories, simple models containing just small parts of the large matrix were created.

This work was focused on studying the interaction of plutonium with humic substances and kaolinite as a model for clay minerals, in binary and ternary systems.

The chemicals used in this work were of "pro analysi" quality, purchased from Merck (Darmstadt, Germany), Riedel de Haen (Seelze, Germany), and Fluka (Buchs, Switzerland). The solutions were prepared using Milli-Q deionised water with 18 MΩ conductivity, produced with a Millipore® (Schwalbach, Germany) installation. The ICP standard solutions were purchased from Merck.

The humic acid was commercially available (Aldrich, München, Germany) sodium salt, charge no. 01816-054 with a PEC=5.43±0.2x10^{-3} eq/g, purified as described by Kim *et al.* (1990). The Gorleben fulvic acid charge no. GoHy-573, PEC=5.63x10^{-3} eq/g, was also isolated and purified as described by Kim *et al.* (1990). The kaolinite was KGa-1b as described in chapter 3. 2. 1.

The stock solutions of plutonium consisted of 99.1wt% ^{239}Pu, 0.88 wt% ^{240}Pu, and 0.014 wt% ^{241}Pu, in 1 M $HClO_4$. It consisted of a mixture of several oxidation states.

The pH was measured by a φ – 310 (Beckmann, Germany) or inoLab pH 720 (WTW, Germany). They were calibrated daily with certified commercial buffers, pH 2, pH 4, pH 7, and pH 9 (Merck, Germany).

5. 1. The binary system Plutonium – Humic Substances

The influence of solved humic substances on the speciation of plutonium in aqueous solutions with respect to its migration behaviour has been studied by different authors (Chopin, 1988), (Kim *et al.*, 1996), (Chopin, 2003) (Marquardt, 2000). All of them have assented to the fact that plutonium is reduced to lower oxidation states in the presence of the humic substances.

At the Institut für Kernchemie in Mainz, a solution containing all four relevant oxidation states of plutonium (Pu(III) 5.1%, Pu(IV) 39.2%, Pu(V) 22.1%, and Pu(VI) 33.6%) with a concentration of [^{239}Pu] ≈ 6 ·10^{-5} M was contacted with Gorleben 573 fulvic acid (GoHy-573) in an aqueous solution at pH ≈ 1. The change in the oxidation states composition was observed by CE-ICP-MS.

The concentration of the fulvic acid was increased in steps of 2 mg/L until the concentration of 36 mg/L was reached. After this point, the concentrations of both components were maintained constant. The experiments were performed under atmospheric conditions at room temperature and light. As presented in Fig. 43, the redox equilibrium is strongly affected by fulvic acid. It was observed that after a relatively short time (in comparison to the half-life of plutonium) Pu(III) and Pu(IV) are the predominant oxidation states found in solution. It was also observed that the reduction of Pu(VI) is much faster than the one of Pu(V).

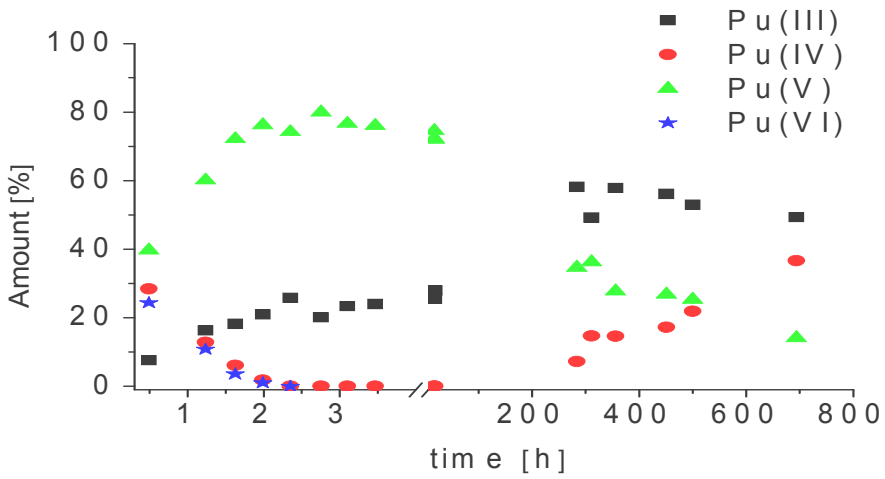

Figure 43: The reduction of plutonium in contact with GoHy-573 fulvic acid as a function of contact time

The same reduction effects were reported for humic acids (Kuczewski, 2004), (Bürger, 2005), (Marquardt *et al.*, 2004)

The reduction occurs faster in the presence of fulvic acids, than in the presence of humic acids. It can be assumed that because of the ubiquitous presence, of humic substances plutonium is reduced if it enters the groundwater after accidental release from nuclear waste repositories.

The work at the "Institut für Kernchemie" was therefore, focused on the study of the most likely oxidation states in ground waters in the presence of humic substances, Pu(III) and Pu(IV). This work comprises the investigation of the interactions of Pu(III) with humic substances and kaolinite in aqueous solutions. The behaviour of Pu(IV) under the same conditions has been conducted by N. Banik, in a parallel work (PhD thesis in preparation).

5. 1. 1. The interactions of Pu(III) with humic substances

Pu(III) was electrolytically prepared as described in chapter 4.2 from a stock solution composed of all oxidation sates of plutonium at a concentration of ~ $1x10^{-4}$ M in $HClO_4$. Roughly three hours were necessary for a complete conversion to Pu(III) for a volume of about 2 ml. The electrolysis was conducted in a hood under aerobic conditions. The oxidation state of the final solution was verified by UV/VIS spectroscopy. Fig. 44 shows a spectrum obtained with the spectrometer described above.

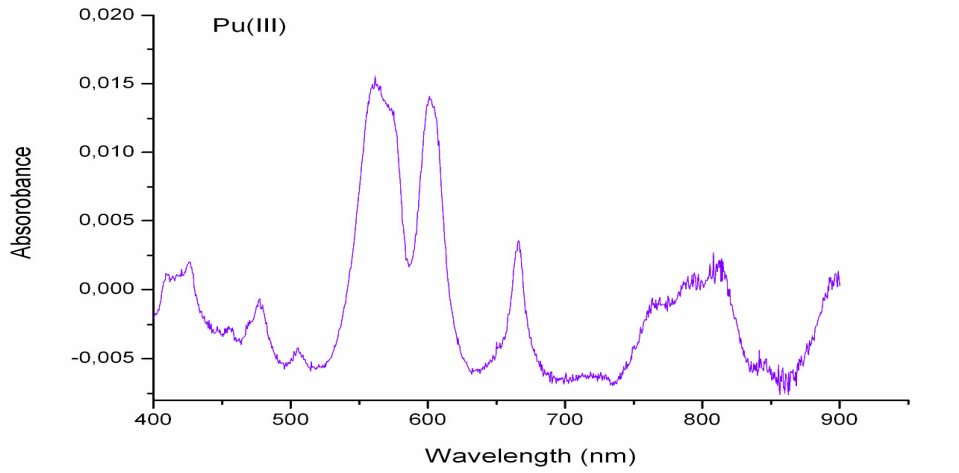

Figure 44: Spectrum of Pu(III) obtained by UV-VIS spectroscopy after 3 h and 15 min. electrolysis time

In order to obtain explicit data on Pu(III), it had to be assured that the oxidation state remains unchanged under the conditions that would be used later on in the experiments.

The stability of a solution of Pu(III) with a concentration ~ $8x10^{-5}$ M in 1 M $HClO_4$ was investigated by UV/VIS spectroscopy. It was found that the solution contained > 95 % Pu(III) even after more than one month from the moment of the preparation. This experiment was conducted at pH < 1, under aerobical conditions, at room temperature. The pH 0.1(1 M $HClO_4$) is however not relevant for natural conditions.

It was stated that the speciation of plutonium in aqueous solutions is strongly dependent on pH (Runde, 2000) (Jianxin et al., 1993) (see also Fig. 12). Therefore, a solution of freshly prepared Pu(III) with a concentration of $7.6x10^{-6}$ M in 0.1 M $NaClO_4$ at pH 5.5 was investigated by CE-ICP-MS over a period of about two weeks with respect to the redox behaviour of plutonium. All the solutions used in the experiment except the plutonium stock solutions, were stored in the inert gas box for minimum one week before they were used in the experiments in order to remove as much as possible of the dissolved oxygen. The pH 5.5 was adjusted in the beginning of the experiment and constantly verified. No pH buffer was used, because this could also influence the complicated chemistry of plutonium. The experiment was conducted in an inert gas box (Ar, $[O_2]$ ~ 1 – 3 ppm) at room temperature. The solution was kept in perfluoroalkoxy fluorocarbon (PFA) vials under continuous stirring. The Eh of the solution was not measured. Fig. 45 illustrates the changes in the oxidation state composition of the solution.

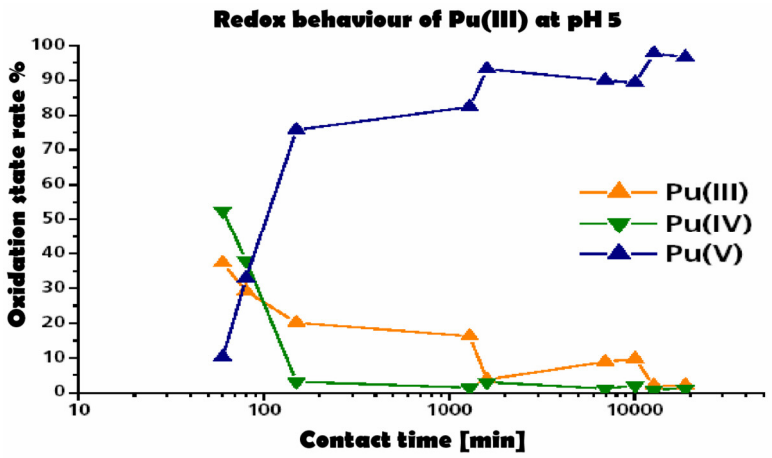

Figure 45: The oxidation of Pu(III) at pH 5.5, under argon atmosphere

The estimated time elapsed between mixing of the plutonium stock solution dissolved in 1 M $HClO_4$, with the aqueous solution and the first analysis, was about one hour. Although the initial solution contained > 95% Pu(III), it can be observed that in the short period of time elapsed, a considerable change in the oxidation state composition occurred.

It was concluded that Pu(III) is rapidly oxidised at neutral pH values. It was also assumed that at higher pH values, the oxidation will take place even faster.

Because the experiments with Pu(III) have been planned over a large pH range (1 – 11) a modality to keep it in the reduced form had to be found.

First, it was tested to stabilise Pu(III) with humic substances as their reducing effect was already known.

Two similar experiments as the one just described above, were performed. The only alteration was that GoHy-573 fulvic acid (GoHy 573 FA) was added in concentrations [GoHy 573 FA] = 1.5 mg/L and [GoHy 573 FA] = 15 mg/L, respectively. The fulvic acid was dissolved previously in Milli Q water, and it was stored at pH ~ 7 in the inert gas box for minimum one week before inserting it in the experiment vessels.

The concentration of 1.5 mg/L of GoHy 573 FA was not sufficient to stabilize the oxidation state in a reduced form. However, the experiment was strongly hindered by sorption of plutonium on the vessel walls. This was determined by emptying the vessels, rinsing them with Milli Q water, and after they were dried out removing the plutonium with a mixture of 0.36 M HCl/0.05 M HF. The amount of plutonium found on the walls was more than 65 % of the starting amount. Therefore, the data could not be reasonably interpreted.

In the solution containing 15 mg/L GoHy-573 FA, plutonium has undergone a fast oxidation followed by a slower reduction so that after 14 days the fraction of Pu(III) in solution was > 90% as shown in Fig. 46. The recovery rate of plutonium in solution was also high, as the wall adsorption was considerably lower (~ 20 %) so an unambiguous interpretation of the CE-ICP-MS spectra was possible.

One explanation for the fast oxidation registered in the first minutes after the mixing of the reactants, could be given by the fact that the solution could still contain a high amount of oxygen dissolved. Another factor that could have an influence on the results is the fact that the CE-ICP-MS analysis cannot be performed inside the inert gas box.

The samples must be exposed to the atmospheric conditions for a short period before they can be analysed. The longest period that could elapse between the contact with the air and the actual

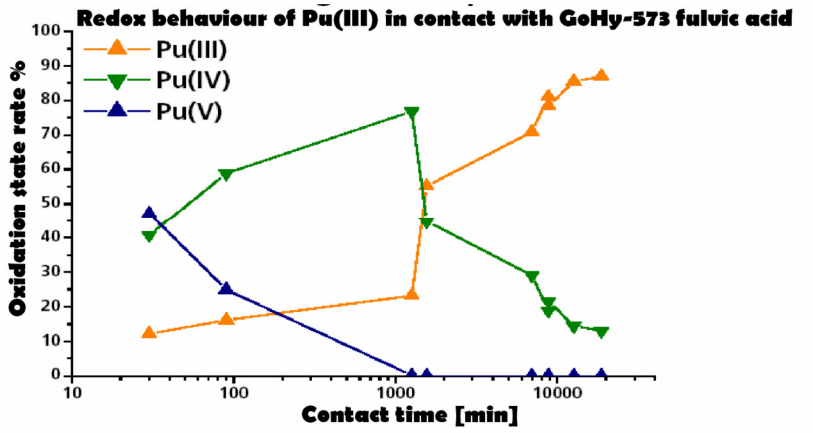

Figure 46: The redox behaviour of Pu(III) in presence of GoHy-573 fulvic acid; [GoHy-573 FA] = 15 mg/L, pH 5.5, argon atmosphere

injection of the sample into the CE, is estimated at < 5 minutes. This is relatively short, but as observed in Fig. 46 the redox kinetics of plutonium at this pH is very fast.

The influence of the air on this solution was investigated. For this, an aliquot of 600 µL from the 2 weeks old solution was taken out, measured by CE-ICP-MS, and left over for two days in contact with air. After two days it was measured again. Fig. 47 presents the two electropherograms obtained for this solution.

It can be concluded that in the presence of air, the fulvic acids cannot stabilize plutonium in the Pu(III) form.

Further reducing agents were tested. Other groups have tried to reduce plutonium with NH_4I or ascorbic acid (Ambard *et al.*, 2005). In this work, the

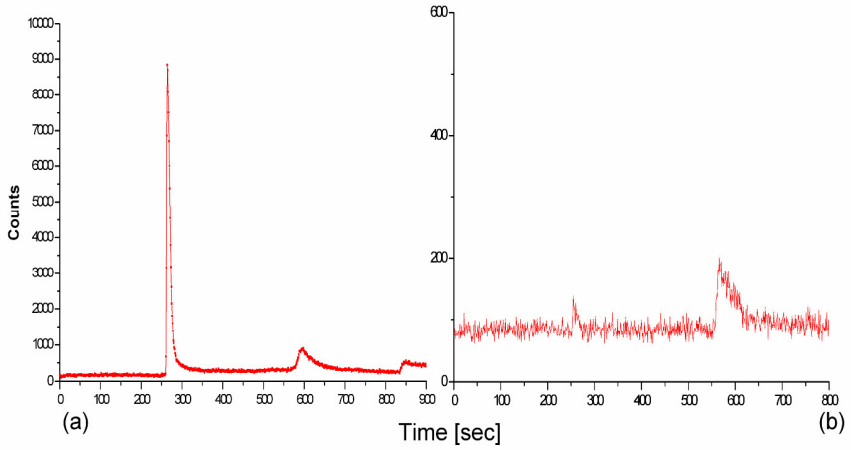

Figure 47: Electropherograms obtained for a solution of Pu(III) in aqueous solution in contact with 15 mg/L GoHy-573 fulvic acid, short after taking it out of the inert gas box (a), and the same solution after 2 days contact with air (b)

potential of hydroxy-amonium hydrochloride, ß-alanin, and ascorbic acid to stabilize Pu(III) was tested.

Because the ICP-MS became inoperable as a result of multiple technical failures, the speciation by CE-ICP-MS could no longer be performed. Liquid-liquid extraction was used instead. This method has the advantage that is more sensitive as the CE-ICP-MS, but has a relatively high experimental uncertainty. Another limitation of the method in the present issue is the fact that the agents used for maintaining Pu(III) in the reduced form, interact with the oxidation agents used by the liquid-liquid extraction in step 2 and 4, (see chapter 4. 3. 2). The correct interpretation of the results is thus problematic. The first step is however not affected by the reducing agents. Therefore, the results of this experiment will refer to the amount of Pu(IV) found in solution, as it was assumed that if its fraction is minor, the amounts of the (V) and (VI) oxidation states will be even lower.

The experiments were performed on a freshly electrolysed Pu(III) solution, under atmospheric conditions and at room temperature. Four solutions of Pu(III) with a concentration of ~ $2x10^{-7}$ M in 0.1 M $NaClO_4$ were prepared at three different pH values (0, 3, and 5). Three of them were mixed separately with hydroxy-amonium hydrochloride, ß-alanin, and ascorbic acid, and the fourth was used as a reference for each pH value independently. The concentration of all the reducing agents was 0.025 M in all the experiments.

The amount of Pu(IV) found in the four solutions at pH 0, was minor.

In the solutions prepared at pH 3, the amount of Pu(IV) found was considerably higher in the solution where no reducing agent was used. Fig. 48 illustrates the effect of the reducing agents on the amount of Pu(IV) formed and found in solutions.

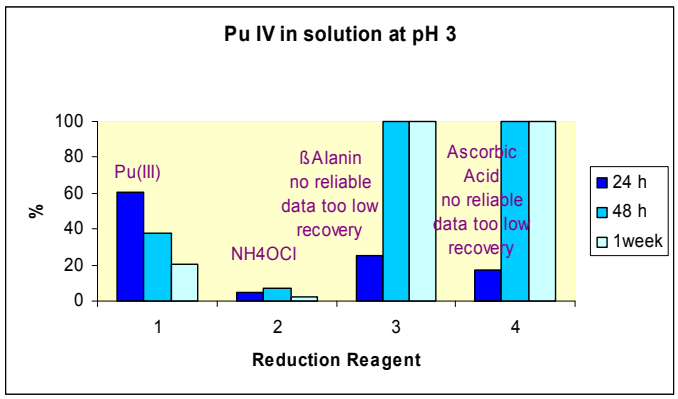

Figure 48: The influence of NH_2OHHCl, ß-alanin, and ascorbic acid on the stabilization of Pu(III) in a $NaClO_4$ 0.1 M solution at pH 3, under atmospheric conditions

It was found that NH_2OHHCl is the most suited agent in order to stabilize a Pu(III) solution under these conditions. The data obtained after 48 hours for the solutions mixed with ß-alanin and ascorbic acid were not reliable, as the recovery of the radioactivity corresponding to plutonium was very low. It was later found that the adsorption on the walls of the vessels (polyethylene,(PE) vials) was exceptionally high in these cases. This was not the case for the solutions mixed with NH_2OHHCl.

The adsorption on the walls of the vessels was extremely high in the experiments with the solutions prepared at pH 5. This is why the data could not be accurately interpreted.

The adsorption of plutonium on the vessel walls was determined by desorbing it with a mixture of 0.36 M HCl/0.05 M HF, after the procedure described earlier on in this paragraph, from the walls. The oxidation state of the desorbed plutonium was determined by liquid-liquid extraction to be almost 100% Pu(IV).

The potential of NH_2OHHCl as a reducing agent was further tested for the stabilization of Pu(III). Therefore, solutions of [Pu(III)] = $5.3x10^{-5}$ M were mixed at pH 3, 3.5, 4, and 4.5 with NH_2OHHCl under the same conditions as in the previous experiments. The higher concentrations were chosen in order to avoid the problems related with the wall adsorption encountered in the earlier experiments. More concentrations of the reducing agent were also tested (0.0025, 0.01, 0.025, and 0.25 M) at all the pH values.

It was found that a concentration of 0.025 is necessary and sufficient in order to maintain the rate of Pu(IV) in solution <7% up to pH 4. For higher pH values this could not be achieved, even with higher concentrations of NH_2OHHCl.

In the frame of this work, there were planned experiments with Pu(III) at higher pH values too (see next chapters). Therefore, a modality to stabilize Pu(III) in solutions at pH > 4 was further searched.

The experiments were conducted this time in an inert gas box (argon, [O_2], [H_2O] < 3 ppm). Only the influence of NH_2OHHCl 0.025 M on the redox behaviour of Pu(III) was investigated based on the experience gained in the previous research. It was found that under argon atmosphere, the ratio of Pu(IV) in solution could be kept under 5 – 7% using this reagent up to pH ~ 5.5 – 6. In a more basic medium, even in the absence of oxygen, plutonium was oxidised to higher oxidation states.

It can be observed that even in the presence of reducing agents, there was always found a small amount of Pu(IV) in solution. This was explained through the equilibrium suggested by the eq. (27).

$$Pu(III) \xrightarrow{pe,pH} Pu(IV)$$
$$Pu(III) \xleftarrow[NH_2OHHCl]{} Pu(IV) \quad (27)$$

Neck *et al*. (2006) have reported a strong influence of the oxidation on the pe and pH.

It is thus possible, in the following experiments to encounter a minor interference effect of the interactions of Pu(IV) with the reagents parallel to the investigated Pu(III).

All the further experiments with Pu(III) have been performed in the presence 0.025 M NH_2OHHCL in order to stabilize as much as possible Pu(III).

5. 1. 2. Investigation of the complexation of Pu(III) with Aldrich humic acid

The complexation of actinides with humic acids could lead to a mobilization of the radiotoxic elements accidentally released from nuclear waste repositories in the groundwater. The heavy actinides could be easier transported once they are bounded to the larger, colloidal humic substances.

Therefore, their complexation has been largely investigated over the last decades (Choppin et al., 1985), (Moulin et al., 1992), (Czerwinski et al., 1996), (Kim et al., 1996, (Marquardt, 2000).

Several models have been produced in order to explain the complexation of the humic acids with metal ions (Ephraim, et al., 1986), (Perdue, 1989), (Tipping, 1993). The models lead to conditional complexation constants that were difficult to compare with one another.

Therefore, J. I. Kim and K. R. Czerwinski (1996) have created a model (metal ion charge neutralization model) based on the concept of metal-ion charge neutralization upon complexation to humic acid functional groups. Hence, the complexation reaction is considered as eq. 28

$$M^{z+} + HA(z) \Leftrightarrow MHA(z) \quad (28)$$

M^{z+} - metal charged with $z+$

HA(z) – humic acid complexation unit (group of complexing sites needed to neutralize metal ion)

MHA(z) – metal ion humate complex

The complexation constant (ß) can be defined based on this equation as:

$$\beta = \frac{[MHA(z)]}{[M^{z+}]_f [HA(z)]_f} \quad (29)$$

[MHA(z]) – concentration of the metal ion humate complex

$[M^{z+}]_f$ – the free metal ion concentration

$[HA(z)]_f$ – the free humic acid concentration

It is considered that a metal ion of higher charge has the capacity to attract proton exchanging sites for charge neutralization even if the latter are not situated at equal distances from the metal. By introducing a term named operational concentration of humic acid ($[HA(z)]_t$) which is calculated from the known proton exchange capacity (PEC), the total amount of humic acid (HA), and the charge of the metal ion (z) (eq. 30), it defines the loading capacity (LC) of the humic acid (eq. 31).

$$[HA(z)]_t = \frac{(HA)(PEC)}{z} \qquad (30)$$

$$LC = \frac{[MHA(z)]_m}{[HA(z)]_t} \text{ or } LC = \frac{z[M^{z+}]^*}{(PEC)(HA)} \qquad (31)$$

$[MHA(z)]_m$ – concentration of humate metal ion complex

$[M^{z+}]^*$ - maximal concentration of metal permissible for complexation with a given humic acid under the experimental conditions

The LC is dependent on the pH, ionic strength, charge of the metal ion and origin of the humic acid (Kim *et al.*, 1991), (Moulin *et al.*, 1987).

Knowing the LC , the concentration of free humic acid in eq. 29 can be calculated as:

$$[HA(z)]_f = [HA(z)]_t LC - [MHA(z)] \qquad (32)$$

The complexation constant (ß) can be calculated combining eq. 29 and eq. 32 as:

$$\beta = \frac{[MHA(z)]}{[M^{z+}]_f ([HA(z)]_t LC - [MHA(z)])} \qquad (33)$$

The LC specific for the reaction conditions can be calculated from the experimental data, and once this is known, ß can be calculated too. This ß value is then independent of the pH, metal ion concentration and origin of humic acid (Kim *et al.*, 1996). In order to simplify the interpretations, it will be expressed as a function logß.

The metal-ion charge neutralization model was used for determining the complexation constants of Aldrich humic acid with Pu(III).

In order to avoid incorrect results induced by possible overlapping reactions such as hydrolysis or formation of carbonate compounds, the humate complexation studies were performed under conditions where these reactions are not expected. pH ≤ 6 was chosen by many authors for trivalent metals (Moulin *et al.*, 1987), (Kim *et al.*, 1996). Fig. 49 presents the speciation of Pu(III) as a function of pH calculated with the programme MEDUSA.

In addition to that, Pu(III) is very fast oxidised at pH > 3, as demonstrated in the previous chapter. Although the

experiments were planned to be conducted under reducing conditions (0.025 M NH_2OHHCl) which can stabilize Pu(III) up to pH 5.5 under inert gas conditions, the highest pH value used for the complexation experiments was pH 4.5. This provided more confidence that the solution will contain mostly Pu(III).

Another limitation concerning the choice of pH was the fact that humic acids precipitate in solutions at pH < 2.5 -3 (see chapter 3. 1). Therefore the pH range for the experiments was pH 3 – 4.5.

The kinetics of the complexation of Pu(III) with Aldrich humic acid was investigated in the presence of 0.025 M NH_2OHHCl, under atmospheric and inert gas conditions. Several solutions of freshly electrolysed [^{239}Pu(III) = 1x10^{-6} M, were mixed with Aldrich humic acid (AHA) at pH 3, 3.5, and 4. The concentrations of humic acid were also varied, ([AHA] = 0, 2.5, 10, 25 mg/L). The ultra filtration technique was employed for these experiments. By simply observing the changes of the ratio free plutonium/complexed plutonium, it was determined that the complexation is fast especially at higher concentrations of AHA. The complexation was completed in maximum one day as shown by Fig. 50 for the solution at pH 3. It can be observed that the recovery of free plutonium after ultrafiltration does not significantly change as a function of time.

For the calculation of the logß these data were not sufficient. Therefore, several additional experiments were performed. The experimental conditions are summarized in the Tab. 22.

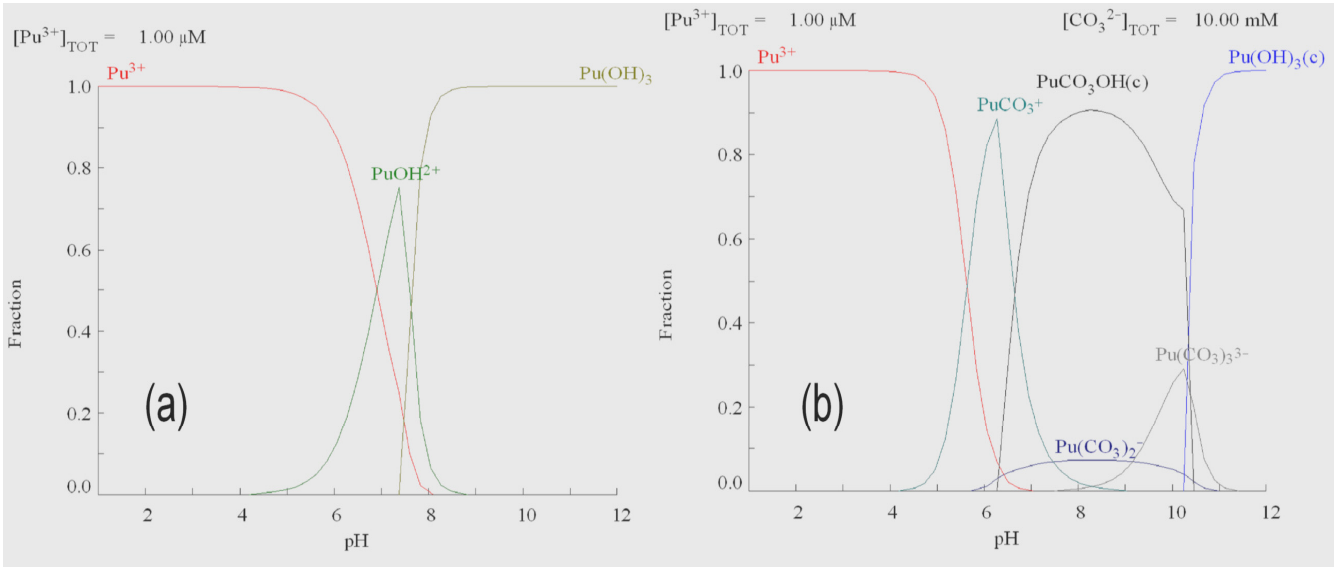

Figure 49: The speciation of Pu(III) in a solution in the absence (a) and presence (b) of CO_2

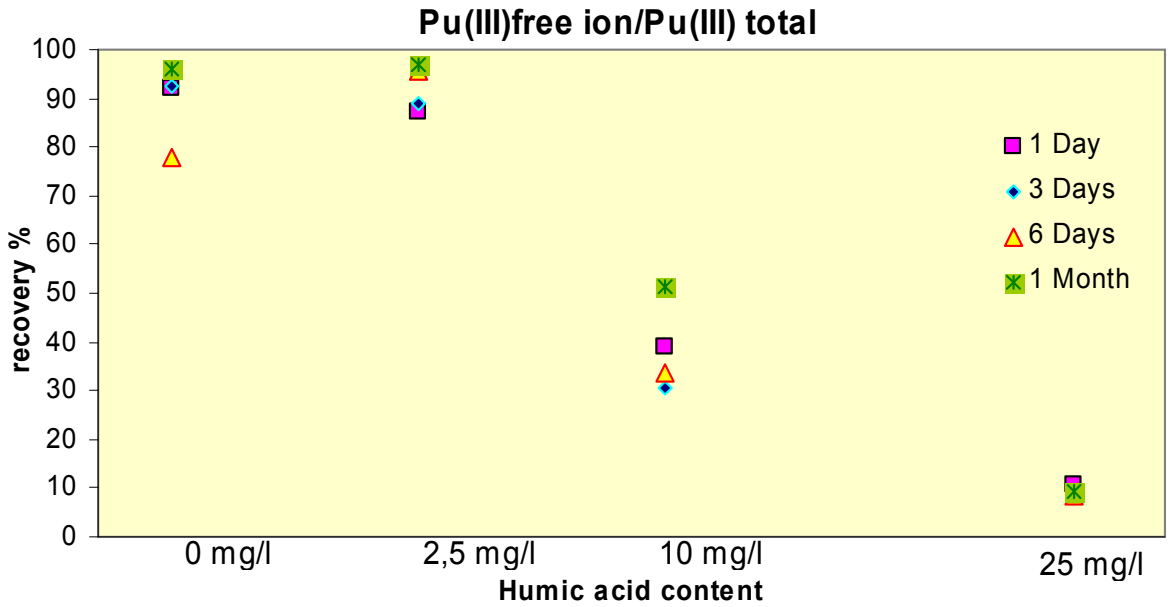

Figure 50: The time dependency of the complexation of Pu(III) with Aldrich humic acid at pH 3 under atmospheric conditions and in the presence of 0.025 M NH_2OHHCl. The experimental failure of the ultra filtration is relatively high

The solutions were prepared in 0.1 M $NaClO_4$, the pH was adjusted, and the activity was immediately checked by LSC. In this way, the precise concentration at the starting point was determined. PE centrifuge vials were used for the preparation and stocking of the solutions.

They were continuously shaken for the entire period of the experiment. After six days, the amount of free metal ion humate complex, respectively, was determined by ultra filtration and subsequently LSC by detecting the activity of the filtrate.

For the accuracy of the results, a correction of the free plutonium sorbed by the filters, walls, and membrane was applied. The solution with no AHA

Table 22: Concentrations and conditions used in the experiments for determining the complexation constant between Pu(III) and Aldrich humic acid

[Pu] mol/L	[AHA] mg/L	pH	Conditions
$1x10^{-6}$	0, 1, 2.5, 5, 7.5, 10, 15 20, 25, 40, 55	3, 4	air and argon
$1x10^{-7}$	0, 1, 2.5, 5, 7.5, 10, 15 20, 25, 40, 55	3, 4	air and argon
$1x10^{-8}$	0, 1, 2.5, 5, 7.5, 10, 15 20, 25, 40, 55	3	air

added, was also filtrated, and the known amount of plutonium lost through the filtration of this solution, was considered the standard loss of free plutonium in the process. For the calculations the PEC of the Aldrich humic acid used was that given by Kim and Czerwinski (1996) (PEC_{AHA} = 5.43±0.2 meq/g). Using this value and performing the calculation as presented above, the following complexation constants were found:

Table 23: The complexation constants of Pu(III) with Aldrich humic acid

pH	LC	logß (L/mol)
3	0.045±0.005	6.21 – 6.86
4	0.11±0.005	6.57 – 6.87

There were no consistent divergences found between the experiments conducted in the inert gas box and those conducted under aerobical conditions.

For the validation of the technique used, the complexation of Am(III) with Aldrich humic acid, following the same steps was also investigated. Am(III) can be considered as an analogue of Pu(III) due to their similar chemistry known so far.

The aim was to compare the data obtained for the experiments performed in our laboratory, with the literature. No literature data was found for the complexation of Pu(III) with humic acid (except for theoretical calculations (Reiller, 2005)), but on the other hand there are a large amount of studies on other trivalent actinides (Kim *et al*., 1991), (Czerwinski *et al*., 1996), (Marquardt, 2000).

A solution of ^{241}Am was contacted with humic acid under similar conditions as in the experiments with plutonium as illustrated in Tab. 24.

The advantage of working with $^{241}Am(III)$ is the certainty that it is always found in the trivalent state in solution and that because of its relatively short half-life (432.2 a (Pfennig *et al*., 1998)) it is possible to work with lower amounts.

The data were processed in the same way as for the calculation of the complexation constants of Pu(III) with AHA.

The loading capacity was found in this case LC ≈ 0.038 and the logß = 6.1–6.7.

The results were in good agreement with the literature as illustrated in Fig.51.

As it can be seen in Fig. 51, the experimental error of the ultra filtration technique is relatively high in spite of the corrections applied. These can be attributed to the pipetting errors, the irregularity of the filters, and the adsorption of plutonium by the vessel walls and the filters.

The interactions of Cm(III) and Am(III) were studied also by time resolved laser fluorescence spectroscopy (TRLFS) (Czerwinski et al., 1996). This method cannot be applied for studies of Pu(III).

Table 24: Concentrations and conditions used in the experiments for determining the complexation constant between Am(III) and Aldrich humic acid

[Am] mol/L	[AHA] mg/L	pH	Conditions
$8x10^{-9}$	0, 0.1, 0.25, 0.5, 1, 2.5, 5, 7.5, 10, 15 20, 30	3.5	air and argon

The coupling of CE-DAD-ICP-MS as an alternative method to the ultra filtration for determining the complexation constants with humic substances is actually under development (see chapter 4. 3. 6).

The complexation constants calculated with the metal-ion charge neutralization model, are directly applicable for geochemical modelling of actinide migration, under variable pH values as expected in nature.

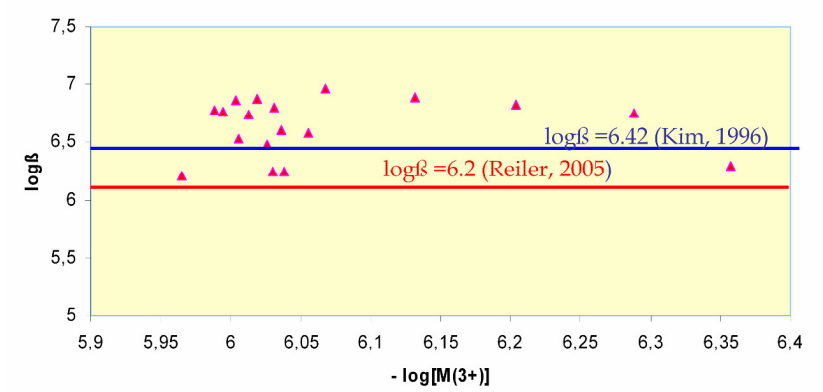

Figure 51: Results from complexation studies of trivalent plutonium (pink triangles) with humic acid compared with experimental data from literature (Kim, 1996) for Am(III) (blue line) and theoretically calculated data for Pu(III) (Reiler, 2005) (red line).

5. 2. The binary system Pu(III) – Kaolinite

It has been mentioned in the earlier chapters that a possibility to prevent the spreading of the radioactive pollutants in the environment after their accidental release from nuclear waste repositories,could be their immediate immobilization by sorption to the host rocks.

Bentonite could be in the future used as backfill material for the disposal of nuclear waste in deep geological formations. Kaolinite, has been chosen as a model mineral for the investigation of the sorption behaviour of Pu(III) on clay minerals (see also chapter 3. 2. 1).

In the frame of the project "*Migration von Actiniden im System Ton, Huminstoff, Aquifer*" it was agreed to perform the sorption studies of actinides on a suspension of 4 g kaolinite/L solution.

The studies carried out in this work were focused on the sorption of Pu(III) onto kaolinite, and Am(III) onto the same solid phase as a analogy study, as Am(III) is an oxidation state analog for the chemistry of Pu(III).

The sorption of Pu(III) onto kaolinite was investigated in batch experiments. For this, a suspension of kaolinite was prepared in 0.1M $NaClO_4$ and the pH was adjusted with 0.1 M NaOH and 0.1 M $HClO_4$. 0.025 M NH_2OHHCl was present from the starting of the experiments as a reducing agent, for the stabilization of Pu(III) (see chapter 5. 1. 1). The solutions were prepared in 15 mL PE centrifuge vials, and were kept in the same vials until the end of the experiments, unless otherwise stated. After the adjustment of the desired pH, the solutions were kept under agitation by rotating the vials end-over-end, for 48 hours. The type of agitation chosen is also important, because if a magnetic stirrer is used, it could lead to a grinding of the kaolinite, increasing thus the sorption surface, hence affecting the results. During the preconditioning time, the pH was monitored and readjusted if necessary.

After 48 hours, stock solutions of freshly electrolysed ^{239}Pu(III) in 1M $HClO_4$ were added, and the pH readjusted. The activity of the solution was measured by LSC immediately after the mixing with Pu(III) for defining the reference for the 0% adsorption of plutonium onto kaolinite. After the contacting time has elapsed, the vials were moved into a centrifuge, positioned under atmospheric conditions. This was not a problem for the experiments conducted under inert gas conditions, as the vials could have been very easy hermetically sealed, and they were opened only inside the inert gas box.

Table 25: Experimental conditions for the investigation of the sorption of Pu(III) onto kaolinite

[Pu(III)] mol/L	[kaolinite] g/L	Ionic strength	pH	Centrifugation min/rpm	Atmosphere
1×10^{-6}	4	0.1 M $NaClO_4$	0.7 – 11	45/2500	argon
1×10^{-7}	4	0.1 M $NaClO_4$	0.7 – 11	45/2500	argon
1×10^{-8}	4	0.1 M $NaClO_4$	0.7 – 11	45/2500	argon
1×10^{-6}	4	0.1 M $NaClO_4$	1 – 10	45/2500	air ($pCO_2=10^{-3.5}$ atm)
1×10^{-7}	4	0.1 M $NaClO_4$	0.7 - 11	45/2500	air ($pCO_2=10^{-3.5}$ atm)

After the centrifugation, aliquots of the samples were extracted from the supernatant, and their activity was detected by LSC. The amount of plutonium found in solution could have been determined in this way as a percentage of the total amount of activity added, and subsequently the amount of metal ion sorbed onto kaolinite was calculated.

The sorption was investigated as a function of pH, under atmospheric conditions ($pCO_2 = 10^{-3.5}$ atm) and also in an inert gas box at room temperature. The experimental conditions are given in Tab. 25. The kinetics of the sorption was investigated for the solutions with the highest concentration, in air as well as under inert atmosphere. There were found only slight changes between the sorption rates obtained from measurements performed 24 hours, and six days, after the contact of kaolinite with plutonium (1-3 % higher sorption after 6 days). Between the sorption rate after 6 days and one month there was no significant difference found.

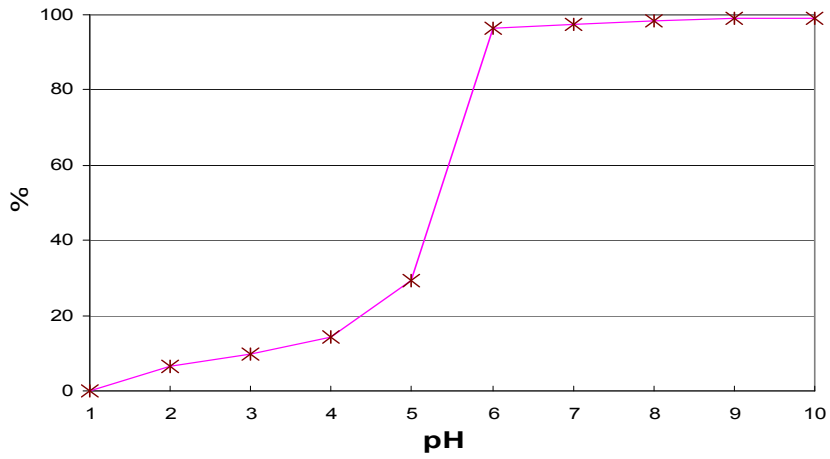

Figure 52: The pH dependency of the sorption of Pu(III) onto kaolinite, [Pu(III)] = $1X10^{-6}$ M, argon atmosphere, no wall adsorption correction

Therefore, the adsorption was measured in the following experiments after 5 – 7 days from the moment of the contact, when it was considered that the process was completed.

Fig. 52 presents the dependence of the sorption on the pH observed for a solution contacted with kaolinite under argon atmosphere.

Parallel to the sorption of plutonium onto kaolinite, the walls of the vessels have also exhibited a tendency to adsorb plutonium. Thus, not all plutonium which was not found in solution had to be necessaryly adsorbed onto kaolinite. Therefore, the adsorption on the walls of the vessels has been determined. For this, the vessels were emptied of the kaolinite suspension, and washed with Milli Q water to remove the last traces of kaolinite. Then, they were dried under a hood, and the plutonium was removed from the walls with 2 ml of a mixture of 0.36 M HCl/0.05 M HF. The activity of this solution was determined by LSC, and the total amount of plutonium found on the walls was calculated and subtracted from the amount of metal considered to be sorbed onto kaolinite.

The wall adsorption was also pH dependent as can be seen in Fig. 53. It can be observed that after the correction of the wall adsorption, the form of the sorption curve has changed to some extent. It could not be determined whether in the absence

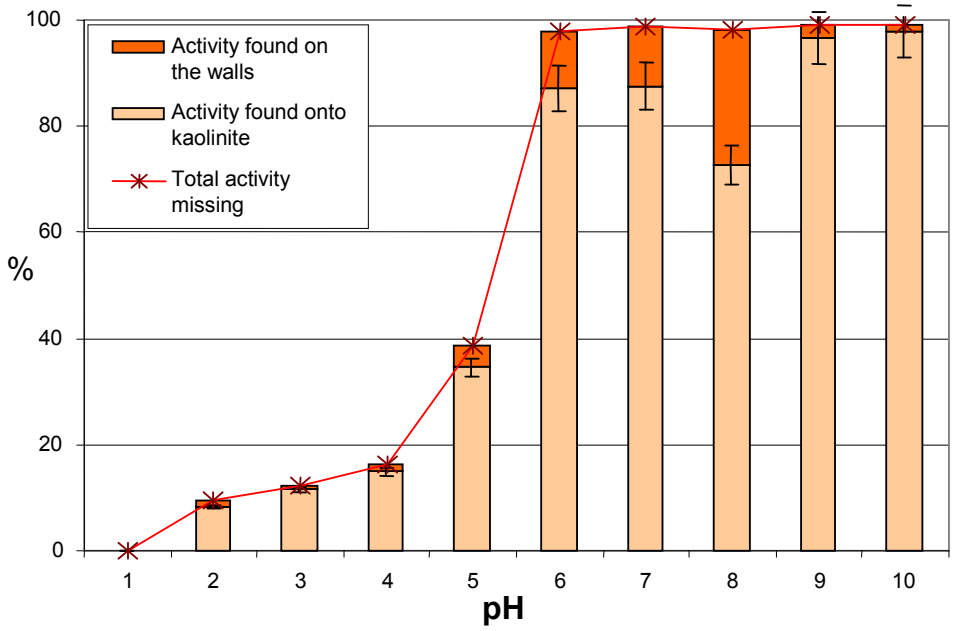

Figure 53: The sorption of Pu(III) onto kaolinite, [Pu(III)] = $1X10^{-6}$ M, argon atmosphere including the wall adsorption correction

of wall adsorption the sorption curves would have the same shape or not. Hence, it is not clear if the slightly lower sorption value encountered at pH 8 is an effect of a weaker adsorption onto kaolinite or of an increased, competitive wall adsorption.

The oxidation state of plutonium desorbed from the walls of the vessels was determined by liquid-liquid extraction and it was found that > 95 % was Pu(IV). It could not be detected whether the metal was sorbed from the beginning as Pu(IV), as it was known that the solution contained a small fraction of Pu(IV). The fraction of Pu(IV) increases with the pH as NH_2OHHCl is only able to keep the solution safely reduced up to pH ~ 6.

There was found no significant influence of the plutonium concentration on the sorption behaviour as illustrated in Fig. 54. The variation of the concentration was however only an order of magnitude in this case.

The pH edge (the point where the sorption onto kaolinite is ~ 50% of the total amount of metal ion) was found at pH ~ 5.5. In order to validate the accuracy of these experiments, the sorption of Am(III) onto kaolinite was also investigated. Am(III) is considered as an analogue of Pu(III) as it resembles much of its chemistry. On the other hand, Am(III) remains in this oxidation state over the entire pH range, giving the confidence that the observed sorption curve is that of a trivalent actinide.

The samples were prepared following the same procedure, and the wall adsorption was corrected. There was observed a slightly higher sorption of Am(III) onto kaolinite at pH 2-4 compared to Pu(III) which could not be explained.

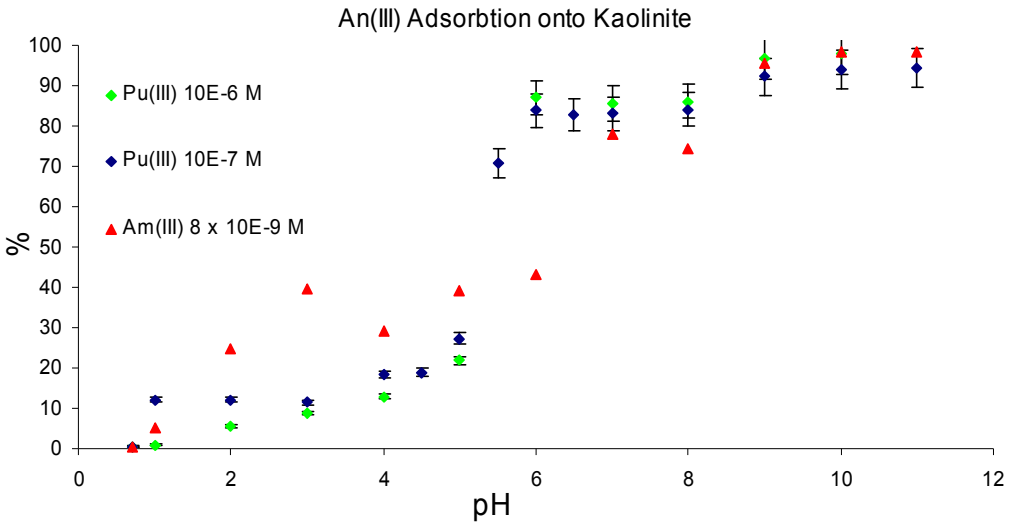

Figure 54: Adsorption of Am(III) and Pu(III) onto kaolinite under argon, as a function of pH

Also, at pH > 6 the sorption rate of Pu(III) was considerably higher, than in the case of Am(III). This could have been explained by the fact that Pu(III) is partially oxidised to Pu(IV), which is much stronger adsorbed by the kaolinite. The same experiments were repeated under aerobical conditions. The pressure of CO_2 was equilibrated at $pCO_2 = 10^{-3.5}$ atm, by adding $NaHCO_3$ at pH > 7. Other than that, the entire procedure was as described above for the experiments under inert gas atmosphere. The sorption of Am(III) was also studied parallel as a comparison study. The wall adsorption was in the same order of magnitude as in the earlier experiments. As shown in Fig. 55 it was found almost a similar sorption behaviour of Pu(III) onto kaolinite as in the earlier case.

It can be observed that the curve of Am(III) remained almost unaltered except of the point corresponding for the sorption at pH 3. This could be an indication that in the earlier case, there was a systematic error.

The sorption curves of Pu(III) maintain the same tendency except of the small decrease of the sorption rate at pH 4 – 5, and the increase at pH 6 – 8. While we cannot offer an explication for the first situation, the stronger adsorption at higher pH values could be explained as an effect of the stronger oxidation of Pu(III) in the presence of air, with a higher influence on the adsorption than in the earlier case.

The pH edge was also determined to be at pH ~ 5. There was no literature data found for the sorption of Pu(III) onto kaolinite. A good agreement was found between our experimental data and the sorption curves published for the sorption of Am(III) on silica (see Fig. 56).

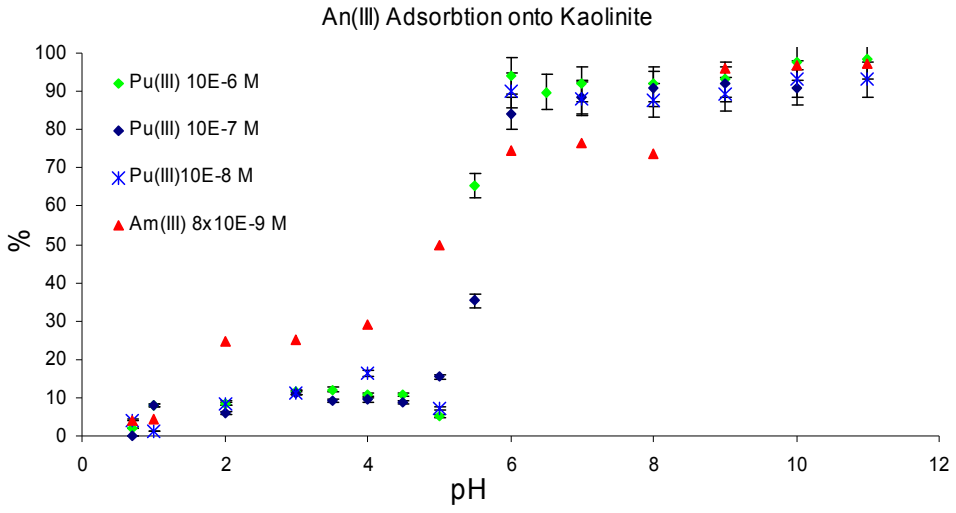

Figure 55: Adsorption of Am(III) and Pu(III) onto kaolinite under air, as a function of pH

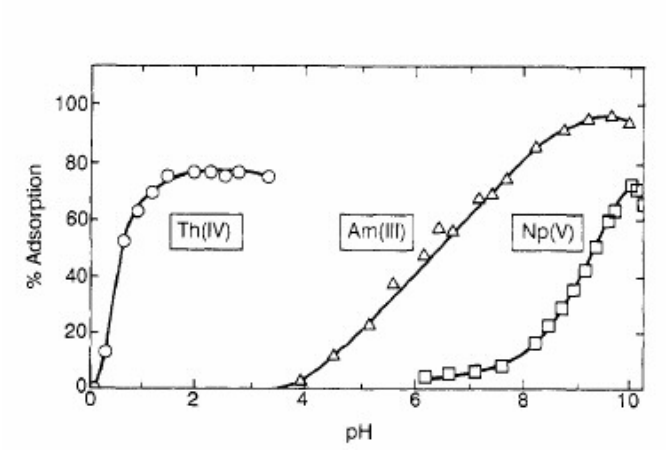

Figure 56: The sorption of actinides on precipitated amorphous silica as a function of pH; (Righetto *et al.*, 1991)

The sorption coefficient, K_d, of Pu(III) onto kaolinite was calculated based on the batch experiment.

K_d is defined by

$$K_d = \frac{\Gamma}{C} \text{ (L/kg)} \qquad (34)$$

(Lippold et al., 2005)

Γ - the adsorbed amount per unit mass of solid [mol/kg]

C – the equilibrium concentration of Pu(III) [mol/L]

The dependence of K_d on the pH is given in the Fig. 57. It was observed a slight difference between the values corresponding to pH > 7, for the different concentrations of plutonium. There were no data found in the literature on the sorption coefficient of Pu(III) onto kaolinite. The K_d values obtained in this work are in good agreement with those obtained by Samadafan et al. (2000) for Cm(III) and Am(III).

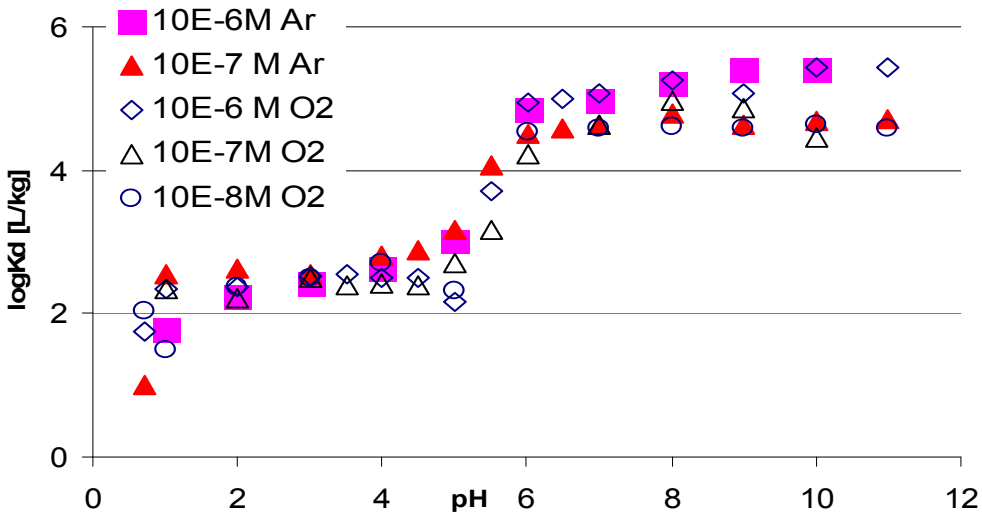

Figure 57: Sorption coefficient as a function of pH and concentration of Pu(III).

Besides the comparison with Am(III), the data obtained for the sorption of Pu(III) were compared with the results obtained by Banik (2006) for Pu(IV) in order to verify the speciation of plutonium. Fig. 58 illustrates explicitly the substantial differences in the pH dependence of the sorption of the two plutonium species onto kaolinite. It presents also the sorption behaviour of pentavalent and hexavalent actinides onto kaolinite.

It can be clearly observed that each one of the four possible oxidation states in which plutonium can be found, exhibit sorption curves substantially different from each other. It can be concluded that the results obtained for Pu(III) in this work are typical for the sorption curves of trivalent actinides onto kaolinite.

The plutonium left in solution at pH 4 was analysed by liquid-liquid extraction. It was determined that > 93% of it was in the oxidation state Pu(III) as expected. At higher pH values, where the oxidation is more likely to take part, it was not possible to perform speciation studies on the plutonium from solution, as the concentration was too low.

The reversibility of the sorption was also investigated. For this, the samples were centrifuged and the supernatant was removed. The solid phase was afterwards resuspended in a fresh solution of 0.1 M $NaClO_4$ with the same pH as the old solution. The suspension was then shaken for 48 hours. After a new centrifugation, the concentration of plutonium was determined measuring the activity of the supernatant by LSC. In all cases it was found that 8 – 10 % of the plutonium sorbed onto kaolinite in the earlier experiments, was desorbed and found in the solution. This could be an indication that the sorption on the surface of the kaolinite is not a physical but a chemical sorption (Allard, 1984), and is mostly irreversible.

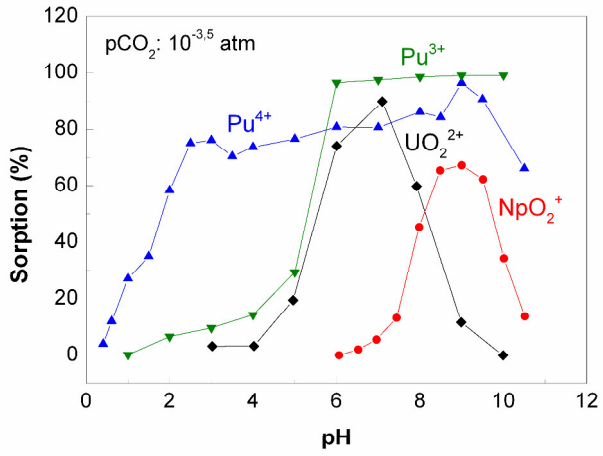

Figure 58: Sorption curves of tri-, tetra-, penta, and hexavalent actinides onto kaolinite as a function of pH (Amayri, 2006)

The pH values of the solutions were next lowered to pH ~ 1 with 0.1 M $HClO_4$, and after 48 hours of shaking the samples, they were again centrifuged and the amount of plutonium measured.

It was determined that > 90% of the sorbed plutonium was desorbed and found in the solution. These results will be used later in chapter 5. 3. In order to understand the processes that take place on the surface of the kaolinite it is necessary to observe also the speciation of the solid phase. Huertas *et al*. (1998) give a detailed description for this. They found that the aluminium layer is positively charged below pH ~5.5 and that the silicon sites contribute to the negative charge under neutral and basic pH (Fig. 59). The overall surface is neutral in a narrow range at pH ~5.5 (point of zero charge, pH_{zpc}), as a result of the balance of positive and negative charges irrespective of the nature of the sites. The negative charge above pH 5.5 is produced by the deprotonation of the > SiOH groups and at pH > 9 of the aluminium groups.

The sorption curves of the positively charged Pu(III) show a considerable increase of the sorption exactly from the point when the solid phase surface is negatively charged. It can be concluded that the charge of the solid phase surface plays an important role with respect to the adsorption behaviour of Pu(III) onto kaolinite. Thus, at pH < 5, the Pu^{+3} ion can be repulsed by the positively charged surface, so the cation exchange with the kaolinite is hindered, explaining the low adsorption rate. At higher pH values, the opposite effect is encountered, so the adsorption is much promoted.

Further studies are necessary in order to describe the interactions in a proper manner.

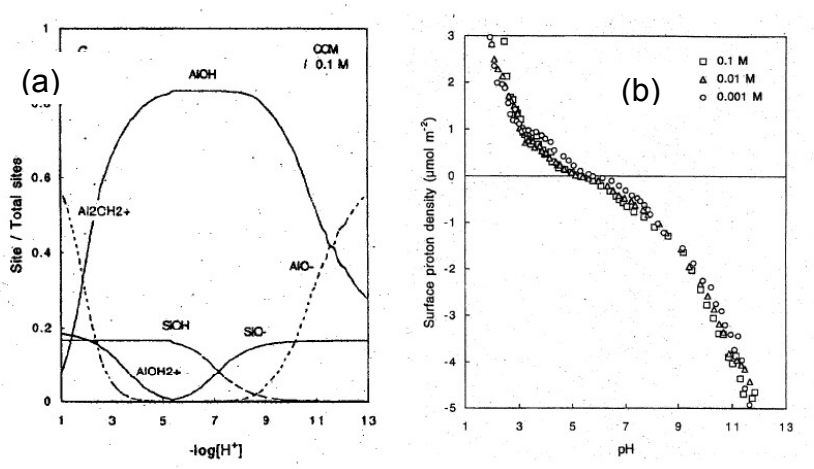

Figure 59: The speciation of the surface of KGa-1 kaolinite as a function of pH at I = 0.1 M, and the charge of the surface of kaolinite as a function of ionic strength and pH. The point of zero charge is also indicated in (b).

5. 2. 1. EXAFS/XANES speciation of plutonium sorbed onto kaolinite

The accurate mechanisms of the adsorption of plutonium onto kaolinite are not yet understood. EXAFS/XANES studies could give indications on the speciation of plutonium sorbed on the surface of kaolinite, as well as on the type of sorption (inner sphere/outer sphere sorption).

In collaboration with the group of Prof. Dr. T. Reich, from the Institut für Kernchemie, Johannes Gutenberg-Universität Mainz, for the first time XAS measurements of plutonium adsorbed onto kaolinite have been conducted.

The samples were prepared in Mainz and the measurements were performed at the INE beamline, at ANKA (Forchungszentrum Karlsruhe).

Based on the sorption curves of Pu(III) and Pu(IV) (Fig. 58), and on the beam time available, four samples of ^{244}Pu sorbed onto kaolinite were prepared at pH 1, 4, and 9 with Pu(IV) and at pH 6 with Pu(III). The choice of pH was motivated as follows: for Pu(III), pH = 6 is the lowest pH value at which almost quantitative sorption onto kaolinite is observed. For Pu(IV), pH = 1 is the end point of the pH-edge, pH = 4 is located in the minimum of sorption at intermediate pH-values, and pH = 9 represents maximum sorption of Pu(IV) onto kaolinite.

The samples of Pu(IV) were prepared in the presence of air, and the one of Pu(III) in an inert gas box.. A suspension of 4 g kaolinite/L in 0.1 M $NaClO_4$ was preconditioned for 48 hours and then the freshly electrolysed plutonium solutions were added. The pH was immediately readjusted. In the case of Pu(III), NH_2OHHCl with a final concentration of 0.025 M, was added in solution for the redox stabilization of plutonium in this oxidation state. The final concentration of plutonium was $1x10^{-5}$M. After centrifugation, the plutonium uptake by kaolinite was determined by LSC. Afterwards, the supernatant was removed, and the wet paste was transferred without drying into 3 mm thick sample holders and sealed with Kapton tape and heat-sealed with two layers of PE foil. The preparation of the sample containing Pu(III) was conducted in an inert gas box, and the sample was transported in a container filled with argon, in order to minimize any air contact with the samples.

The final concentration of the samples is given in Tab. 26.

The Pu L_{III}-edge spectra were collected in the fluorescence mode at room temperature using a Ge solid state detector. The data were analysed by the colleagues from the group of Prof. T. Reich, using the suite of programs

EXAFSPAK (George *et al.*, 2000) and FEFF 8.20 (Ankuninov *et al.*, 2002), (Conradson *et al.*, 1998).

Table 26: Description of the samples examined by XAFS

Sample	Description
Pu(IV) (A)	pH 1, air, 94 ppm
Pu(III) (B)	pH 6, argon, 243 ppm
Pu(IV) (C)	pH 4, air, 370 ppm
Pu(IV) (D)	pH 9, air, 412 ppm

The XANES spectra are presented in the left part of Fig. 60. No shift in the absorption edge energy is evident, neither a significant structural difference at the high energy side of XANES, for the four spectra, indicating that the oxidation state of the plutonium sorbed at the surface of kaolinite is Pu(IV). There are several possible explanations for this unexpected result with respect to sample B:

• the plutonium was sorbed as Pu(III) but oxidized to Pu(IV) during the transport at from Mainz to the INE beamline at Anka (it is important to note that there was obviously no beam-induced oxidation of Pu during the EXAFS measurements)

• Neck *et al.*, (2006) reported that Pu(III) hydroxides ($Pu(OH)_3(s)$), are unstable and rapidly transform into Pu(IV); this could happen also on the surface of kaolinite if Pu(III) hydroxides are sorbed

A pseudo radial distribution function of the plutonium near-neighbor surrounding was determined from the Fourier transform of the EXAFS spectra illustrated in Fig. 60, right.

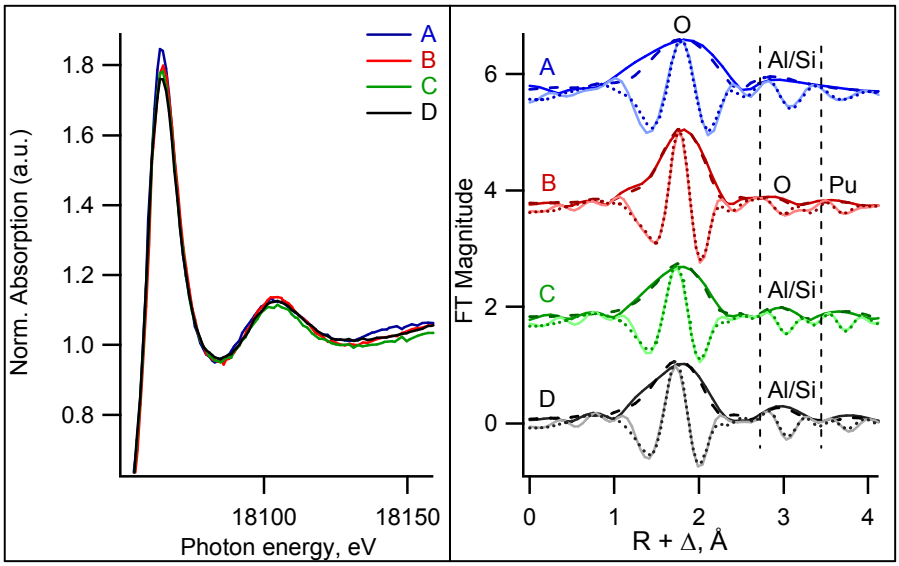

Figure 60: Pu L_{III}-edge XANES (left) and the Fourier transform (right) spectra of the four samples

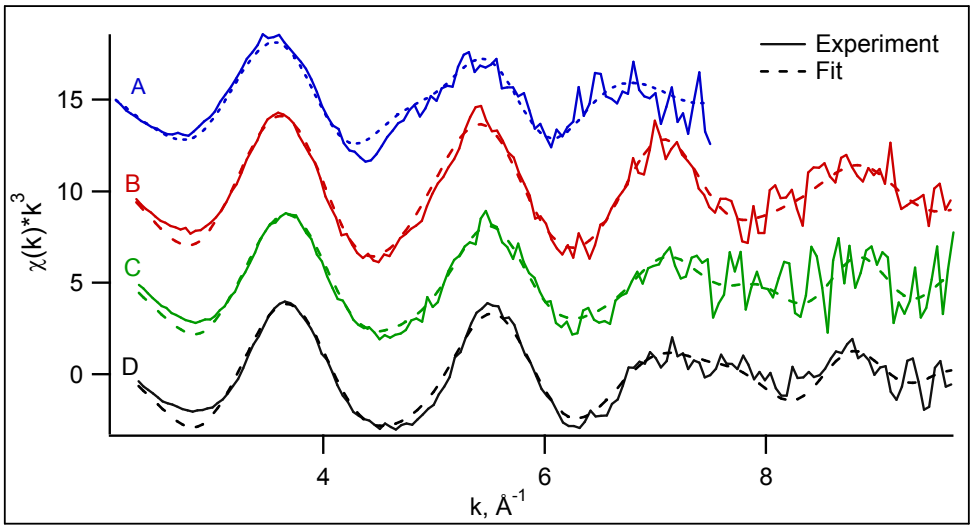

Figure 61: Pu L_{III}-edge EXAFS data and fits for all four samples

The most prominent peak in all spectra was found at ≈ 1.8 Å corresponding to the backscattering caused by eight oxygen atoms coordinated to Pu(IV). The formation of polynuclear Pu species at the surface of kaolinite was indicated by Pu-Pu interactions at ≈ 3.7 Å with two Pu atoms.

From the k^3-weighted experimental EXAFS data and fits presented in Fig. 61, it can be observed that sample B exhibits a different EXAFS pattern in particular in the k range 6 - 8 Å.

While EXAFS indicates a Pu-Al/Si coordination shell at 3.62 – 3.66 Å which can be rationalized by an inner-sphere sorption of the polynuclear Pu(IV) species formed in solution to the kaolinite surface, the EXAFS spectrum of the sample B could not be modelled with a Pu-Al/Si shell. The best fit was obtained by including a Pu-O interaction at 3.25 Å (see Tab. 27).

More specific information on the interpretation of the spectra is given by Reich *et al.* (2006).

Table 27: Distances to Pu neighbours in Å

	8 x O_1	2 x O_2	2 x Al/Si	2 x Pu
A	2.34	-	3.66	3.70
B	2.31	3.25	-	3.70
C	2.28	-	3.62	3.69
D	2.27	-	3.62	3.68

In order to corroborate the findings, EXAFS spectra with better statistics are needed. Further experiments for the speciation of Pu(III) are planned at ANKA (INE beamline)in the future.

5. 3. The binary system kaolinite-humic acid

The interaction between humic substances and clay minerals needs to be studied independently in order to understand their influence on the migration of actinides in the multicomponent systems containing all the components expected under conditions relevant to the natural environment.

The sorption of Aldrich humic acid by KGa-1b kaolinite was investigated as a function of pH. The experiments were conducted under inert gas atmosphere.

The concentration of kaolinite was 4 g/L as in all the previous experiments. The concentration of Aldrich humic acid was 25 mg/L and the ionic strength of the aqueous solution was 0.1 M $NaClO_4$. The two phases were contacted after the preconditioning of the kaolinite surface in the solutions at the desired pH for 48 hours at room temperature. A solution of humic acid with the concentration 25 mg/L was prepared in the same electrolyte, without mixing it with kaolinite, and it was used as standard for the light absorption in the UV/VIS spectrometer. After 72 hours of continuous mixing, the phases were separated through centrifugation. The solution containing no kaolinite was also centrifuged, in order to avoid possible errors induced by deposition of humic colloids. The concentration of humic acid in the supernatant was measured by UV/VIS spectroscopy at 310 nm, and the adsorption rate was calculated.

A strong pH dependence was obtained similar to that obtained by other authors (Lippold *et al.*, 2005), (Wang *et al.*, 2006), (Righetto *et al.*, 1991) as presented in Fig. 62.

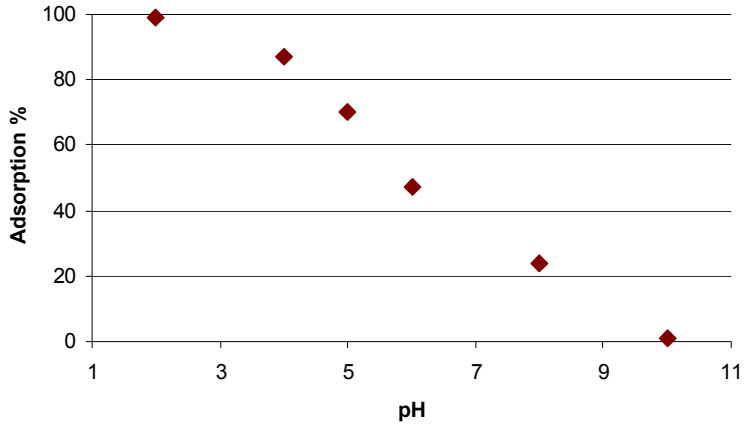

Figure 62: pH dependence of the adsorption of Aldrich humic acid onto kaolinite, I = 0.1 M $NaClO_4$

The form of the sorption curve can be explained by the surface charges of the two components. The humic substances are negatively charged. The surface of the kaolinite is positively charged at pH < pH_{zpc} and negatively at pH > pH_{zpc} as shown in Fig. 59. Thus, the negatively charged humic substances are easily sorbed at low pH and then their sorption rate decreases with increasing pH at pH>pH_{zpc} (Montavon *et al.*, 2002).

The sorption of fulvic acid on kaolinite, as well as the influence of the humic acid concentration on the sorption behaviour of Aldrich humic acid, is described more detailed by Banik (2006).

5. 4. The ternary system Pu(III)-humic acid-kaolinite

After studying the three binary systems individually, the question in which way do they influence each other when all interact at the same time, has been tried to answer.

Many authors have performed studies of the interaction of similar minerals with humic acid and trivalent actinides or lanthanides (Wang, *et al*., 2006), (Wang et al., 2004), (Lippold et al., 2005), (Takashi et al., 2001), (Samadfam et al., 2000). There was no literature found for the interaction of Pu(III) in the ternary system described above.

The investigation of a system containing Pu(III), kaolinite, and humic substances, is not an easy task due to the multitude of parameters that have to be dealt with. The studies performed in this work have been the first steps in understanding the influence of the humic acids on the sorption of Pu(III) onto kaolinite. Thus, the experiments were conducted using just one concentration for each component, at room temperature, under inert gas atmosphere, and at ionic strength 0.1 M $NaClO_4$. All the experiments were performed in the presence of 0.025 M NH_2OHHCl.

The question whether or not the sequence of metal ion and humic acid addition to the solid phase influences the sorption of plutonium is discussed controversially (Wang *et al.,* 2004), (Wang *et al*., 2006), (Panak, 2005). Therefore, four different approaches were considered. The experimental conditions and the components addition sequence in the ternary system are summarized in Tab. 28. The shortcuts are explained as follows: for example in case (A) K-Pu(III)-AHA means that the kaolinite was preconditioned, mixed first with Pu(III) and after a contact time of 48 hours after verifying the sorption of Pu(III) onto kaolinite, the Aldrich humic acid was added.

The kaolinite was preconditioned like in the earlier experiments for 48 hours at the working pH before mixing it with the other components. The activity of the solutions was measured immediately after adding the freshly electrolysed ^{239}Pu(III) by LSC. The concentration of humic acid was also determined by UV/VIS spectroscopy for a solution with 25 mg Aldrich HA/L in the same aqueous phase as used in the experiments. These were considered the start concentrations before any sorption could take part, as the measurements were conducted just some seconds after the mixing of the phases. After mixing the first two fractions the solutions were agitated by end-over-end rotation.

In the case (A) and (B) before adding the humic acid or Pu(III), respectively, the

Table 28: Experimental conditions and the addition sequence of the components for the investigations of the ternary system

Addition sequence	Concentration			pH	3rd component added
	K	Pu	AHA		after
(A) K- Pu(III)-AHA	4 g/L	$1x10^{-6}$M	25 mg/L	1 - 10	48 hours
(B) K-AHA-Pu(III)	4 g/L	$1x10^{-6}$M	25 mg/L	2, 4, 5, 6, 8, 10	48 hours
(C) AHA-Pu(III)-K	4 g/L	$1x10^{-6}$M	25 mg/L	2 – 10	28 days
(D) All together	4 g/L	$1x10^{-6}$M	25 mg/L	2, 4, 5, 6, 8, 10	all at the same time

K – kaolinite, AHA – Aldrich humic acid

suspension was centrifuged, and the adsorption rate of Pu or AHA onto kaolinite was determined by LSC or UV/VIS spectroscopy, respectively. These two methods were used over the entire duration of the experiments as standards for determining the concentration of Pu and AHA.

In the case (C) a longer time has been left before adding the kaolinite. It was assured in this way that the redox equilibrium was achieved (see Fig. 46). The concentration of AHA was chosen in this sense above the concentration 15 mg/L which was known to stabilize Pu(III) under argon atmosphere (see chapter 5. 1. 1). The experiments in that situation were however carried out in the presence of GoHy-573 fulvic acid, which is expected to have a stronger reduction effect on the redox behaviour of plutonium implying a faster kinetics. To make sure that Pu(III) will be stabilized, the concentration of AHA was chosen 25 mg/L and the contact time was 28 days.

In the case (D) the activity of the suspension was measured immediately after mixing all the three phases, and this value was considered, as presumed before, the one corresponding to 0 % adsorption of plutonium onto kaolinite.

After certain periods, in which the solutions were continuously agitated, they were centrifuged for 45 minutes at 2500 rpm. The concentration of Pu and/or AHA in the supernatant was determined, and then this fraction was ultrafiltrated through filters with pore size 1 kDalton. The amount of free plutonium in the filtrate was also measured. In this way it was possible to determine the rate of plutonium fixed on kaolinite, complexed with AHA, and free plutonium. It was also possible to find out the adsorption rate of AHA onto kaolinite.

In the following section, every experiment will be discussed individually.

The sorption of Pu(III) onto kaolinite, and the influence of AHA on the sorption was monitored, thus the discussion of the results will refer to the amount of plutonium and humic acid found free in solution after the separation from the solid phase.

The amount of plutonium found in solution after various periods of time in the experiment (A) after the separation from the solid phase through centrifugation (a CF) before and after the ultrafiltration (b UF and a UF) as a function of pH can be seen in Fig. 63.

At pH 1 and 2 there are observed no significant influence of the humic acid on the sorption of plutonium on kaolinite (see also Fig. 54) as at this acidic pH the adsorption rate is anyhow low, and the humic acid is precipitated. At pH 4 it was observed that the amount of plutonium found free in solution after the separation from AHA is slightly increasing with time. There was no explanation found for this, as the amount of AHA in solution remained roughly constant as presented in Fig. 64.

Most notable is the increase of plutonium found after the centrifugation in solution at pH 7-10 after longer periods of time. The data resulting from the subsequent ultrafiltration, presented in the right part of Fig. 63, show clearly that this plutonium is complexed with humic acid, as it is not found in solution after the ultra filtration. This is a clear indication that the humic acid found free in solution, is interacting with the plutonium sorbed on the surface of the kaolinite, and manage to draw some parts of it into solution leading thus to a mobilization of it.

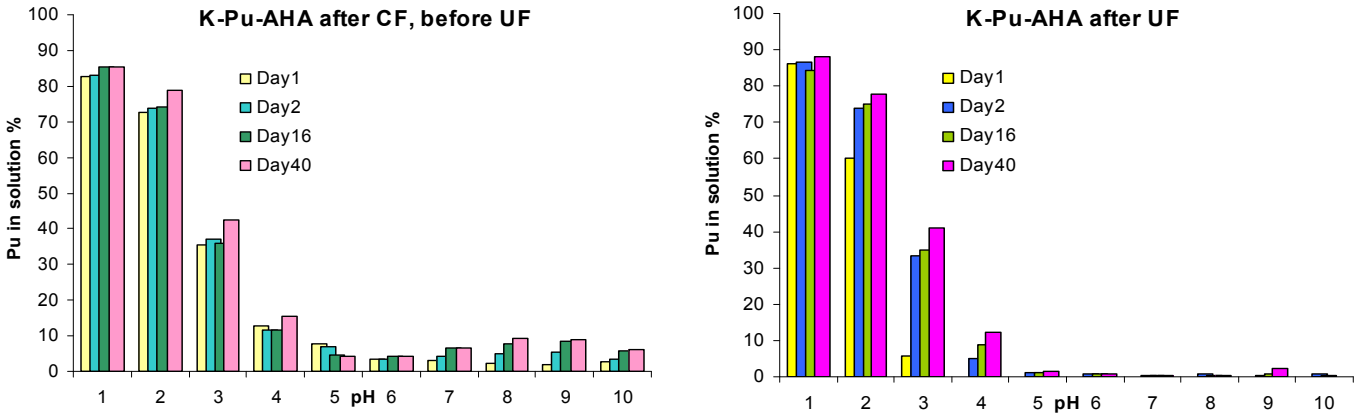

Figure 63: The influence of Aldrich humic acid on the sorption of Pu(III) onto kaolinite as a function of pH and time; the measurements were performed 1, 2, 16, and 40 days after adding the AHA to the Pu(III)-K suspension

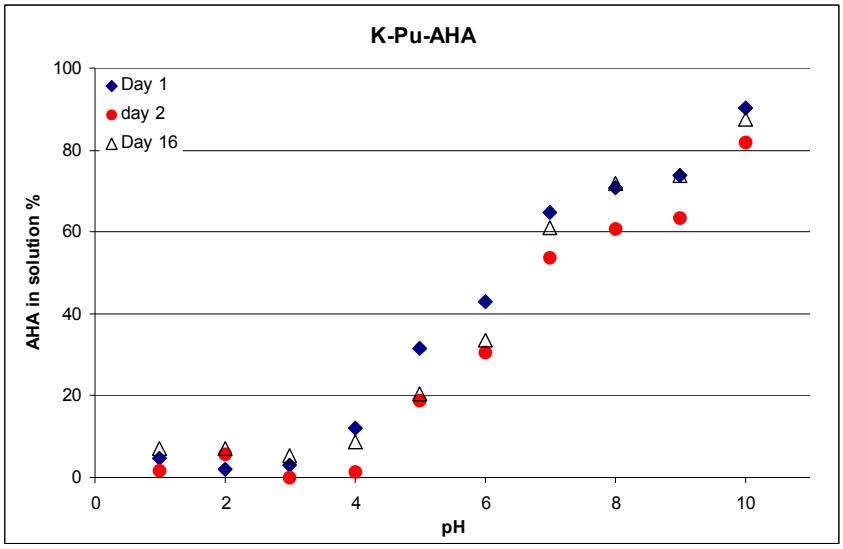

Figure 64: AHA and AHA-Pu complexes found dissolved in solution after the separation from kaolinite

This is possible since at these high pH values the humic acid is no longer sorbed onto kaolinite, so its presence in the solution leads to a slight remobilization of plutonium previously sorbed onto kaolinite.

A completely different sorption curve was found in the experiment (C) as presented Fig. 65. It was found that at pH 3 the rate of plutonium found free in solution after centrifugation, was lower compared to experiment (A). Analysing Fig. 65 and Fig. 66, it can be concluded that most of the plutonium not sorbed onto kaolinite at pH 3, is not complexed with the humic acid, as the amount of humic acid found free in solution at this pH is very low and plutonium is found in solution after ultrafiltration,.

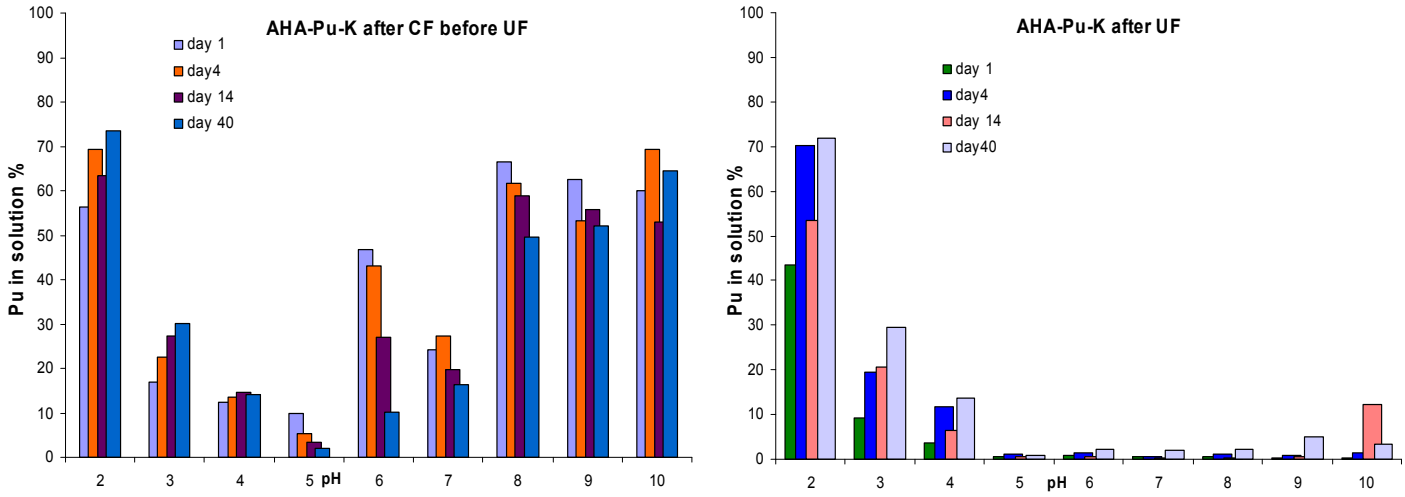

Figure 65: The adsorption of plutonium complexed with Aldrich humic acid, onto kaolinite

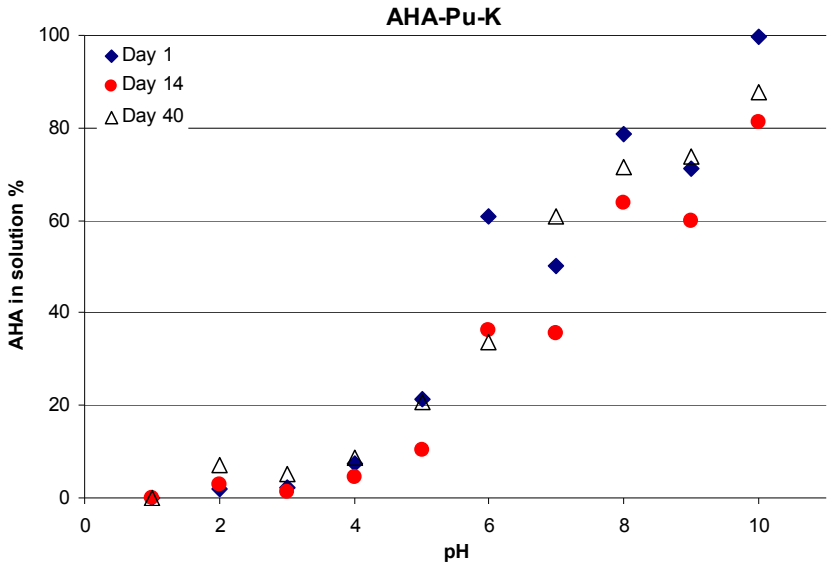

Figure 66: The humic acid found in solution after the centrifugation

On the other hand, through complexation with the strongly sorbed humic acid, plutonium is fixed at a higher rate at pH 4 and 5 compared to the situation when no humic acid is present (see Fig. 55). The humic acid is sorbed in proportion of ~ 80% at these pH values. It also forms strong complexes with plutonium at this pH as shown in chapter 5. 1. 2. Thus, by complexing with the humic acid plutonium is stronger fixed.

The opposite situation was found at pH 6 – 10, when plutonium remains in solution complexed with humic acid. This is also suggested by the ultrafiltration experiment, which has shown that there is no plutonium found in solution after the filtration.

There was also found a time dependency of the sorption of plutonium onto kaolinite at pH 6 showing that the sorption was increased after longer contact time.

In conclusion, in this experiment was found that the humate-plutonium complexes are stronger sorbed at pH < 6, than the uncomplexed metal. At pH ≥ 6 the situation changes completely, so it can be observed that plutonium is strongly mobilized by the presence of Aldrich humic acid.

Between the experiments (B) and (D) there was found only one significant difference. At pH 4 the sorption of Pu(III) onto kaolinite with the surface covered with a layer of sorbed humic acid, is lower than in all the other cases. This could be explained by a blocking of the cation exchanging sites of the kaolinite by the humic acid film. The sorption is however higher than in the absence of humic acid,

suggesting that surface humate-plutonium complexes are formed.

It was also observed that in the experiment (B) at pH 4 almost all the plutonium not sorbed onto kaolinite was found in solution after the ultrafiltration, indicating that the humic acid was completely adsorbed onto kaolinite. However, this could not be confirmed by UV/VIS spectroscopy, which perceived no difference between the spectra of the different addition sequence experiments at this pH as presented in Fig. 68.

It can be observed that in experiment (B) at pH > 6 the sorption of plutonium onto kaolinite is lower than in the case (A), but not so low as in the experiment (C).

Observing the kinetics of the sorption of plutonium in Fig. 67 and AHA in Fig. 68, it can be presumed that a sorption of humate-plutonium complexes takes part, as the amount of plutonium and AHA found in solution after centrifugation decreases as a function of time. This sorption is slower than that of the uncomplexed metal.

It was found that the sequence in which the components are added, has a strong influence on the sorption of plutonium onto kaolinite over the entire pH range and thus on the mobilization/immobilization of these compounds.

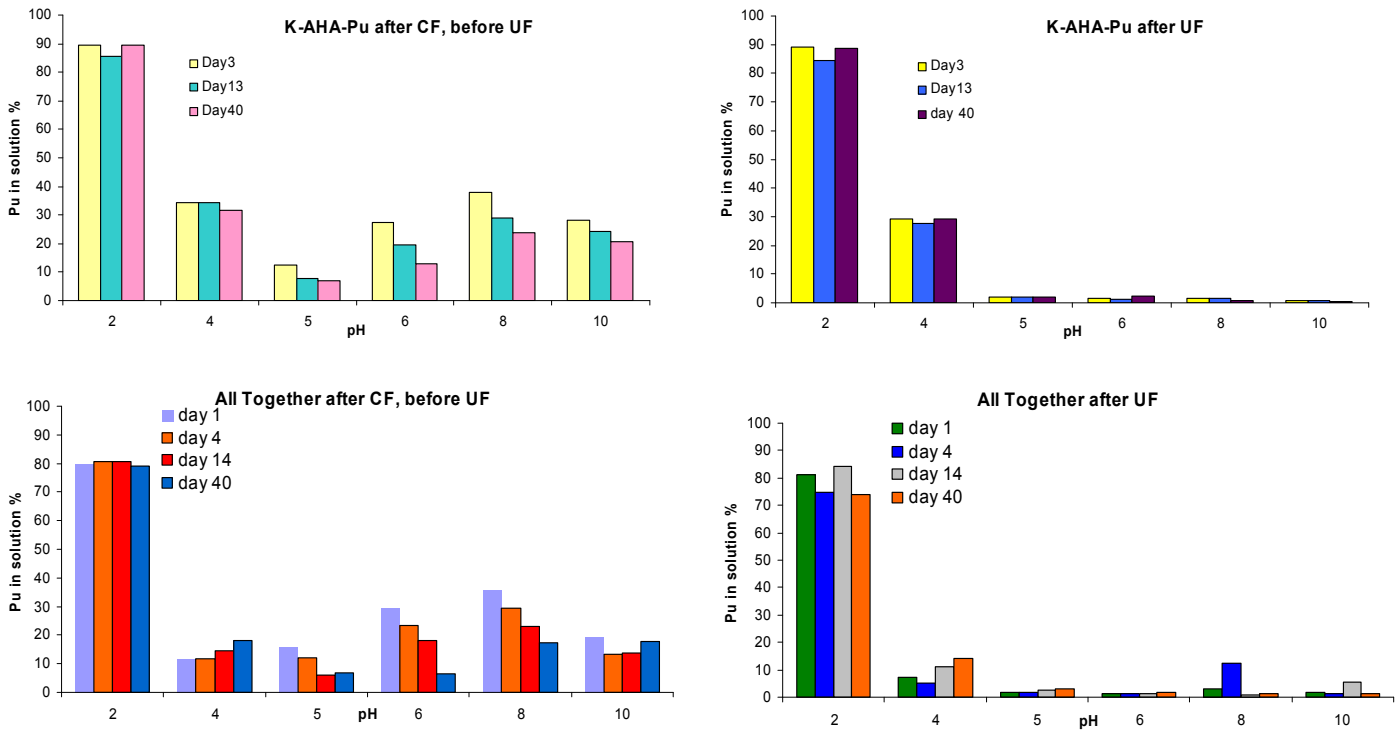

Figure 67: The adsorption of Pu(III) onto kaolinite in the presence of Aldrich humic acid, comparison between two different addition sequence of the components

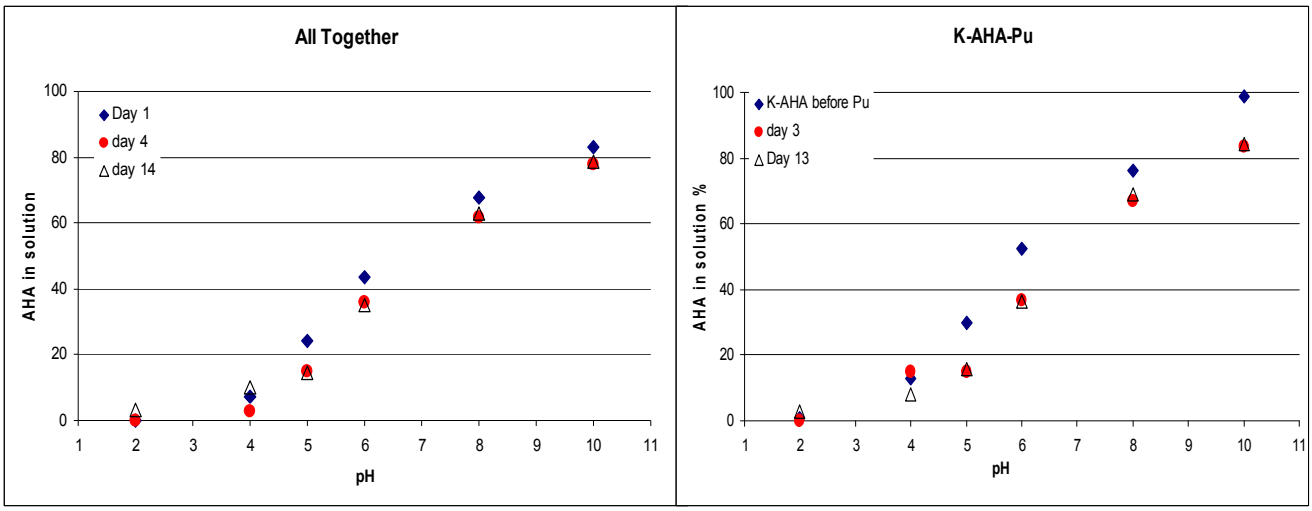

Figure 68: The humic acid found in solution after the centrifugation in the experiments (D) and (B)

The sorption on the walls of the vessels was determined in the same way as in the experiments from chapter 5. 2. It was determined that it was negligible in these experiments (< 3%).

The influence of humic acid on the sorption coefficient K_d of plutonium onto kaolinite was also investigated. The K_d values were calculated as described in chapter 5. 2, using the experimental data obtained after 40 days from the moment of contact of all three phases. They are presented in Fig. 69 in comparison with the results obtained for the sorption of Pu(III) with the same concentration, under argon atmosphere, in the absence of humic acid. It is observed that at pH < 6 the humic acid enhances the sorption of metal ion onto kaolinite when the addition sequence is that from the experiments (A), (B), and (C). When the components come in contact all at the same time, the adsorption coefficient are almost not affected by the presence of Aldrich humic acid at pH < 6. It can also be observed that the humate-plutonium complexes are sorbed easier than the free plutonium onto kaolinite, or onto a humic acid coated kaolinite surface at pH < 6.

Beyond pH 6 the sorption of Pu(III) onto kaolinite is hindered by Aldrich humic acid depending strongly on the components adding sequence. In this pH range, the sorption of the humate-plutonium complexes is much lower than the one corresponding for the sorption of uncomplexed plutonium. This is expected, as the humate-metal complexes can be negatively charged, and the surface of kaolinite is also negatively charged at this pH (see chapter 5.3).

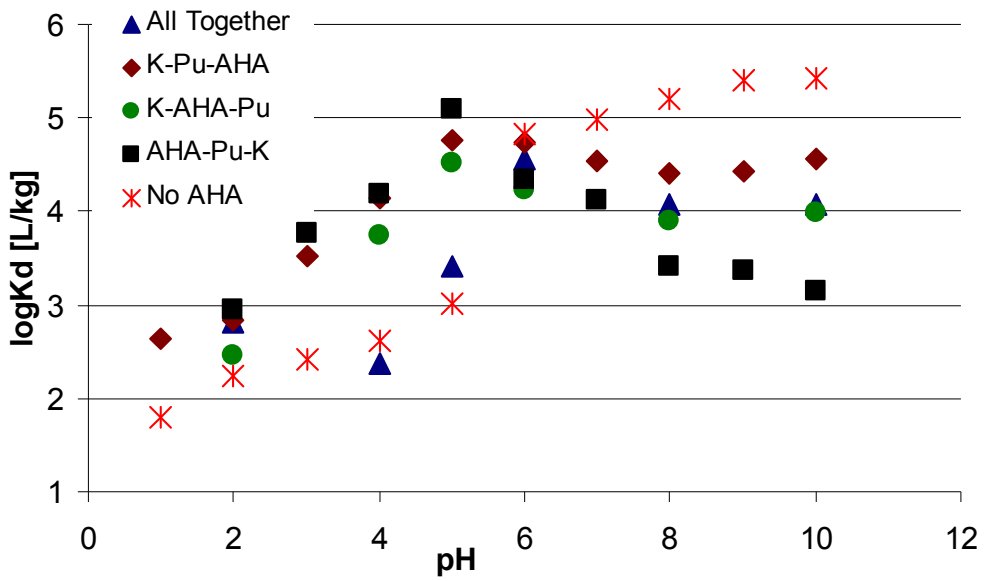

Figure 69: The K_d values for the sorption of plutonium(III) onto kaolinite as a function of pH; Comparison between different adding sequences of humic acid (AHA), kaolinite (K), and plutonium (Pu); I = 0.1 M $NaClO_4$, [K] = 4 g/L, [AHA] = 25 mg/L, and PU(III)] = $1x10^{-6}$ M.

With increasing pH, the dissociation of acidic groups leads to a gain in metal binding sites on the humic colloids. A competitive situation arises thus, between metal sorption onto kaolinite and humate complexation. Moreover, even after the sorption of plutonium onto the solid phase has taken part, it can be desorbed partially by Aldrich humic acid at pH ≥ 7.

In the pH range 4 - 5 the strongest sorption of Pu(III) is encountered, probably due to the combined effect of the sorption of plutonium as metal directly onto kaolinite and of humate-metal complexes, or sorption of the metal ions onto the already fixed humic acid.

It can be concluded that the sequence in which the components are added in the solution plays an important role concerning the K_d value too.

The results obtained are in good agreement with those obtained by Lippold et al. (2005) for studies on the system Tb(III)-humic acid - kaolinite and by Samadafan *et al.* (2000) for the influence of humic acid on the sorption coefficients of Cm(III) and Am(III) onto kaolinite as presented in Fig. 70. The authors found also an increase in the sorption of the two trivalent actinides for pH < 6. They found that this effect depends on the concentration of humic acid, as suggested by the points situated above the red line marking the sorption in the absence of humic acids.

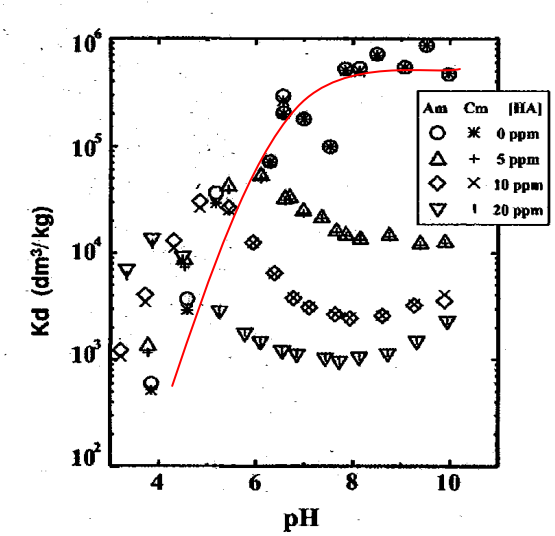

Figure 70: The influence of humic acid on the sorption coefficients of trivalent actinides onto kaolinite (Samadfam *et al.*, 2000)

At pH > 6 the K_d values drop drastically over more orders of magnitude depending also on the concentration of the humic acid as indicated by the points situated under the red line in Fig. 70. Our results obtained for a concentration of [AHA] = 25 mg/L are comparable with the results obtained by Samadafan *et al.* (2000) for [HA] = 20 mg/L.

The reversibility of the sorption was investigated following the procedure described earlier in chapter 5. 2. When a fresh solution was mixed with the solid phase at the same pH the amount of plutonium desorbed from kaolinite was considerably lower than in the experiments conducted in the absence of humic acid.

The question whether the metal ion is directly sorbed onto kaolinite or a humate mediated sorption takes place is difficult to answer using classical chemical methods. Several hypotheses can be taken into account:

- the sorption of metal ion (M) and humic substances are independent of each other
- a K-AHA-M bridge is formed
- a K-M-AHA bridge is formed

Several authors have concluded that the metal complexation with sorbed humic substances is stronger than humate complexation in solution (Tipping et al., 1983), (Laxen, 1985), so the first hypothesis is less likely to happen.

Attempts to determine chemically the form of binding to the solid surface were performed. It was proven in chapter 5. 2 that at pH ~ 1 Pu(III) is almost completely desorbed from kaolinite while at pH > 10 it is very strongly fixed. On the other hand it was shown in chapter 5. 3, that humic acid is strongly sorbed onto kaolinite at lower pH values, but dissolved at pH > 10. Assuming that no other interactions take part, if a K-AHA-M bridge is formed, it should be desorbed from the kaolinite when the pH of the solution is > 10. On the contrary, when a K-M-AHA bridge is formed, it will remain fixed at pH > 10 and will only be desorbed when the pH is lowered. For this, the pH of the solutions was first raised to pH ~ 11.5 by adding NaOH. They were agitated for 48 hours,

centrifuged and the activity of the supernatant determined (basic desorption).

Afterwards, the supernatant was removed and ultrafiltrated with the purpose to determine whether the desorbed plutonium is complexed by AHA or not.

A fresh solution of 0.1 M $NaClO_4$ with pH < 1 was mixed with the separated solid phase from the earlier experiment. After another 48 hours of agitating, the solutions were again centrifuged, and the activity of the liquid phase was determined by LSC providing information on the sorption in acidic conditions (acid desorption). The supernatant was also ultrafiltrated and the free plutonium ion content was determined by LSC in the filtrate.

The obtained data are not yet completely understood. The following discussions are just speculative, and only the data resulting from experiments (A) and (C) are presented in Fig. 71as an example of the different results obtained. Further details will be given in Buda (2006).

It could be interpreted that the low amount of plutonium sorbed onto kaolinite in experiment (C) (see Fig. 65) is not sorbed as a complex but as metal ion, thus it is readily desorbed at pH < 1 similar to the case when no humic acid is present. This theory was also sustained by the fact that plutonium was found in the filtrate after ultrafiltration. The part of plutonium sorbed as a humate complex is only in smaller amounts desorbed at either basic or acidic pH. It could be concluded that, although the sorption of Pu(III) onto kaolinite is impaired by the presence of humic acids, once sorbed the plutonium-humate complexes are stronger desorbed over the entire pH range, than the metal alone.

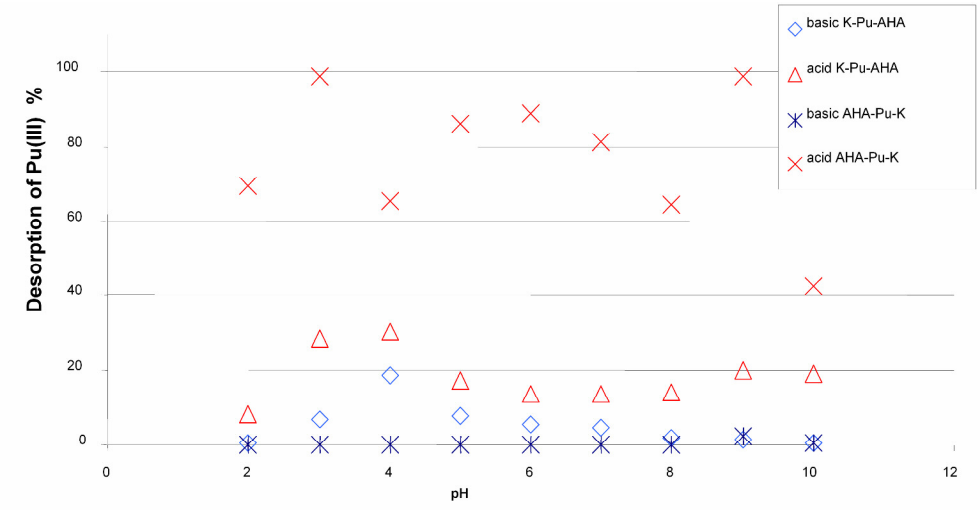

Figure 71: The influence of the components adding sequence on the desorption of Pu respectively Pu-AHA complexes from kaolinite

So far, it was not possible to determine in which form plutonium and the humic acid are sorbed onto kaolinite in the ternary system (over K-Pu-AHA bridges or K-AHA-Pu bridges), but it is very likely that they are not bonded separately. This answer could be given by EXAFS/XANES, and therefore future experiments are planed with this technique.

Lippold *et al*. (2005) have concluded that the enhancement of metal sorption at low pH is attributable to co-adsorption of metal loaded humic acid, rather than the formation of a K-M-AHA surface complex as it is assumed for inorganic ligands. The impaired metal adsorption encountered at higher pH in the presence of humic acid can be interpreted as the effect of the competitive situation between sorption of the metal ions onto the solid phase, on one hand, and the complexation with humic acids dissolved in solution, on the other hand.

The question of mobilization versus immobilization of actinides in the natural environment was long debated. It was thought that due to their high tendency towards the sorption of metals, the clay minerals could create a very effective geological barrier in the path of radiotoxic waste accidentally released from nuclear facilities. It was clearly proven in this study that Aldrich humic acid has a considerable influence on the sorption of Pu(III) onto kaolinite.

Besides the influence of the addition sequence of the components, recognized by other authors too (Wang *et al*., 2005), other factors can also influence the effect of humic acids on the sorption of metal ions onto kaolinite, *e.g*., the concentration of humic acid (Samadfam *et al*., 2000), ionic strength, and nature of humic acid (Wang *et al*., 2005).

6. Summary and outlook

For the safety assessments of nuclear waste repositories in deep geological formations, the interactions of the radiotoxic pollutants with the environmental compounds must be well understood. Since plutonium is the major contribution to the radiotoxicity of spent nuclear fuel, stored for periods of > 1000 years, it is very important to predict its behaviour after possible, accidental release into the environment.

New speciation methods

For the detection of plutonium in natural samples, Resonance Ionization Mass Spectrometry (RIMS) has been applied. It was shown in chapter 4. 1. 3, that the method is extremely sensitive and element selective being able to distinguish between different isotopes of plutonium. By coupling RIMS offline to Capillary Electrophoresis (CE) it was possible to determine the speciation of plutonium in solutions with a detection limit ~ 2 orders of magnitude lower compared to the online coupling of CE with ICP-MS, which was routinely used for the study of the redox chemistry of plutonium in contact with humic substances.

In chapter 4. 3. 6, there were presented the first steps carried out for the establishing a new technique which could offer an alternative to ultratfiltration, for determining the complexation constants of plutonium with humic substances. The method based on coupling of CE with two detection systems simultaneously, namely Diode Array Detector (DAD) and ICP-MS, could enable the detection of free metal ions, metal-humate complexes, and uncomplexed humic substances, separately. Based on this data, the calculation of the complexation constants of plutonium with humic and fulvic acids should be possible.

Interactions of Pu(III) with humic acid and kaolinite in binary and ternary aqueous systems

A mixture of all oxidation states of plutonium is reduced in aqueous solutions to Pu(III) and Pu(IV) in the presence of humic substances (chapter 5. 1). The present work was focused on the investigation of Pu(III) with respect to its migration behaviour under environmental conditions. Humic substances are

ubiquitously found in ground water and their presence could enable the transport of heavy metals over larger distances by complexation of the metals with humic colloids which are easily carried away. The metals sorption onto clay minerals could form a geological barrier in the path of leaked radioactive contaminants.

The interaction of Pu(III) with humic acid and kaolinite as a model for clay minerals, was studied in the binary systems as well as in the more complicated ternary system in chapter 5.

Using the ultrafiltration technique, the complexation of Aldrich humic acid with Pu(III) was studied. The complexation constant (logß = 6.5±0.3) is in good agreement with those found by other authors for other trivalent actinides (chapter 5.1.2).

The sorption of Pu(III) onto kaolinite was investigated in batch experiments. It was determined that the pH edge is at pH 5.5 comparable with results published for other trivalent actinides. In addition, the speciation of plutonium on the surface of kaolinite was investigated by EXAFS/XANES at the INE beamline at ANKA. It was discovered that, although the experiments were conducted in an inert gas box starting from a Pu(III) solution, the plutonium on the surface was Pu(IV) (chapter 5. 2. 1).

In chapter 5. 3 it was shown that the sorption of humic acid onto kaolinite is pH dependent.

The studies performed on the ternary system have shown that the sorption of Pu(III) onto kaolinite is strongly influenced by the presence of Aldrich humic acid. While at pH < 5 a changeover from mobility to demobilization of plutonium occurs as an effect of the co-adsorption of metal-loaded humic acid, at higher pH the sorption is strongly hindered through a competitive complexation with humic acid found free in solution at neutral and basic pH.

The sequence of addition of the kaolinite, Pu(III), and humic acid in solution, plays a significant role in the changes that occur in the system as a result of the presence of humic acid, as described in chapter 5. 4.

Further experiments are planned, and more detailed speciation of plutonium on the surface of kaolinite will be performed by means of EXAFS/XANES.

In the presence, further efforts are carried out for the development and the optimization of CE-DAD-ICP-MS for studies of the complexation between actinides and humic substances.

The potential of RIMS for speciation experiments with the CE-RIMS coupling was still not entirely exploited. In the future, the detection limits of this method,

and its possible background problems will be more accurately determined.

Although, just a small part of the complex environmental system has been characterized in this work, the way to comprehensive knowledge is open; hence continuing the research, will deliver the information necessary for establishing the suitable key for the convoluted enquiry for locating a nuclear waste repository.

Figures Index

Table Index

Literature:

1. Agilent Technologies,internet site, *http://www.home.agilent.com* .
2. Allard, B., Olofsson, U., and Torstenfelt, B. (1984) Environmental actinide chemistry. *Inorganic Chimica Acta*, **94**, 205-221.
3. Albers, R. C., (2001), Condensed-matter physics: An expanding view of plutonium, *Nature*, **410**, 759-761.
4. Amayri, S., (2006). oral presentation. at "Workshop des Verbundprojektes Migration von Actiniden im System Ton, Huminstoff, Aquifer", Mainz.
5. Ambard, C., Delorme, A., Baglan, N., Aupiais, J., Pointurier, F., and Madiac, C. (2005) Interfacing capillary electrophoresis with inductively coupled plasma mass spectrometr for redox speciation of plutonium. *Radiochimica Acta*, **93**, 665-673.
6. Ambartzumian, R. V. and Letokhov, V. S. (1972), *Applied Optics*, **11**, 354.
7. ANKA Synchrotron Light Source, web site: http://ankaweb.fzk.de
8. Ankudinov, A. L. (2002). Parallel calculation of electron multiple scattering using Lanczos algorithms. *Physical Reviews* B, **65**, 104107
9. Bagnall, K. W., (1972), The actinides elements, in Robinson, P. L. (Ed.), *Topics in inorganic and general chemistry*, Monograph **15**, Elsevier Publishing Company, Amsterdan.
10. Banik, N. L. (2006). PhD Thesis, *Institut für Kernchemie, Johannes Gutenberg-Universität Mainz,* in preparation
11. Barbot, C., Czerwinski, K., Buckau, G., Kim, J. I., Moulin, V., Vial, M., Pieri, J., Durand, J._P., and Goudard, F. (2002). Characterization of a humic gel synthesized from an activated epoxy silica gel. *Radiochimica Acta*. **90**, 211-218
12. Baxter, M. S., Fowler, S. W., and Povinec, P. (1995). Observation on plutonium in the oceans. *Applied radiation and Isotopes*, **46**, 1213-1223.
13. Beckmerhagen, I. A., Berg, H. –P., and Brennecke, P. W. (2004). Recent waste management related developments in Germany. *Journal of Nuclear Science and Technology*, **41**, 393-398.
14. BfS, Bundesamt für Strahlenschutz, internet site: www.bfs.de
15. Bitea, C., Kim, J. I., Kratz, J. V., Marquardt, C. M., Neck, V., Seibert, A., Walther, C., Yun, J. I. (2002). A study of colloid generation and disproportionation of Pu(IV) in aquatic solutions by LIBD and LPAS. *Institut für Kernchemie, Johannes Gutenberg-Universität Mainz,* **C4**, Annual Report

16. Bitea, C. (2005). Laser-induzierte Breakdown Detektion (LIBD): Quantifizierung der Kolloidbildung vierwertiger Actiniden und Homologen. *Institut für Nukleare Entsorgung, Wissenschftliche Berichte*, **FZKA 7083**.
17. Breiner, J. M., Anderson, M. A., Tom, H. W. K., and Graham, R. C. (2006). Properties of surface-modified colloidal particles. *Clay and Clay Minerals*, **54**, 12-24.
18. Bryan, N. D.; Jones, M. N.; Birkett, J.; Livens, F. R. (2001). Application of a new method of analysis of ultracentrifugation data to the aggregation of humic acid by copper(II) ions. *Analytical Chimica Acta*., **437,** 281-289.
19. Buda, R. A., Banik, N. L., Bürger, S., Kratz, J. V., Kuczewski, B., Trautmann, N. (2006) Interaction of trivalent plutonium with humic acid and kaolinite, **in preparation**.
20. Bundesamt für Strahlenschutz (BfS), Deutsche Gesellschaft zum Bau und Betrieb von Endlagern für Abfallstoffe GmbH (DBE), *Nuclear waste management in Germany.*
21. Bundesamt für Strahlenschutz, Internet site: http://www.bfs.de/ion/wirkungen/plutonium.html
22. Buerger, S., Riciputi, L. R., Turgeon, S., Bostick, D., McBAy, E., and Lavell, M. (2006). A high efficiency cavity ion source using TIMS for nuclear forensic analysis, *Abstract Plutonium Futures o6 Conference*, Pacific Grove, California, USA.
23. Bunzl, K., and Kracke, W. (1987). Simultaneous determination of plutonium and americium in biological and environmental samples. *Journal of Radioanalytical and Nuclear Chemistry,* **115 (1),** 12-21.
24. Bürger, S. (2005). Spurenalyse von Uran und Plutonium sowie Speziationsuntersuchungen an Plutonium mit massenspektrometrischen und kapillarelektrophoretischen Methoden, Doctoral Thesis, Johannes Gutenberg-Universität Mainz, Institut für Kernchemie, Mainz.
25. Cashen, G. H. (1959). Electric charges of kaolinite. *Trans Faraday Society*, **55**, 477-486.
26. Choppin, G. R. (1985). Complexes of Actinides with naturally occurring organic compounds, *Handbook of the Physics and Chemistry of the Actinides*, Vol. 3, eds. A. J. Freeman and C. Keller, Elsevier Science Publications, **11**
27. Choppin, G. R. (1988). Humics and radionuclide migration. *Radiochimica Acta,* **44/45**, 23-28.
28. Choppin, G. R. (2003). Actinide speciation in the environment. *Radiochimica Acta,* **91**, 645-649.
29. Choppin, G. (2004). Actinide chemistry: from weapons to remediation to stewardship. Radiochimica Acta, **92**, 519-523.

30. Clark, D. L. (2000). The chemical complexities of plutonium. *Los Alamos Science*, **26**, 364-381
31. Cohen, D. (1961). Electrochemical studies of plutonium ions in perchloric acid solution. *Journal of Inorganic and Nuclear Chemistry*, **18**, 207-210.
32. Cohen, B. L., Ott, O. K. (1989). The myth of plutonium toxicity, (*from Karl Otto and Bernard, I. Spinard, eds. Nuclear Energy, New York: Plenum Press*), 355-365.
33. Conradson, S. D. (1998). Applied Spectroscopy, 52, 252A
34. Cornelis, R., Caruso, J., Crews, H., and Heumann, K. (2003). *Handbook of elemental speciation*. Wiley.
35. Cunningham, B. B. and Werner, L. B. (1949). The first isolation of plutonium, *Journal of the American Chemical Society*, **71**, 1521.
36. Czerwinski, K. R., Kim, J. I., Rhee, D. S., and Buckau, G. (1996). Complexation of trivalent actinide ions (Am 3+, Cm 3+) with humic acid: The effect of ionic strength, *Radiochimica Acta*, **72**, 179-187.
37. DBE Technology GmbH, internet site: www.dbetec.de.
38. Delaney, M. S., Dahlam, R. C., and Craig, R. B. (1979). An investigation of plutonium concentration and distribution in a Burrowing Crayfish from the White Oak Creek floodplain, *National Technical Information Service*, Springfiled VA 22161, **101**, 9.
39. Dobschütz von , P. Ch., Fischer, B. (2003). The German policy and strategy on the storage of spent fuel. IAEA-CN-102/**64.**
40. Drits, V. A. and Kashaev, A. A. (1960). The X-ray study of kaolinite single crystal, *Kristallografiya*, **5**, 224-227.
41. Ehmann, T., Bächmann, K., Fabry, L., Rüfer, H., Serwe, M., Ross, G., Pahlke, S., and Kotz, L. (1998). Capillary preconditioning for analysis of anions using indirect UV detection in capillary zone electrophoresis. Systematic investigation of alkaline and acid prerinsing techniques by designed experiments. *Journal of Chromatography A*, **816**, 261-275.
42. Eichler, B., Hübener, S., Erdmann, N., Eberhardt, K., Funk, H., Herrmann, G., Köhler, S., Trautmann, N., Passler, G., and Urban, F. –J. (1996). Eine Atomstrahlquelle für Actinoide-Konzeption, Aufbau und Wirkungsweise. *PSI-Bericht*, **96-03**.
43. Erdmann, N. (1998). Resonazionisationsmassenspektrometrie zur Bestimmung der Ionisationsenergie von Berkelium un Californium und zur Spurenanalytik von Plutonium, PhD Thesis, *Institut für Kernchemie*, Johannes Gutenberg-Universität Mainz
44. Erdmann, N., Nunnemann, M., Eberhardt, K., Herrmann, G., Huber, G., Köhler, S., Kratz, J. V., Passler, G., Peterson, J. R., Trautmann, N., and Waldek, A. (1998).

Determination of the first ionization potential of nine actinide elements by resonance ionization mass spectrometry (RIMS). *Journal of Alloys and Compounds*, **271-273**, 837-840.

45. Ephraim, J., Alegret, S., Mathuthu, A., Bicking, M., Malcolm, R. L., and Marinski, J. A. (1986). Unified physicochemical description of the protonation and metal ion complexation equilibria of natural organic acids (humic and fulvic acids). 2.Influence of polyelectrolyte properties and functional group heterogeneity on the protonation equilibria of fulvic acid, *Environmental Science and Technology*, **20**, 354-366.
46. Euratom. (1989). European Council. Council Regulation No. 3954/87 laying down the maximum permitted levels of radioactive contamination of foodstuffs and feedingstuffe following a nuclear accident or any other case of radiological emergency. *Off J Eur Commun*, L371/11 (1987), amended by Council Regulation 2218/89, *Off J Eur Commun*, L211/1.
47. Frisch, O. R. (1939). Physical evidence for the division of heavy nuclei under neutron bombardment , *Nature*, **143**, 276.
48. FZK. (2001). Radioaktivität und Kernenergie; Forschungszentrum Karlsruhe, internet site: ww.fzk.de.
49. Garner, C. S., Bonner, N. A., and Seaborg, G. T.,(1948). Search for elements 94 and 93 in nature. Presence of 94^{239} in Carnotite. Paper 1.10. *Journal of American Society,* **70**, 3453.
50. George, G. N. and Pickering, I. J. (2000). EXAFSPAK-A suite of computer programs for analysis of X-ray absorption spectra, Stanford.
51. Gomper, K. (2001). Zur Abtrennung langlebieger Radionuklide. *Radioaktivität und Kernenergie, Forschungszentrum Karlsruhe*, 153-167.
52. Grüning, C. (2001). Spektroskopie und Ultraspurenanalyse von Plutonium mittels Resonanzionisations-Massenspektrometrie. PhD Thesis, *Institut für Kernchemie, Johannes Gutenberg-Universität Mainz.*
53. Grünning, C., Huber, G., Klopp, P., Kratz, J. V., Kunz, P., Passler, G., Trautmann, N., Waldek, A., and Wendt, K. (2004) Resonance ionization mass spectrometry for ultratrace analysis of plutonium with a new solid state laser system. *International Journal of Mass Spectrometry*, **235**, 171-178.
54. Hardy, E. P., Krey, P. W., and Volchok, H. L. (1973). Global inventory and distribution of fallout plutonium. *Nature,* **241,** 444-445
55. Hecker, S. with the Los Alamos Staff (2000). The plutonium challenge, Environmental issues. *Los Alamos Science*, **26**, 36-47.
56. Herforth, L. and Koch, H. (1981). Praktikum der Radioaktivität und Radiochemie, *Birkhäuser* Publishing, 182.

57. Hoffman, P. and Lieser, K. (1991). Methoden der Kern- und Radiochemie. *VCH Verlagsgesellschaft mbH.*
58. Holleman, A. F., Wiberg, E., and Wiberg, N. (1987). *Lehrbuch der Anorganischen Chemie.* Walter de Gruyter.
59. Hotzl, H., Rosner, G. and Winkler, R., (1983). Radionuclide concentrations in ground level air and precipitations in South Germany from 1976 to 1982. *GSF-Report S-956.* Gesellschaft für Strahlen und Umweltforschung MBH.
60. http://www.nuclearfaq.ca/cask.htm
61. Huertas, J. F., Chou, L., and Wollast, R. (1998). Mechanism of kaolinite dissolution at room temperature and pressure: Part 1. Surface speciation, *Geochimica et Cosmochimica Acta*, **62**, 417-431.
62. IAEA. (1998). *Safe handling and storage of plutonium, Safety reports series No. 9.* International Atomic Energy Agency.
63. IAEA. (2004). *The Nuclear Safety Review for the Year 2004.* International Atomic Energy Agency.
64. IAEA. (2006). *Data base.* International Atomic Energy Agency.
65. IEER, (1992). : *Plutonium, Deadly Gold of the Nuclear Age*, International Physicians for the Prevention of Nuclear War and The Institute for Energy and Environmental Research (Cambridge, Massachusetts: International Physicians Press).
66. ICRP (1988).Metabolic data for plutonium, *Reports*, **19**, issue 4
67. IUPAC, (1997). IUPAC Compedium of Chemical Terminology **2nd** Edition, 1991, 63, 902.
68. Jarvis, K. E., Gray, A. L., and Houk, R. S. (1992). Handbook of Inductively Coupled Plassma Mass Spectrometry. *Chapman and Hall*. New York
69. Jennings, C. *D.*, Delfanti, R., and Papucci, C. (1985). The distribution inventory of fallout plutonium in sediments of the Ligurian Sea near La Spezia, Italy. *Journal of Environmental Radioactivity,* **2**, 293-310.
70. Jianxin, T., Yaozhong, C., and Zhangji, L. (1993). A kinetic study of the reduction of plutonium with humic acid. *Radiochimica Acta*, **61,** 73-75.
71. Joliot, F., von Halban, H., and Kowarski, L. (1939) . Liberation of neutrons in the nuclear explosion of uranium. *Nature*, **143**. 470-471.
72. Katz, J. J., Seaborg, G. T., Morss, L. R., (1986) The chemistry of the actinide elements, 2nd ed., Vol. **2**, *Chapman and Hall*, New York, 1133-1146.
73. Kautenburger, R., Nowotka, K., Beck, P. H. (2006). Modelluntersuchungen zu Wechselwirkungen im System Metall/Huminsäure/Kaolinit, oral presentation at

„Abschlussworkshop Verbundprojekts Migration von Actiniden im System Ton, Huminstoff, Aquifer“, Mainz.

74. Keller, C. (1971). The transuranium elements. Verlag Chemie Gmbh.
75. Kersting, A. B., Efurd, D. W., Finnegan, D.L., Rokop, D. J., Smith, D. K., and Thompson, J. L. (1999). Migration of plutonium in ground water at the Nevada Test Site. *Nature*, **397**, 56-59.
76. Kim, J. I. and Buckau, G. (1988). Characterisation of reference and site specific humic acids, *Report RCM – 02188*, Institut für Radiochemie, TU München.
77. Kim, J.I., Buckau, G., Li, G. H., Duschner, H., and Psarros, N. (1990). Characterization of humic and fulvic acids from Gorleben groundwater, *Fresenius Journal of Analytical Chemistry*, **338**, 245-252.
78. Kim, J. I., Rhee, D. S., Buckau, G. (1991). Complexation of Am(III) with humic acids of different origin, Radiochimica Acta, 52/53, 49-55
79. Kim, J. I. and Czerwinski, K. R. (1996). Complexation of metal ions with humic acid: metal ion charge neutralization model. *Radiochimica Acta*, **73**, 5-10.
80. Klopp, P. (1997). Aufbau eines Festkörper-Lasersystems für die Resonazionisations-Massesnspektroskopie am Plutonium. Diploma Thesis, *Institut für Kernchemie, Johannes Gutenberg-Universität Mainz.*
81. Kok, W. (2000). Capillary electrophoresis: instrumentation and operation. *Chromatographia*, **51**, 1-89.
82. Koshurnikova, N. A., Bolotnikova, M. G., Ilyin, L. A., Keirim-Markus, I. B., Menshikh, Z. S., Okantenko, P. V., et al. (1998). Lung Cancer Risk Due to Exposure to Incorporated Plutonium. *Radiation Research***. 149**: 366-371
83. Kuczewski, B., Marquardt, C. M., Seibert, A., Geckesi, H., Kratz, J. V., and Trautmann, N. (2003). Separation of plutonium and neptunium species by capillary electrophoresis-inductively coupled plasma-mass spectrometry and application to natural groundwater samples. *Analytical Chemistry*, **75,** 6769-6774.
84. Kuczewski, B. (2004) Trennung der Oxydationsstufen des Plutoniums mit CE-ICP-MS und Untersuchung des Redoxverhaltens von Plutonium im Grundwasser. PhD work, *Institut für Kernchemie, Johannes Gutenberg Universität Mainz*.
85. Landers, J. P. (1996). Handbook of Capillary Electrophoresis, *CRC Press.*
86. Lead, J. R.; Wilkinson, K. J.; Balnois, E.; Cutak, B. J.; Larive, C. K.; Assemi, S.; Beckett, R. (2000). Diffusion coefficients and polydispersities of the Suwannee River fulvic acid: comparison of fluorescence correlation spectroscopy, pulsed-field gradient nuclear

magnetic resonance and flow field-flow fractionation. *Environmental Science and Technology*, **34**, 3508-3513

87. Letokhov, V. S., (1972) Nonlinear Laser Chemistry, *Springer Series in Chemical Physiscs*, **22**.
88. Li, S.F.Y. (1993). Capillary Electrophoresis: Principles, Practice and Applications, *Elsevier*, Amsterdam.
89. Liang, L. and Morgan, J. J. (1990). In Chemical modelling of aqueous systems II, *American Chemical Society*, Washington, DC, 193-308.
90. Lide, D. R., (1997-1998), *Handbook of Chemistry and physics*, **78th** Ed.
91. Lidskog, R., Andersson, A. C. (2001). The management of radioactive waste . A description of ten countries, *Svensk Kärnbräslehantering AB.*
92. Lippold, H., Müller, N., and Kupsch, H. (2005) Effect of humic acid on the pH-dependent adsorption of terbium (III) onto geological materials, *Applied Geochemistry*, **20**, 1209-1217.
93. Ma, C., and Eggleton, R. A. (1999). Cation exchange capacity of kaolinite, C*lay and Clay Mineraly*, **47**, 174-180.
94. Marquardt, C. M. (1989). Trennung von Neptunium (IV) und (V) in sehr geringen Konzentrationen, *Diploma Thesis*, Institut für Kernchemie, Johannes Gutenberg-Universität Mainz.
95. Marquardt, C. M. (Ed.) (2000). Influence of humic acid on the migration behaviour of radioactive and nonradioactive substances under conditions close to nature*, Final report, Project no.02 E 8795 8 and 02 E 8815 0, Scientific report FZKA 6557*, Karlsruhe
96. Marquardt, C. M., Seibert, A., Artinger, R., Denecke, M. A., Kuczewski, B., Schild, D., and Fanghänel, T. (2004). The redox behaviour of plutonium in humic rich groundwater. *Radiochimica Acta*, **92**, 617-623.
97. McMillan, E. (1964). Nobel Lectures, *Chemistry 1942-1962*, Elsevier publishing Company, Amsterdam.
98. Meitner, L. and Frisch, O. R. (1939). Disintegration of uranium by neutrons: a new type of nuclear reaction. *Nature*, **143**, 239-240.
99. Mermut, R., A. and Cano, A., F. (2001). Baseline studies of the clay minerals society source clays: Chemical analyses of major elements. *Clay and Clay Minerals*, **5**, 381-386.
100. Moli, W. F. Jr. (2001). Baseline studies of the clay minerals society source clays: Geological origin. *Clay and Clay Minerals*, **49**,374-380.

101. Montavon, G., Markai, S., Anders, Y., Grambow, B. (2002). Complexation studies of Eu(III) with alumina –bound polymaleic acid: effect of organic polymer loading and metal ion concentration. *Environmental Science and Technology*, **36**, 3303-3309.

102. Montero, P. R. and Sanchez, A. M., (2001). Plutonium contamination from accidental release or simply fallout: study of soils at Palomares (Spain). *Journal of Environmental Radioactivity*, **55**, 157-165.

103. Moulin, V., Robouch, P., Vitorge, P., Allard, B. (1987). Spectroscopic study of the interaction between Am(III) and humic materials. *Inorganic Chimica Acta*, **140**, 303-308

104. Moulin, V. and Moulin, C. (2001). Radionuclide speciation in the environment: a review. *Radiochimica Acta*, **89**, 1-16.

105. Moulin, V. and Tits J. (1992). Complexation behaviour of humic substances towards actinides and lanthanides studied by Time-Resolved Laser –Induced Spectrofluorometry, *Radiochimica Acta*, **58/59**, 121-128.

106. Murray, H., Bundy, W., Harvey, C. (1993). Kaolin genesis and utilization. *Clay Minerals Society*, Boulder Colorado.

107. Neck, V., Altmaier, M., and Fanghänel, Th. (2006). Solubility and redox reactions of $PuO_2{\cdot}xH_2O$(s). Private comunication at Institut für Kernchemie, Johannes Gutenberg-Universität Mainz

108. Neu, M. P., and Hoffman, C. D. (1994). Comparison of chemical extractions and laser photoacustic spectroscopy for the determination of plutonium species in near-neutral carbonate solutions. *Radiochimica Acta*, **66/67**, 251-258.

109. Newville, M. (2004). Fundamentals of X-ray absorption fine structure. *Consortium for advanced radiation sources*, University of Chicago.

110. Niitsu, Y., Sato, S., Ohashi, H., Sakamoto, Y., Nagao, S., Ohnuki, T., and Muraoka, S. (1997). Effects of humic acid on the sorption of neptunium(V) on kaolinite, *Journal of Nuclear Materials*, **248**, 328-332.

111. Nitsche, H., Lee, S. C., and Gatti, R.C. (1988). Determination of plutonium oxidation states at trace levels pertinent to nuclear waste dsiposal. *Journal of Radioanalytical and Nuclear Chemistry, Articles*, **124,** 171-185.

112. Nitsche H., Gatti, R. C., Standifer, E. M., Lee, S. C., Müller, A., Prussin, T., Deinhammer, R. S., Maurer, H., Becraft, K., Leung, S., and Carpenter, S.A. (1993) Measured solubilities and speciations of neptunium, plutonium, and americium in a typical groundwater (J-13) from the Yucca Mountain Region Milestone Report 3010-WBS 1.2.3.4.1.3.1 *Rep. LA-12562-MS, Los Alamos National Laboratory.*

113. Nitsche, H. and Silva, R. J (1996) Investigations of the carbonate complexation on Pu(IV) in aqueous solution. *Radiochimica Acta,* **72,** 65-72.

114. Olesik, J. W., Kinzer, J. A., and Olesik, S. V. (1995). Capillary electrophoresis inductively coupled plasma spectrometry for rapid elemental speciation. *Analytical Chemistry,* **67**, 1-12.

115. Panak, P. J. (2005). Aquatische Chemie von Actiniden in natürlichen kolloidalen Systemen, Private communication at Institut für Kernchemie, Johannes Guttenberg-Universität Mainz.

116. Passler, G., Erdmann, N., Hasse, H. U., Hermann, G., Huber, G., Köhler, Kratz, J. V., Mansel, A., Nunnemann, A., Trautmann, N., and Waldeck, W. (1997). Application of laser mass spectrometry for trace analysis of plutonium and technetium. *Kerntechnik*, **62**, 85-90.

117. Perdue, E. M. (1989). Effeccts of humic substances on metal speciation, *Aquatic Humic Substances Influence on Fate and Treatment of Pollutants.* (I. H. Suffet, and P. MacCarthy eds.) American Chemical Society

118. Perelygin, V. P. and Chuburkov, Y. T. (1997). Man-made plutonium in environment-Possible serious hazard for living species. *Radiation Measurement*, **28**, 385-392.

119. Peuser, P., Gabelmann, H., Lerch, M., Sohnius, B., Trautmann, N., Weber, M., Herrmann, G., Denschlag, H.O., Ruster, W., and Bonn, J. (1981). Detection methods for trace amounts of plutonium. IAEA-SM-252/40, Pg 257-262.

120. Pfenning, G., Klewe-Nebenius, H., Seelmann-Eggebert, W., (1998), *Karlsruher Nuklidkarte*, corrected version of the 6th Edition

121. Prange, A., Schaumlöffel, D. (1999). Determination of element species at trace levels using capillary electrophoresis-inductively coupled plasma sector field mass spectrometry. *Journal of Analytical Atomic Spectrometry*, **14**, 1329-1332.

122. Prutt, T. E. (1993). Sampling and analysis of KGa-1B well-crystallized kaolin source clay. *Clay and Clay Minerals*, **41**, 514-519

123. Puukko, E., Hakanen, M., Lindberg, A. (2003). Characterization of the natural kaolinite KGa-1b, Working report 2003- **17**. Posiva internet site.

124. Redwood, P. S., Lead, J. R., Harrison, M. R., Jones, P. I., and Stoll, S. (2005). Characterization of humic substances by environmental scanning electron microscopy.

125. Rehr, J. J. Theoretical approaches to x-ray absorption fine structure. *Reviews of Modern Physics*, **73**, 621-654.

126. Reich, T. Ye., Banik, N. L., Buda, R. A., Amayri, S., Drebert, J., Kratz, J. V., Trautmann, N., and Reich, T. (2005). EXAFS study of plutonium sorption onto kaolinite*, Institut für Kernchemie, Johannes Gutenberg Universität Mainz, Annual Report*

127. Reiller, P. (2005). Prognosticating the humic complexation for redox sensitive actinides through analogy, using the charge neutralisation model. *Radiochimica Acta*, **93**, 43-55.

128. Riciputi, L. R. and Turgeon, S. (2004). The high efficiency cavity source for isotope analysis of small samples, *Abstract International Geological Conference*, 32.

129. Righetto, L., Bidoglio, G., Azimonti, G., and Bellobono, I. R. (1991). Competitive actinide interactions in colloidal humic acid-mineral oxide, *Environmental Science and Technology*, **25**, 1913-1919.

130. Runde, W. (2000). The chemical interactions of actinides in the environment. *Los Alamos Science*, **26**, 392-411.

131. Samadfam, M., Jintoku, T., Sato, S., Ohashi, H., Mitsugarashira, T.,Hara, M., and Suzuki, Y. (2000). Effects of humic acid on the sorption of Am(III) and Cm(III) on kaolinite. *Radiochimica Acta*, **88**, 717-721.

132. Savrasov, S. Y., Kotliar, G. & Abrahams, (2001), *E. Nature*, **410**, 793-795.

133. Schaumlöffel, D. and Prange, A. (1998). *German Patent*, **198 41 288.6**.

134. Schroth, B. K. and Sposito, G. (1997). Surface charge properties of kaolinite. *Clay and Clay Minerals*, **45**, 85-91.

135. Seaborg, G. T. (1964). Nobel Lectures, *Chemistry 1942-1962*, Elsevier publishing Company, Amsterdam

136. Seaborg, G. T.,McMillan, E. M., Kennedy, J. W., and Wahl, A. C., (1946). Radioactive element 94 from deuterons on uranium. *Physical Review,* **69,** 367.

137. Seaborg, G. T. and Perlman, M. L., (1948). Paper 1.3, *Journal of American Society.* **70,** 1571.

138. Stevenson, F. E. (1982). Humus Chemistry. *Wiley-Interscience*, New-York.

139. Stieve, F. E. (1976). Radiation protection and cardiac pacemakers with radionuclide batteries. *Strahlenschutz Forsch Prax*. **15**. 178-91.

140. Stumpe, R., Kim, J. I., Schrepp, W., and Walther, H. (1984). Speciation of actinides ions in aqueous solution by laser-induced pulsed photoacustic spectroscopy. *Applied Physics B*, **34,** 203-206.

141. Taylor, R. N., Warneke, T., Milton, J. A., Croudace, I. W., Warwick, P. E. and Nesbitt, R. W. (2003). Multiple ion counting determination of plutonium isotope ratios using multi-collector ICP-MS. *Journal of Analytical Atomic Spectrometry*, **18**, 480-484.

142. Takashi, Y., Kimura, T., and Minai, Y. (2001). Direct observation of Cm(III)-fulvate species on fulvic acid-montmorillonite hybrid by laser-induced fluorescence spectroscopy, *Geochimica et Cosmochimica Acta*, **66**,1-12.

143. Terabe, S., Otsuka, K., Ichikawa, K., Tsuchiya, A., and Ando, T. (1984). Electrokinetic separations with micellar solutions and open-tubular capillaries, *Analytical Chemistry*, **56**, 111-113.

144. Tipping, E. (1993). Modelling the binding of europium and the actinides by humic substances, *Radiochimica Acta*, **62**, 141-152.

145. Tokarskaya, Z. B., Okladnikova, N. D., Belyaeva, Z. D., and Drozhkoo, E. G. (1997). Multifactorial Analysis of Lung Cancer Dose-response Relationships for Workers at the Mayak Nuclear Enterprise. *Health Physics*. **73** (6). 899-905.

146. Trautmann, N., Passler, G., and Wendt, K. D. A. (2004). Ultratrace analysis and isotope ratio measurements of long-lived radioisotope by resonance ionization mass spectrometry (RIMS). *Analytical and Bioanalytical Chemistry*, **378**, 348-355.

147. Triay, I. R. *et al.* (1996) Radionuclide sorption in Yucca Mountain tuffs with J-13 Well-Water: Neptunium, uranium, and plutonium *Rep. LA-125956-MS, Los Alamos National Laboratory.*

148. Truscott, J. B., Jones, P., Fairman, B. E., and Evans, E. H. (2001). Determination of actinide elements at femtogram per gram levels in environmental samples by on-line solid phase extraction and sector-field-inductively coupled plasma-mass spectrometry. *Analyticy Chimica Acta*, **433**, 245-253.

149. Tuniz, C., Bird, J. R., Fink, D., and Herzog, G. F. (1998). (eds) Accelerator mass spectrometry. CRC Press LLC, Boca Raton.

150. Urban, F. –J. (1994). Resonanzionistionsmassenspektroskopie an Plutonium mit einem Reflektron-Flugzeitmassenspektrometer. PhD Thesis, *Institut für Physik*, Johannes Gutenberg-Universität Mainz.

151. Voelz, G. L., Buican, I. G. (2000). Plutonium and Health how great is the risk?. *Los Alamos Science*, **26**, 74-89

152. Walther, C. Cho, H. R., Marquardt, C. M., Neck, V., Seibert, A., Yun, J. I., Fanghänel, Th. (2005). Redox behaviour of plutonium(IV) in acidic Solutions, Poster, *Migration 2005 Conference*.

153. Walther, C.,.Bitea, C., Yun, J. I., Kim, J. I., Fanghänel, Th., Marquardt, C. M., Neck, V., Seibert, A. (2003). Nanoscopic approaches to the aquatic plutonium chemistry. Conference proceeding, Plutonium Future – The Science Conference. Los Alamos National Laboratory.

154. Wang, X. K., Rabung, Th., Geckeis, H., Panak, P. J., Klenze, R., and Fanghänel, Th. (2004). Effect of humic acid on the sorption of Cm(III) onto γ-Al_2O_3 studied by the time-resolved laser fluorescence spectroscopy, *Radiochimica Acta*, **92**, 691-695.

155. Wang, X., Xu, D., Chen, L., Tan, X., Zhou, X., Ren, A., and Chen, Ch. (2006). Sorption and complexation of Eu(III) on alumina: Effects of pH, ionic strength, humic acid and chelating resin on kinetic dissociation study, *Applied radiation and Isotopes*, **64**, 414-421.

156. Warneke, T., Croudace, I. W., Warwick, P. E., and Taylor, R. N. (2002). A new ground-level fallout record of uranium and plutonium isotopes for northern temperate latitudes. *Earth and Planetary Science Letters*, **203**, 1047-1057

157. Watters, R. L., Edginton, D. N., Hakonson, T. E., Hanson, W. C., Smith, M. H., Whicker, F. W., and Wildung, R. E. (1980). Synthesis of the research literature. *W. C. Hanson*: *Transuranic elements in the environment*.

158. Wendt, K., Blaum, K., Bushaw, B. A., Grünning, C., Horn, R., Huber, G., Kratz, J. V., Kunz, P., Müller, P., Nörtershäuser, W., Nunnemann, M., Passler, G., Schmitt, A., Trautmann, N., and Waldeck, W. (1999). Recent developments in and applications of resonance ionization mass spectrometry. *Fresenius Journal of Analytical Chemistry*, **364**, 471-477.

159. Winkler, S., Ahmad, I., Gosler, R., Kutschera, W., Orlandini, K. A., Paul, M., Priller, A., Steier, P., Valenta, A., and Vockenhuber, C. (2004). Developing a detection method of environmental ^{244}Pu, *Nuclear Instruments and Methods in Physics Research*, **B 223-224**, 817-822.

160. World Nuclear Association, Internet site *http://www.world-nuclear.org*

161. Wunderlich, T. (2006)Abtrennung von Plutonium aus Umweltproben. Diploma thesis, *Institut für Kernchemie*, Johannes Gutenberg-Universität Mainz.